ROLE OF ß-GLUCURONIDASE IN THE CHEMOPREVENTIVE EFFICACY OF ORAL CURCUMIN: A PRODRUG HYPOTHESIS

A DISSERTATION

SUBMITTED TO THE FACULTY OF THE GRADUATE SCHOOL OF

THE UNIVERSITY OF MINNESOTA

BY

Garvey Liu

IN PARTIAL FULFILLMENT OF THE REQUIREMENTS

FOR THE DEGREE OF

DOCTOR OF PHILOSOPHY

IN PHARMACEUTICS

Jayanth Panyam

November 2015

Acknowledgements

I would like to take this honored opportunity to acknowledge and express my gratitude to the individuals that have influenced me throughout the four years of my graduate education and contributed to the work in this dissertation. This journey would have been impossible to tread without the guidance, support, and assistance of these phenomenal people surrounding me.

First and foremost, I would like to extend my deepest gratitude to my graduate advisor, Dr. Jayanth Panyam. The level of appreciation that I have for his mentorship, guidance, and wisdom over the course of my graduate studies is immense. Entering graduate school, I had a very limited set of experimental and research skills, but rather than perceiving this as a shortcoming, Dr. Panyam continued to broaden my knowledge in the fields of drug delivery and biopharmaceutics. His teachings and philosophies have instilled in me a greater appreciation for scientific inquiry, and his limitless encouragement and support have made me a better scientist. Thank you very much for giving me this opportunity to write a great scientific story, and for always motivating me to strive to be my very best.

I would like to thank my thesis committee members – Dr. William Elmquist, Dr. Karunya Kandimalla, and Dr. Kaylee Schwertfeger – for their critical reviews, suggestions, and comments on my dissertation and research work. Thank you Dr. Elmquist, for your valuable contributions and recommendations as I conducted my pharmacokinetic studies; Dr. Kandimalla, for the guidance on principles of drug delivery

and pharmacokinetics; and Dr. Schwertfeger, for providing insight into the various breast adenocarcinoma cell lines and cancer biology.

My gratitude extends to all of the faculty members, staff, graduate students, and postdoctoral fellows in the Department of Pharmaceutics. The enriching intellectual interactions and academic environment in the department has made my graduate educational career a truly memorable chapter in my life. I treasure my friends in the department – especially Ameya Kirtane, Mehak Mehta, Karen Parrish, Pinal Mistry, Nidhi Sharda, Michelle Fung, Hyunjoon Kim, and Sampada Koranne – for always being there for lively chats, support, and whenever I needed a helping hand. A special thanks to Dr. Calvin Sun, for being my temporary advisor during my lab rotation, and Dr. Timothy Wiedmann, for all of your advice and the constructive conversations throughout the program. My thanks also go to Candy McDermott, Erica Stapic, Jeanene Noll, and Katie James for the administrative assistance.

Working side-by-side and in collaboration with fellow members of the Panyam lab has been a true pleasure over the years. I am sincerely grateful for the friendships, comradery, company, and support of both senior and current members of the lab: Dr. Alex Grill, Dr. Tanmoy Sadhukha, Dr. Suresh Swaminathan, Dr. Marina Usacheva, Dr. Lin Niu, Dr. Ameya Kirtane, Dr. Mingxia Yu, Steve Kalscheuer, Hyunjoon Kim, Drishti Sehgal, and Vidhi Khanna. Many thanks to Alex, for helping me in becoming integrated into the lab during my first year; Tanmoy, for all of the insight he has provided to my many questions; Steve, for his guidance and assistance in cell culture and animal work; and Hyunjoon, for our valuable discussions and conversations. I would like to especially

thank Ameya, for not only being there from the beginning as a friend and a lab mate, but for all of our insightful discussions and his dedication to our project collaborations.

This thesis would not have been possible without the valuable contributions of numerous faculty, staff, and researchers on both the Minneapolis and St. Paul campuses at the University of Minnesota. I would like to thank Jim Fisher in Clinical Pharmacology Analytical Services for his guidance and input with the LC-MS/MS analyses. I am grateful for Josh Parker and his colleagues at the Comparative Pathology Shared Resource for their assistance with histology and immunohistochemistry. I want to thank everyone in Research Animal Resources, especially Brenda Koniar for her diligent work and immeasurable assistance with the animal studies.

At this time, I would like to acknowledge and express my utmost gratitude for the most important people in my life. My sincere thanks to my aunt, Chen Hong Li, who has always been supportive of my endeavors. Her optimistic, one-of-a-kind personality never fails to bring a smile to my face. I thank my grandparents, Shu Lin Li and Ji Xiang Li, for their endless love and care.

Finally, words can do no justice in expressing how whole-heartedly grateful I am to have such extraordinary parents, and how much I am deeply indebted to them for becoming the person I am today. My parents, Da Hao Liu and Chenlee Liu, have always been at my side for whatever interests I may pursue. They have been my biggest supporters and greatest role models, teaching me the most important lessons in life through example. Their belief in me, continuous motivation, and teachings to be an independent thinker has led me to build character and become a stronger individual. They have truly shown me that nothing is impossible to achieve once you set your mind to it

and persevere towards that goal. I am incredibly thankful for their unconditional love, determination, encouragement, and support that has brought me to this point in my educational career. I can only hope that I make them nearly as proud of me as I am of them. I dedicate this thesis to my most beloved parents.

Dedication

This thesis is dedicated to my beloved parents, Da Hao Liu and Chenlee Liu, who have always been at my side in the pursuit of my endeavors. Your affection, love, dedication, determination, encouragement, support, and hard work are truly an inspiration in life.

Abstract

Curcumin, a dietary polyphenol, has been shown to have several preventive and therapeutic benefits in epidemiological studies. The chemopreventive potential of curcumin is related to its anti-inflammatory activity and is largely mediated through inhibition of the transcription factor NF-kB. However, curcumin has rather poor oral bioavailability (<1%). Much of orally dosed curcumin undergoes glucuronidation, resulting in the formation of inactive glucuronides. Thus, it is not clear how dietary curcumin exhibits chemopreventive activity despite not being absorbed into the systemic circulation in its active form. We proposed a prodrug hypothesis to explain this 'bioavailability paradox' of curcumin.

β-glucuronidase is an enzyme that hydrolyzes the glycosidic bond of glucuronides. Previous studies have shown that the expression of this enzyme is elevated under inflammatory conditions and overexpressed in necrotic regions of tumors. Increased β-glucuronidase activity in the tumor tissue in comparison to its relatively minimal activity in normal cells potentially explains the bioavailability paradox with curcumin. *We hypothesized that curcumin glucuronide is an inflammation-responsive natural prodrug that gets converted back to curcumin 'on-demand' at the site of action.*

Our studies were aimed at determining specific activity of β-glucuronidase based on mammary tumor type, stage, and model. β-glucuronidase activity was determined in mammary tumor tissues with HER-2+ (BALB-*neu*T, TuBo) and triple negative (4T1, JC, MDA-MB-231) phenotypes. Activity assay results showed that the highest rate of conversion was in 4T1 tumors as compared to the other tumor types.

Immunohistochemistry (IHC) studies on primary human breast tumor tissue samples showed β-glucuronidase expression levels to be highest in HER-2+ type breast cancer compared to triple negative and ER/PR+ types. Also determined from the microarray of human tissue samples, as well as from Western blotting and fluorescence imaging studies, was the strong correlation between enzyme expression levels and stage of cancer: normal and benign stages showed the lowest levels of β-glucuronidase while the invasive/metastatic stage showed the highest expression levels.

Using a self-microemulsifying drug delivery system (SMEDDS) formulation that was developed to improve the oral absorption, we aimed next to investigate the chemopreventive efficacy of curcumin following oral administration. Daily oral dosing of curcumin for one month in the orthotopic models described above showed that those with higher β-glucuronidase specific activities (JC, MDA-MB-231, and 4T1) benefitted the most from curcumin in limiting tumor growth rate. Pharmacokinetic studies with oral dosing of curcumin SMEDDS showed elevated levels of the glucuronide metabolite in plasma as compared to negligible levels of curcumin while the trend was reversed in the tumor tissue, providing further support to the prodrug activation hypothesis. The pharmacokinetics of curcumin glucuronide following intravenous dosing also confirmed conversion of the glucuronide to the parent compound in the tumor tissue.

Overall, the work presented in this thesis demonstrated the potential of oral curcumin for breast cancer chemoprevention based on the enzymatic prodrug activation hypothesis.

Table of Contents

List of Tables

List of Figures

List of Abbreviations

ACN	Acetonitrile
Akt	Protein kinase B
ANOVA	Analysis of variance
AP-1	Activated protein-1
AUC	Area under the curve
CG	Curcumin Glucuronide, 4-[(1E,6E)-7-(4-Hydroxy-3-methoxyphenyl)-3,5-dioxo-1,6-heptadien-1-yl]-2-methoxyphenyl β-D-Glucopyranosiduronic Acid
CL	Clearance
COX-2	Cyclooxygenase-2
C_{ss}	Steady state concentration
CUR	Curcumin, (1*E*,6*E*)-1,7-Bis(4-hydroxy-3-methoxyphenyl)-1,6-heptadiene-3,5-dione
CPT-11	Irinotecan
DMSO	Dimethyl sulfoxide
EGF	Epidermal growth factor
EGFR	Epidermal growth factor receptor
EMT	Epithelial to mesenchymal transition
ER	Estrogen receptor
FDA	Food and Drug Administration
g	Gram

GUSB	β-glucuronidase
H&E	Hematoxylin and eosin
HER-2	Human epidermal growth factor receptor-2
HER-2+	Overexression of HER-2
HMR 1826	N-[4-β-Glucuronyl-3-nitrobenzyloxycarbonyl]doxorubicin, a doxorubicin glucuronide prodrug
HPLC	High performance liquid chromatography
hr	Hour
HRP	Horseradish peroxidase
IKK	IκB kinase
IL	Interleukin
IP	Intraperitoneal
IV	Intravenous
kDa	Kilodaltons
kg	Kilogram
Ki-67	Cellular marker for proliferation
K_m	Michaelis constant
L	Length
LC-MS/MS	Liquid chromatography-mass spectroscopy/mass spectroscopy
M	Molar
MAPK	Mitogen activated protein kinase
mg	Milligram
min	Minute

mL	Milliliter
μL	Microliter
mM	Millimolar
μM	Micromolar
mm	Millimeter
μm	Micrometer
MMTV-LTR	Mouse mammary tumor virus-long terminal repeat
mTOR	Mammalian target of rapamycin
MW	Molecular weight
NF-κB	Nuclear factor-kappa B
ng	Nanogram
NIR-TrapG	Activity-based near-infrared difluoromethylphenol−glucuronide fluorescent probe
nM	Nanomolar
nm	Nanometer
NP	4-Nitrophenol
NPG	4-Nitrophenyl β-D-glucuronide
NSAID	Non-steroidal anti-inflammatory
p53	Tumor suppressor protein
PI3K	Phosphatidylinositol-4,5-bisphosphate 3-kinase
pmol	Picomole
PR	Progesterone receptor
RNS	Reactive nitrogen species

ROS	Reactive oxygen species
rpm	Rotations per minute
S.C.	Subcutaneous
SD	Standard deviation
SEM	Standard error of mean
SMEDDS	Self micro-emulsifying drug delivery system
SN-38	Active metabolite of irinotecan; potent topoisomerase I inhibitor
SN-38G	SN-38 glucuronide, an inactive metabolite of SN-38
SULT	Sulfotransferase
$t_{1/2}$	Half-life
TNF-α	Tumor necrosis factor-α
UDPGA	Uridine 5'-diphospho-glucuronic acid
UGT	UDP-glucuronosyltransferase
VEGF	Vascular endothelial growth factor
V_{max}	Maximum reaction velocity
w/v	weight by volume
w/w	weight by weight

Chapter I

Overview and Introduction

1.1 Physico-chemical Properties and Composition of Curcumin

Curcumin, a brilliant yellow-orange colored polyphenol, is the main bioactive ingredient extracted from the dried ground rhizome of the perennial herb *Curcuma longa Linn* (commonly known as turmeric), an herb of the curcuma species. Turmeric has been traditionally used for many centuries to give the distinctive flavor and color to curry spice, and curcumin has long been employed in traditional Indian and South Asian medicine (Ayurveda) for the treatment of a wide range of ailments. The molecular formula of curcumin is $C_{21}H_{20}O_6$, and it has a molecular weight of 368.37 g/mol, melting point of 183 °C, and a predicted logP value of 3.62. Spectrophotometrically, the maximum absorption (λ_{max}) of curcumin in methanol was observed to be at 430 nm and in acetone at 415-420 nm [1]. The polyphenol was first isolated in 1815 by Vogel and Pelletier [2], obtained in crystalline form in 1870 [2, 3], and its chemical structure of (1*E*,6*E*)-1,7-Bis(4-hydroxy-3-methoxyphenyl)-1,6-heptadiene-3,5-dione or diferuloyl-methane was confirmed by Lampe and Milobedezka in 1910 [4]. The major curcuminoids, or chemically related structures to and derivatives of curcumin, in turmeric include curcumin, demethoxycurcumin, and bisdemethoxycurcumin. Commercial curcumin consists of curcumin (77%), demethoxycurcumin (17%), and bisdemethoxycurcumin (3%) [5].

Curcumin is an oil-soluble compound due to its hydrophobic nature, making it readily soluble in ethanol, methanol, acetone, dimethyl sulfoxide (DMSO), alkali, ketones, acetic acid and chloroform, and practically insoluble in water at acidic or neutral pH [4]. The compound can exist in both the enolic and beta diketone forms, with the enol form being more stable in solution and solid phase. In acidic pH conditions (≤ 6),

curcumin is relatively stable, but at neutral and basic pH (> 7), curcumin is rapidly degraded to ferulic acid and feruloylmethane, with vanillin being identified as a minor degradation product. However, one of the major metabolites of curcumin, tetrahydrocurcumin (THC), is stable at neutral and basic pH, but only for 1-2 hours [6]. Curcumin is a highly protein bound compound, making it more stable in cell culture medium containing protein such as 10% fetal bovine serum and in human blood [7].

1.2 Molecular Targets and Mechanisms of the Therapeutic Benefits of Curcumin

Deregulation of various cell signaling and transduction pathways because of alterations in a wide array of regulatory proteins is the key hallmark of cancer. Curcumin modulates and interacts with many regulatory proteins to modify their expression and activity, including inflammatory cytokines and enzymes, transcription factors, growth factors, and gene products that are associated with cell survival, proliferation, invasion, and angiogenesis. Studies have found that curcumin inhibits several signaling pathways and molecular targets involved in cancer progression and inflammation. This was observed from documentation of curcumin inhibiting proliferation and growth of various tumor cells in culture, and limiting the growth rate of human tumors xenografted in animal models. The various molecular targets of curcumin which are involved in several cell signaling pathways are presented in the following.

Curcumin is known to inhibit the activation of several transcriptional factors, including activator protein (AP)-1, nuclear factor-kappa B (NF-κB), β-catenin, early growth response gene (EGR)-1, signal transducers and activators of transcription (STAT)-3, hypoxia inducible factor (HIF)-1, and Notch-1, which are all upregulated in

cancer. Such transcription factors play a role in cell proliferation, invasion, metastasis, and angiogenesis. Studies have shown curcumin to inhibit both inducible and constitutive STAT3 activation and its nuclear translocation by inhibiting Janus kinase (JAK)-2 phosphorylation in several myeloma cell lines [8]. Constitutive STAT3 activation was also inhibited in peripheral blood mononuclear cells from myeloma and pancreatic cancer patients [9, 10]. In AP-1 signaling, curcumin has been observed to inhibit AP-1 activation by tumor promoters, which in turn inhibits C-Jun N-terminal kinase (JNK) activation by carcinogens [11, 12]. Notch-1 signaling, which cross-talks with another important cell growth and apoptotic pathway (NF-κB), is also limited due to curcumin-induced reductions in Notch-1 levels [13]. Wnt/β-catenin signaling, a pathway that is important in tissue development, homeostasis, and regeneration and often deregulated in human cancer, is inhibited by reducing levels of β-catenin and Tcf-4 proteins, as shown in studies with gastric, colon and intestinal cancer cell lines [14, 15]. It has been also shown that curcumin suppresses the induction of transcription factor Egr-1, a gene regulator in vasculature growth, differentiation, wound healing, blood clotting, and immune response. This suppression of Egr-1 by curcumin modulates the Egr-1 gene in fibroblasts, endothelial cells [16], and colon cancer cells [17].

NF-κB is a major transcription factor that is modulated by curcumin. NF-κB mainly serves as a gene regulator that controls cell proliferation and cell survival. The NF-κB heterodimer – NF-κB complexed with the inhibitory protein IκBα – exists in the cytosol in an inactivated state. Extracellular signals stimulate and activate the enzyme IκB kinase (IKK) through integral membrane receptors, causing IKK to phosphorylate and thus mark the IκBα protein for dissociation and degradation [18]. The activated NF-

κB then translocates to the nucleus where it may bind to response elements (RE) at certain sequences of DNA and therefore initiate transcriptional activity for cell survival [19]. Curcumin inhibits NF-κB signaling and induces apoptosis by inhibiting IKK signaling and phosphorylation of IκBα, causing NF-κB to remain bound to inhibitory IκBα [20].

Not only does curcumin inhibit IKK signaling, but it also inhibits inflammatory cytokines such as interleukins and tumor necrosis factor-alpha (TNF-α). TNF-α plays key roles in immunity, cellular remodeling, apoptosis, and cell survival [21]. Since TNF-α is also largely responsible for the cause of inflammation, many efforts have been put forth to develop antagonists for the receptors of TNF-α in the treatment of inflammation and cancer. Curcumin has significant activity against TNF-α-induced signaling, as it not only modulates the signaling, but also inhibits the expression of the cytokine. It is known to inhibit expression of TNF-α mRNA in rat livers with CCl_4-induced hepatic fibrosis [22]. Curcumin reduced TNF-α levels in sodium taurocholate-induced acute pancreatitis in rats [23], diabetic encephalopathy in rats, and cisplatin-induced nephrotoxicity in mice [24]. In addition, curcumin has been shown to be a potent inhibitor of interleukins as well, a class of pro-inflammatory cytokines that are involved in the induction of metalloproteinases, adhesion molecules, and pro-angiogenic factors [25]. Studies have shown curcumin to inhibit IL-1 [26], IL-2 [27], IL-5 [28], IL-8 [26], IL-12 [29], and IL-18 [30] expression. In one study, curcumin inhibited IL-6-induced phosphorylation of STAT3 in myeloma cells [8].

The mitogen-activated protein kinase (MAPK) and PI3K/Akt/mTOR cellular signaling pathways are other pathways that curcumin modulates. MAPKs play important

roles in converting various extracellular signals into intracellular responses via serial phosphorylation cascades [31]. Environmental stress stimuli such as cytokines (TNF-α, interleukins), ultraviolet (UV) light, and ionizing radiation induce activation of MAPKs (ERK, JNK, and p38), which can in turn phosphorylate transcription factors that include c-myc, c-jun, Sin1-associated protein (SAP-1), GADD153, myocyte enhancer factor-2C (MEF2C), and activating transcription factor-2 (ATF2), thus eventually causing alterations in gene expression [32-34]. Regulation of MAPK signaling by curcumin has been shown to contribute to suppression of tumorigenesis and inflammation. Studies have reported curcumin inhibiting the upregulation of COX-2 and MMP-9 by blocking ERK1/2 phosphorylation in MCF10A human breast epithelial cells [35]. In addition, JNK activation was inhibited by curcumin in human Jurkat T (leukemia) cells and human embryonic kidney 293 cells [36]. This inhibition of several signaling modules by curcumin in the MAPK cascade enhances the induction of apoptosis in both *in vitro* and *in vivo* tumor models [37].

The PI3K/Akt/mTOR signaling pathway is a key regulator of the cell cycle, survival, and apoptosis. There have been several reports of curcumin inducing apoptosis in cancer cells due to the inhibition of multiple components in the PI3K/Akt/mTOR pathway. One key component that is modulated is the dephosphorylation of Akt, as observed with acute T-cell leukemia [38]. Since Akt is a protein kinase that promotes cell survival by phosphorylating Bcl-2-associated agonists of cell death, curcumin limits B lymphoma cell growth by inhibitng Akt and its target genes [39]. Levels of phosphorylated Akt, an indication of activated Akt, dramatically decreased as a response to receiving high doses of curcumin [40]. Additionally, PI3K/Akt/mTOR signaling is

stimulated by activation of membrane receptors, such as EGFR, via external cytokines and growth factors. Curcumin functions to not only inhibit EGF-stimulated phosphorylation of Akt, but the polyphenol also limits the levels of the cytokines themselves that are stimulating membrane receptors in breast cancer cells and thereby facilitate the induction of apoptosis [41].

Curcumin is known to modulate the activity of enzymes that are involved in inflammation and cancer, including cyclooxgenase-2 (COX-2), matrix metalloproteinases (MMPs), and inducible nitric oxide synthase (iNOS). Overexpression of COX-2 has been linked with many types of cancers, including that of the colon, lung, and breast. Cycolooxygenase is an enzyme that converts arachidonic acid to prostaglandins and thromboxanes, and COX-2 specifically is overexpressed at inflammatory sites, which may play a critical role in tumor promotion and tumorigenesis. Studies have demonstrated that curcumin inhibits COX-2, the inducible form of COX, but not COX-1, the constitutively active form of COX that is responsible for homeostatic functions [42]. This effect is due mainly to the inhibition of the IKK signaling complex in the NF-κB pathway to phosphorylate inhibitory IκBα, and thereby blocking the activation of NF-κB [43]. Curcumin was shown to inhibit COX-2 initiation by the colon tumor promoter TNF-α due to inhibition of NF-κB activation in human colon epithelial cells [44]. In addition, it has been reported that curcumin also suppressed the chenodeoxycholate-(CDC) or phorbol ester 12-*O*-tetradecanoylphorbol-13-acetate (TPA) mediated induction of COX-2 and inhibited synthesis of prostaglandin E_2 in several gastrointestinal cell lines [45]. Expression of COX-2 in peripheral blood mononuclear cells from pancreatic cancer [10] and myeloma [9] patients was inhibited by curcumin. A specific inhibitor of COX-2,

Celecoxib, is approved by the Food and Drug Administration (FDA) for the treatment of inflammatory conditions.

Matrix metalloproteinases (MMPs) are endopeptidases, which are overexpressed in tumor infiltration. MMP-2 and MMP-9 are mainly associated with tumor angiogenesis via their roles of extracellular matrix (ECM) degradation [46]. It has been demonstrated that curcumin limits the invasion and metastasis of cancer cells through suppression of MMPs. Inhibition of TPA-induced ERK activation and NF-κB transcriptional activation in human breast cancer epithelial cells by curcumin has been reported [36]. Curcumin downregulates MMP-9 expression, which is associated with brain tumors, by inhibiting NF-κB and AP-1 binding to the DNA promoter region [47]. It has been also shown that curcumin inhibits expression of MMP-9 in orthotopically transplanted pancreatic [48] and ovarian [49] tumors in nude mouse models. Moreover, iNOS, another enzyme associated with inflammation and metastasis, is also inhibited by curcumin, as was the case in inhibiting its production in *in vitro* cultured Balb/c mouse peritoneal macrophages [11, 50].

Cytokine signaling receptors and growth factors are also molecular targets of curcumin. Suppression of the expression of growth factors such as EGF, HER-2, FGF, VEGF, TNF-α, insulin growth factor (IGF-1), and their receptors is essential in suppressing tumor growth. Numerous reports exist of curcumin being a key modulator in the expression and activity of these various growth factors. Epidermal growth factor receptor (EGFR) is overexpressed in several tumor types, including lung, head and neck, colorectal, and breast cancer, and curcumin has been shown to inhibit EGFR1 overexpression [11, 12]. HER-2, another member of the EGFR class, is also

overexpressed in many cancers. While Trastuzumab (trade name: Herceptin®) is currently one of the main FDA approved antagonists for the treatment of HER-2+ breast cancer, curcumin has shown promising results in inhibiting HER-2 overexpression in A431 cells [51]. There is evidence that curcuminoids modulate the fibroblast growth factor (FGF-2) angiogenic signaling pathway as well as inhibit expression of vascular endothelial growth factor (VEGF), thus limiting angiogenesis and tumor growth. Bevacizumab (trade name: Avastin®) is the only VEGF inhibitor approved by the FDA for the treatment of non-small cell lung cancer, and studies have shown that curcumin inhibited VEGF expression levels in NIH3T3 cells and transcript levels of two major angiogenesis factors, VEGF and bFGF, in the triple negative MDA-MB-231 breast cancer cells [52, 53] at similar levels as Avastin. Curcumin also inhibited VEGF expression in orthotopically implanted ovarian [49] and pancreatic tumors [48] in nude mouse models. Furthermore, expression and activation of hormone (estrogen, progesterone) receptors (ER/PR) are also suppressed by curcumin. Estrogen and estrogen receptors alpha and beta (ER-α and ER-β) play a major role in tumorigenesis, as two-thirds of breast cancers are associated with overexpression of these functional receptors. Studies have reported that curcumin not only inhibits proliferation of ER-positive cells, but also ER-negative cells as well (i.e., breast adenocarcinoma cells of the triple negative subtype), which suggests that curcumin has chemopreventive effects in both an ER-dependent and ER-independent manner [54].

Other effects on molecular targets include activating pro-apoptotic caspases, downregulating anti-apoptotic proteins such as Bcl-2 and Bcl-X_L, upregulating tumor suppressor p53, and suppressing the expression of cyclin D1. Studies have revealed

curcumin to induce cytotoxicity and apoptosis via caspase-3 activation in human colon cancer cells, promoting expression of tumor suppressor protein p53 and inhibiting expression of anti-apoptotic Bcl-2 and Bcl-X_L proteins [55]. Curcumin induces apoptosis in human malignant mesothelioma cells and human mantle cell lymphoma by downregulating Bcl-2 and Bcl-X_L expression [56]. In addition, p53, a tumor suppressor protein that plays a pivotal role in cell cycle control, genomic stability, cellular response to DNA damage, signal transduction and apoptosis, is upregulated by curcumin [57]. As a tumor suppressor, functional p53 activates transcription of downstream genes such as $p21^{cip1/waf-1}$ and $p27^{kip-1}$ to induce apoptosis, inhibit the growth of DNA damaged cells, and block cell cycle progression [58]. Curcumin serves to upregulate p53 gene expression, as seen in the growth arrest and induction of apoptosis in BKS-2 cell lymphoma [59], human melanoma [60], and glioma [61] cells. Moreover, cyclin D1, a component of the subunit of cyclin-dependent kinase CDK4 and CDK6, is overexpressed in a variety of tumor cells, thus causing alterations and deregulation in cell cycle progression. Curcumin has been known to inhibit cyclin D association with CDK4/CDK6 and phosphorylate tumor suppressor pRb, which blocks cell cycle progression from G1 to S phase [62]. Through upregulation of CDK inhibitors (CDKIs) and downregulation of cyclin B1 and cdc2, curcumin induces G0/G1 or G2/M phase cell cycle arrest in umbilical vein endothelial (ECV304) cells [63]. Downregulation of cyclin D1 *in vivo* was observed to be at both the transcriptional and translational levels.

The ability of curcumin to inhibit several signaling pathways and modulate molecular targets that are key to tumorigenesis and inflammation, in combination with

minimal systemic cytotoxicity and side effects at high oral doses, suggests the high potential of this polyphenol to be widely used as a chemopreventive compound.

1.3 Curcumin for Chemoprevention

Curcumin has several pharmacological effects that make it an excellent candidate for use in cancer chemoprevention. The compound itself is safe and relatively non-toxic when ingested orally. It has been shown that large doses of curcumin administered orally for extended periods of time is safe – no significant toxicity was observed in pilot phase I clinical trials in healthy human volunteers who consumed daily doses of up to 12 grams of curcumin orally for 3 months [73]. Cytotoxicity primarily occurs with diseased tissue and cells, as curcumin regulates and restores several signaling pathways that contribute to cancer. Downregulation of overexpressed proteins and cytokines, such as interleukins and tumor necrosis factor-α (TNF-α), as well as various growth factors also play a key role in tumor cell cytotoxicity [74]. Since curcumin is a common and naturally occurring compound that mainly functions by intervening with only abnormal cellular processes, it is a strong candidate for being widely used as a chemopreventive agent.

1.4 Bioavailability of Curcumin

Numerous pre-clinical studies and phase I clinical trials have shown that curcumin possesses diverse pharmacological effects, but exhibits poor bioavailability (<1%). Low plasma and tissue levels of curcumin are attributed to its poor absorption along the gastrointestinal tract, extensive first-pass metabolism in the liver, and rapid elimination from the body. The lipophilicity and low aqueous solubility of curcumin

limits its rate of dissolution in the gastrointestinal tract upon oral administration, and hence a greater portion of the dose remains unabsorbed and is excreted. It has been reported that very low levels of curcumin were present in serum after oral dosing, a strong indication of low bioavailability. In a study involving the intravenous dosing of rats with curcumin at 10 mg/kg, the maximum concentration observed in serum was 0.36 ± 0.05 μg/mL, whereas a 500 mg/kg dose (50-fold higher than IV dose) administered orally yielded only 0.06 ± 0.01 μg/mL at maximum serum levels [70]. For rats, the maximum serum concentration of curcumin at 45 minutes after an oral dose at 1 g/kg was 0.5 μg/mL [77]. Another study reported that at 50 minutes after an oral dose of curcumin, the maximum concentration was found to be only 6.5 ± 4.5 ng/mL [78].

In addition to poor absorption, curcumin undergoes rapid first-pass metabolism as well, both within the enterocytes along the gastrointestinal wall immediately upon absorption and in the hepatocytes of the liver, where a significant portion of the absorbed curcumin is either sulfonated or glucuronidated by phase II metabolism. Studies have reported that gut bacteria play a role in phase I metabolism of curcumin [79]. It has been shown that the NADPH-dependent curcumin/dihydrocurcumin reductase (CurA) enzyme originating from Escherichia coli (E. coli) present in the gastrointestinal tract metabolizes curcumin in a two step-reduction, first to intermediate dihydrocurcumin (DHC), and then to the end product tetrahydrocurcumin (THC). Some studies have observed THC and other reduced curcumin metabolites to possess even greater potency than curcumin in terms of anti-inflammatory [80], antidiabetic, and antihyperlipidemic [81] activity, as well as equal potency in terms of antioxidant activity [82]. Moreover, phase II metabolism of curcumin also contributes to its low bioavailability. Sulfonation and

glucuronidation of curcumin in the first-pass effect of the liver yields inactive conjugated metabolites of the polyphenolic compound in the systemic circulation.

Several approaches have been developed and studied in attempts to increase the bioavailability of curcumin. Concomitant administration of adjuvants has been used to inhibit metabolic pathways as major means of improving its bioavailability. In one study, it was noted that the effects of piperine, a known inhibitor of intestinal and hepatic glucuronidation, when co-administered with curcumin, effectively increased the bioavailability of curcumin by 2000% [83]. Additionally, other novel formulations that have been studied and showed promising results in increased curcumin bioavailability and delivery include nanoparticles [84-85], micelles [86-87], liposomes [88-90], and phospholipid complexes [91-92].

In the studies presented in this thesis, a self-microemulsifying drug delivery system (SMEDDS) formulation (see below) was developed to enhance the solubility of curcumin and thus improve the bioavailability of oral curcumin.

1.5 Pharmacokinetics of Curcumin

Numerous studies have investigated the pharmacokinetics of curcumin following oral, intravenous (IV), and intraperitoneal (IP) dosing, revealing its poor absorption and rapid elimination from the body. When curcumin powder is administered orally, low levels of curcumin have been found in the plasma and a major fraction of the dose is excreted unchanged in the feces. In rats, a 400 mg oral dose of curcumin resulted in 40% of the dose to be eliminated unchanged in the feces with no detectable levels in the urine and heart blood, and only trace levels in the portal blood and kidneys. The same study

showed 90% of the curcumin remaining in the gastrointestinal tract 30 minutes after administration, and only 1% remaining in the kidneys after 24 hours post-dose [64]. Another study reported negligible levels of curcumin in plasma of rats following oral administration of 1 g/kg of curcumin, indicating poor absorption of the drug from the gut [65]. In studies with mice, an IP dose of 100 mg/kg resulted in 2.25 μg/mL of curcumin in the plasma within the first 15 minutes of dosing. In the same study, at 1 hour post IP dose, curcumin levels in the intestine, spleen, liver, kidneys, and brain had levels of 177.04, 26.06, 26.09, 7.51, and 0.41 μg/g, respectively [66].

Clinical trials in human subjects further revealed the low levels of curcumin in plasma following oral administration. In Taiwan, 25 patients with cancer lesions were administered varying doses of 4, 6, and 8 grams of curcumin per day. After treatment for 3 months, peak serum concentrations were found to be 0.51 ± 0.11, 0.64 ± 0.06, and 1.77 ± 1.87 μM, respectively. Lower doses resulted in undetectable levels in the serum [67]. In another clinical study with colorectal cancer patients, 1.8 g and 3.6 g of curcumin were administered orally for seven days, resulting in serum concentrations of 7.7 ± 1.8 and 12.7 ± 5.7 nmol/g, respectively [68]. After an IP dose of 100 mg/kg curcumin in human patients, intestinal tissue levels reached 300 nmol/g, as compared to 1 nmol/g in the brain and 72 nmol/g in the liver [69].

Distribution of curcumin in tissue and elimination from the body are important factors in its pharmacological activity. Studies investigating curcumin distribution have used ^{14}C curcumin as a method to measure curcumin levels in various tissues. In an *in vivo* study with C57B1/6J mice, a single IP dose of 100 mg/kg ^{14}C curcumin resulted in the following observed peak drug concentrations: intestine: 200 ± 23 nmol/g, liver: 73 ±

20 nmol/g, brain 2.9 ± 0.4 nmol/g, heart: 9.1 ± 1.1 nmol/g, lung: 16 ± 3 nmol/g, kidney: 78 ± 3 nmol/g, and muscle: 8.4 ± 6.0 nmol/g. In the same study, radioactivity of ^{14}C declined rapidly after reaching between 20 – 33% of the peak values at 4 or 8 hours post-dose [72]. Other studies have determined the elimination half-life values of curcumin for an IV dose of 10 mg/kg in rats to be 28.1 ± 5.6 hours and for an oral dose of 500 mg/kg to be 44.5 ± 7.5 hours [70].

1.6 Clearance of Curcumin

In addition to being poorly absorbed following oral administration, curcumin also undergoes extensive metabolism in both the enterocytes of the gastrointestinal wall and the hepatocytes of the liver. Both phase I (reduction) and phase II (conjugation) metabolic pathways play prominent roles in limiting its bioavailability.

1.6.1 Phase I Metabolism

Phase I metabolism involves the formation of a new or modified functional group or cleavage, such as in the case of oxidation, reduction, and hydrolysis reactions. Such reactions are non-synthetic, and typically consist of conversion of a parent drug to a more polar metabolite by the insertion of a polar functional group. Curcumin is readily reduced to dihydrocurcumin, tetrahydrocurcumin, hexahydrocurcumin, and octahydrocurcumin upon IV and IP administration [93]. These reduction reactions are catalyzed primarily by alchohol dehydrogenase in the liver. *In vitro* studies have confirmed the phase I metabolism of curcumin, as evidenced by reductive metabolite levels being prominent following incubation of curcumin with precision-cut liver slices from rats. In one *in vitro*

study, curcumin incubated with Sprague-Dawley rat liver slices yielded five reductive but no oxidative metabolites, and the major reductive metabolites were hexahydrocurcuminoids [94]. In addition, incubating curcumin with pure alchohol dehydrogenase enzyme yields significant levels of reduced metabolite products, further confirming that these products are in fact due to phase I metabolism. It has also been observed that many of the reduced phase I metabolites of curcumin are further metabolized and undergo phase II conjugation metabolism.

1.6.2 Phase II Metabolism

Phase II metabolism consists of conjugating the active drug compound with an endogenous substance, such as glucuronic acid, sulfate, or glycine. These reactions are synthetic and result in a metabolite that has higher molecular weight, higher polarity, and less activity than the parent drug. Due to the higher polarity of the metabolite, phase II metabolites are more readily excreted through the kidneys.

Curcumin is either glucuronidated by UDP-glucuronosyltransferases (UGTs) or sulfated by sulfotransferases (SULTs). There exist numerous isoforms of both UGTs and SULTs, but only a select few are important to curcumin metabolism. UGT1A1 and UGT1A3 isozymes, both specific to the liver, account for the highest activity of curcumin glucuronidation, as has been shown using recombinant UGTs. Intestinal UGT1A8 and UGT1A10 predominantly catalyze the glucuronidation reaction in the enterocytes along the gut wall [95]. One *in vivo* study showed that following oral dosing, 99% of curcumin in the plasma was present as curcumin glucuronide [96]. While the four isoforms of UGT mentioned above are mainly responsible for the glucuronidation of curcumin, metabolic

activity levels vary between human and rodent microsomes, and by whether it is taking place in the intestine or the liver. Enzymatic activity levels were shown to be similar between human hepatic (4641 ± 126 pmol/min/mg protein) and rat hepatic (4589 ± 170 pmol/min/mg protein) microsomes, but the levels of human intestinal metabolic activity by UGTs (12687 ± 1138 pmol/min/mg protein) is approximately 3-fold higher as compared to rat intestinal enzyme activity (3933 ± 104 pmol/min/mg protein) [97]. Such differences between species in metabolic activity must be taken into account when translating from pre-clinical trials involving animal models to clinical trials involving human patients. In another study, it has been shown that glucuronidation accounts for ~82% of all metabolites observed. Sulfonation, mediated by SULT1A1 and 1A3, account for the remainder of the fraction of phase II curcumin metabolism (~15%) [98]. Overall, curcumin undergoes extensive phase II metabolism via glucuronidation and sulfonation, which contributes greatly to its limited bioavailability of reaching the systemic circulation in its active form.

1.7 Bioavailability Paradox

Curcumin is known to have a wide range of preventive and therapeutic effects, and has been employed for the treatment of diseases and ailments that range from digestive, hepatic, and biliary disorders, to wound healing, sinusitis, rheumatism, and inflammation. Pharmacologically, curcumin has been shown to have anti-cancerous, anti-proliferative, anti-oxidant, and anti-inflammatory properties in numerous studies on both the pre-clinical and clinical levels. Reports of southern Asia – a region of the world in which Indian curry spice containing curcumin is prevalent in regular dietary consumption

– having some of the lowest rates of colorectal and lung cancer [176] have further supported the idea that the polyphenol has chemopreventive effects.

Though curcumin possesses many health benefits and has demonstrated its preventive and therapeutic potential when administered orally, less than 1% of orally administered curcumin is bioavailable because of its poor intestinal absorption and extensive metabolism. A majority of the curcumin absorbed undergoes rapid glucuronidation in the intestinal wall or the liver, and thus yielding the inactive metabolite curcumin glucuronide as the primary form present in systemic circulation. Thus, it is unclear how dietary curcumin exhibits chemopreventive activity despite not being absorbed into the systemic circulation in its active form. The objectives of this thesis is to investigate the mechanisms behind this 'bioavailability paradox' by determining the pharmacokinetics of curcumin and its metabolite curcumin glucuronide as well as anticancer efficacy following the oral administration of curcumin in a microemulsion formulation that improves its oral absorption.

1.8 Prodrug Hypothesis

The prodrug activation hypothesis is a proposal for the mechanism of chemopreventive action of oral curcumin. It proposes to explain the 'bioavailability paradox' of curcumin, in which despite its poor bioavailability, oral curcumin has been repeatedly shown to have several preventive and therapeutic benefits. When curcumin is orally administered and reaches the gastrointestinal tract (GIT), curcumin is absorbed along the GIT, which is then delivered to the liver via the hepatic portal vein. Curcumin undergoes phase II metabolism by UDP-glucuronosyltransferases (UGTs) in either the

enterocytes along the gastrointestinal wall or the hepatocytes of the liver to form curcumin glucuronide. The inactive metabolite curcumin glucuronide is the predominant form that circulates in plasma. Curcumin glucuronide that reaches a site of inflammation or tumor in which the enzyme β-glucuronidase is overexpressed would then be converted back to active curcumin at the site of action. Minimal to no activation in healthy tissue with marginal enzyme expression is expected. Any metabolite remaining in the systemic circulation would be cleared by renal filtration due to its high water solubility and low cell permeability. In essence, oral curcumin is metabolized in either the gastrointestinal wall or liver to curcumin glucuronide, followed by subsequent activation back to active curcumin by β-glucuronidase at the site of disease or inflammation.

The prodrug activation hypothesis ultimately suggests that curcumin glucuronide is an inflammation-responsive natural prodrug that gets converted back to curcumin 'on-demand' at the site of action. Curcumin glucuronide is deconjugated by β-glucuronidase present in the tumor tissue and sites of inflammation to generate the active parent compound curcumin, which can then exert its pharmacological effects at the target site (Figure 1.1).

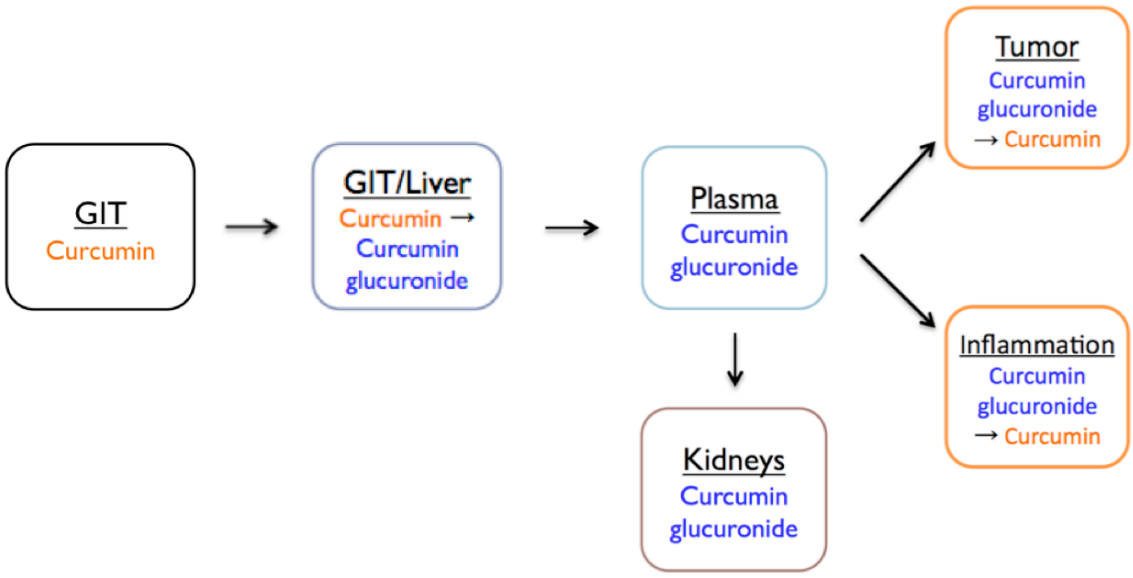

Figure 1.1. Schematic of the prodrug activation hypothesis. Oral curcumin is metabolized either in the gastrointestinal wall upon absorption or liver to curcumin glucuronide, which predominates in plasma circulation. Curcumin glucuronide is activated by β-glucuronidase in sites of disease or inflammation to active curcumin. Remaining curcumin glucuronide is eliminated by renal filtration.

Based on previous reports and data presented in this thesis, we propose that the prodrug activation hypothesis is the main mechanism of curcumin chemopreventive action. The lipophilic nature of curcumin that is activated from curcumin glucuronide in the tumor would allow for accumulation within the disease tissue. This key chemical property that allows for such accumulation within the tumor microenvironment is essential in the therapeutic efficacy of curcumin. Slow but steady accumulation over time increases the concentration of active curcumin at the site of action, and therefore greater efficacy from higher levels of the active drug.

It has been previously reported in literature that steady, regular low doses of drug being administered over a period of time is a more effective therapeutic approach than single, high-dose treatments [75, 76]. This may very well be due to the accumulation of lipophilic drug in the tissue that occurs over time, in which a higher concentration of drug leads to an increased efficacy and more effective treatment. Single, high-dose treatments may not be effective due to the pharmacokinetics of the drug, in that although there may be a higher maximum concentration of drug in plasma or site of action immediately after administration, these levels would unlikely be maintained for long due to drug clearance. The concept of "metronomic chemotherapy" describes this phenomenon, in which tumor growth inhibition occurs by administering regular and consistent, low-dose chemotherapy. Even though conventional high-dose chemotherapy directly kills tumor cells, side effects are often a major issue with such dosage regimens. While further studies are necessary, a sustained and near-constant maintenance of drug levels in the systemic circulation through regular, low dosages would be a more desired approach both

in the aspects of limiting systemic toxicity and maximizing efficacy through drug accumulation [75, 76].

This concept of "metronomic therapy" applies to the prodrug activation hypothesis of chemoprevention by curcumin as well. Regular, daily oral doses of curcumin would yield steady and near-constant concentrations of curcumin glucuronide in the plasma. While administered doses of curcumin may be low or sub-therapeutic, the steady metabolism of curcumin to curcumin glucuronide would generate sufficient levels of the metabolite in the circulation. These low levels of curcumin glucuronide would be activated by β-glucuronidase at inflammation sites, causing a slow but steady accumulation of curcumin. It is a combination of the moderate and regular activation of curcumin glucuronide in disease sites overexpressing β-glucuronidase plus the lipophilic nature of curcumin that would ultimately contribute to its accumulation in the tumor, which is essential in successful chemoprevention.

1.9 Curcumin Glucuronide as a Natural Prodrug

A prodrug is a bioreversible derivative of a drug molecule that undergoes an enzymatic and/or chemical transformation *in vivo* to release the active parent drug, which can exert the desired pharmacological effect at the target site of action [99, 100]. Prodrugs are typically inactive until activated through certain catabolic processes. One example of such an activation reaction is the hydrolysis of an ester. The purpose of formulating a prodrug is to enhance the bioavailability and pharmacokinetics of a drug, in which the absorption, distribution, metabolism, and/or excretion (ADME) is modified to improve drug delivery [101, 102]. They may also be used to improve selectivity of the

drug to a specific target site of action, or reduce adverse or unintended side effects of a drug. This is particularly important in chemotherapy treatments where undesirable side effects are often caused by non-specific cytotoxicity.

Curcumin glucuronide serves as a natural prodrug in that orally administered curcumin undergoes rapid phase II metabolism and is conjugated with a glucuronide promoiety by natural metabolic processes. Due to this metabolism and the hydrophilic nature of the glucuronide, curcumin glucuronide is the main form of curcumin that is present in systemic circulation, and not active curcumin itself. The glucuronide would circulate in plasma and upon reaching a site of disease or inflammation that naturally overexpresses deconjugating enzymes (i.e., β-glucuronidase), the glucuronide promoiety would be cleaved, leaving active curcumin at the site of action. This mechanism of chemoprevention by oral curcumin has multiple benefits: 1.) both curcumin and curcumin glucuronide are relatively nontoxic to normal, healthy cells; 2.) curcumin upon absorption is naturally metabolized to curcumin glucuronide; and 3.) enzymes that de-conjugate the glucuronide to re-form active curcumin are naturally overexpressed at sites where the active drug is desired.

1.10 β-Glucuronidase

Human β-glucuronidase is a 332 kDa homotetrameric glycoprotein with four identical subunits of 78 kDa molecular weight [103]. While β-glucuronidase is primarily localized in the cell lysosome, the enzyme is also found in significant quantities in the necrotic areas of many tumors, especially in larger tumors containing many necrotic cells [104]. The optimal pH for human β-glucuronidase activity is ~4, resembling the pH in

lysosomes. At physiological pH of 7.4, the enzyme exhibits ~10% of normal catalytic activity. β-glucuronidase remains stable and intact at temperatures up to 70°C [105]. Catalytic activity as determined by protein structural analysis is associated primarily with three amino acid residues in the active site: Glu^{540} serves as a nucleophile, Glu^{451} is an acid-base catalyst/proton donor, and Tyr^{504} is also important, though its role has yet to be determined [106]. Structurally, β-glucuronidase contains a type of β-barrel known as a jelly roll barrel as well as a TIM barrel, in which eight α-helices and eight parallel β-strands alternate along the peptide backbone [107].

To understand the role of β-glucuronidase in cancer chemoprevention, a brief overview of phase II drug metabolism via glucuronidation is essential. The conjugation of glucuronic acid to xenobiotics is a fundamental mechanism in nature for detoxifying and eliminating lipophilic compounds from the body [108]. Glucuronidation is a primary pathway of phase II metabolism, in which UDP-glucuronosyltransferase (UGT) conjugates glucuronic acid to a lipophilic drug molecule. Substrates for UGTs include phenols, alcohols, carboxylic acids, and aromatic acids. The conjugation reaction requires the cofactor uridine diphosphateglucuronic (UDP-glucuronic) acid and is catalyzed by UGTs located mainly in the endoplasmic reticulum of hepatocytes. Glucuronide metabolites are polar, hydrophilic, and water-soluble, causing these compounds to be more readily excreted from the body via renal or biliary clearance. Excretion is promoted by the carboxylic acid moiety of glucuronic acid, which is ionized at physiological pH and thus increases the aqueous solubility of the drug. As a result, the hydrophilic glucuronide metabolite is recognized by biliary and renal organic anion transport systems and is subsequently eliminated.

β-glucuronidase is an enzyme that hydrolyzes the glycosidic bond of glucuronides and is overexpressed in the necrotic regions of many human tumors [110]. Its primary physiological function is to catalyze the breakdown of complex carbohydrates. Overexpression of β-glucuronidase in the tumor microenvironment in comparison to its relatively minimal expression levels in normal cells holds potential in targeting chemotherapeutic agents specifically to the tumor site [109, 110]. A key approach that is developed for tumor selective prodrug conversion is prodrug monotherapy, in which the endogenous enzyme that is elevated in tumors is exploited for therapeutic benefit; β-glucuronidase at the tumor site converts relatively nontoxic prodrugs into active cytotoxic compounds, allowing for better selectivity and efficacy for chemopreventive and chemotherapeutic agents. A wide range of malignancies, including breast, lung and gastrointestinal tract carcinomas, and melanomas have shown high levels of β-glucuronidase localized in necrotic areas, as evidenced by enzyme immunohistochemistry (IHC) on tumor biopsies [111]. Previous studies have shown significant differences in growth inhibition effects between small non-necrotic tumors and larger tumors when human tumor xenograft models are treated with a glucuronide prodrug. It was observed then that the extent of chemopreventive efficacy was strongly associated with the expression of β-glucuronidase in areas of tumor necrosis [104, 112, 113]. Expression of β-glucuronidase is due largely to the liberation of monocytes (macrophages), granulocytes (neutrophils), and other factors involved in inflammatory response in the necrotic areas of human tumor tissue. Disintegrating tumor cells contribute minimally to β-glucuronidase release [114]. Previous studies have shown that an increased β-glucuronidase expression results in the increased activity of the enzyme in tumor tissue as

opposed to normal tissue, where there is practically no expression. For example, studies have shown that, after isolated perfusion with a glucuronide prodrug of doxorubicin, uptake of doxorubicin into bronchial carcinoma was much greater as compared to uptake levels into normal lung lobes extracted from the same patients [109]. Correlating enzyme expression in pancreatic carcinoma homogenates with glucuronide prodrug bioactivation of doxorubicin also yielded similar findings [115]. These studies convey the chemopreventive potential of elevated β-glucuronidase levels in tumor tissue.

1.11 β-Glucuronidase Hydrolysis Reaction

Hydrolysis is a reaction in which a chemical bond in a molecule is cleaved by the addition of water. The chemical process in which a water molecule is added to a molecular compound involves the degradation of that compound into its component molecules. Such a process is essential to biological systems, as in the case of breaking down complex carbohydrates into its component sugar molecules. Hydrolysis is often catalyzed by an enzyme. β-glucuronidase, an enzyme of the glycosidase family that aids in breakdown of complex carbohydrates, catalyzes the hydrolysis of β-D-glucuronide from the non-reducing end of glycosaminoglycans [116-118]. The products of the reaction are an alcohol and the cleaved β-D-glucuronic acid moiety (Figure 1.2). In the case that "R" is a drug molecule in the β-glucuronidase hydrolysis reaction, the enzyme substrate would be an inactive glucuronidated drug, and the product yielded would be an active drug molecule. For the reaction shown in Figure 1.2, β-D-glucuronide is the inactive glucuronidated drug, the alcohol is the active drug molecule, and the β-D-glucuronic acid is the cleaved glucuronide moiety.

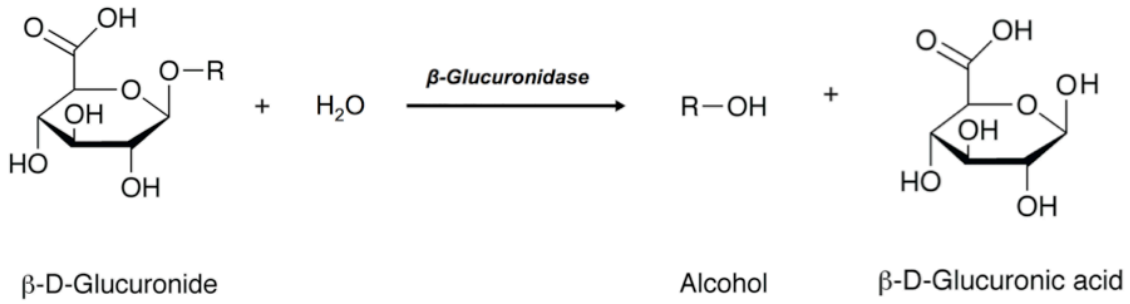

Figure 1.2. Hydrolysis Reaction with β-Glucuronidase.

1.12 Curcumin Metabolism and De-Glucuronidation

A major metabolic pathway of curcumin upon oral administration is phase II metabolism, in which curcumin undergoes glucuronidation [119]. UDP-glucuronosyltransferases (UGTs) present within the enterocytes along the gastrointestinal tract and hepatocytes within the liver catalyze a glucuronide transfer reaction from co-substrate uridine 5'-diphosphoglucuronic acid (UDPGA) to a hydroxy functional group of curcumin [120]. This glucuronidation reaction yields curcumin glucuronide, an inactive molecule that is readily excreted due to its hydrophilic nature. [119]. Curcumin glucuronide that reaches β-glucuronidase at sites of inflammation or disease, however, undergoes a hydrolysis reaction in which the glucuronide moiety is cleaved from the inactive metabolite, thus yielding active curcumin as the product along with the byproduct β-D-glucuronic acid (Figure 1.3).

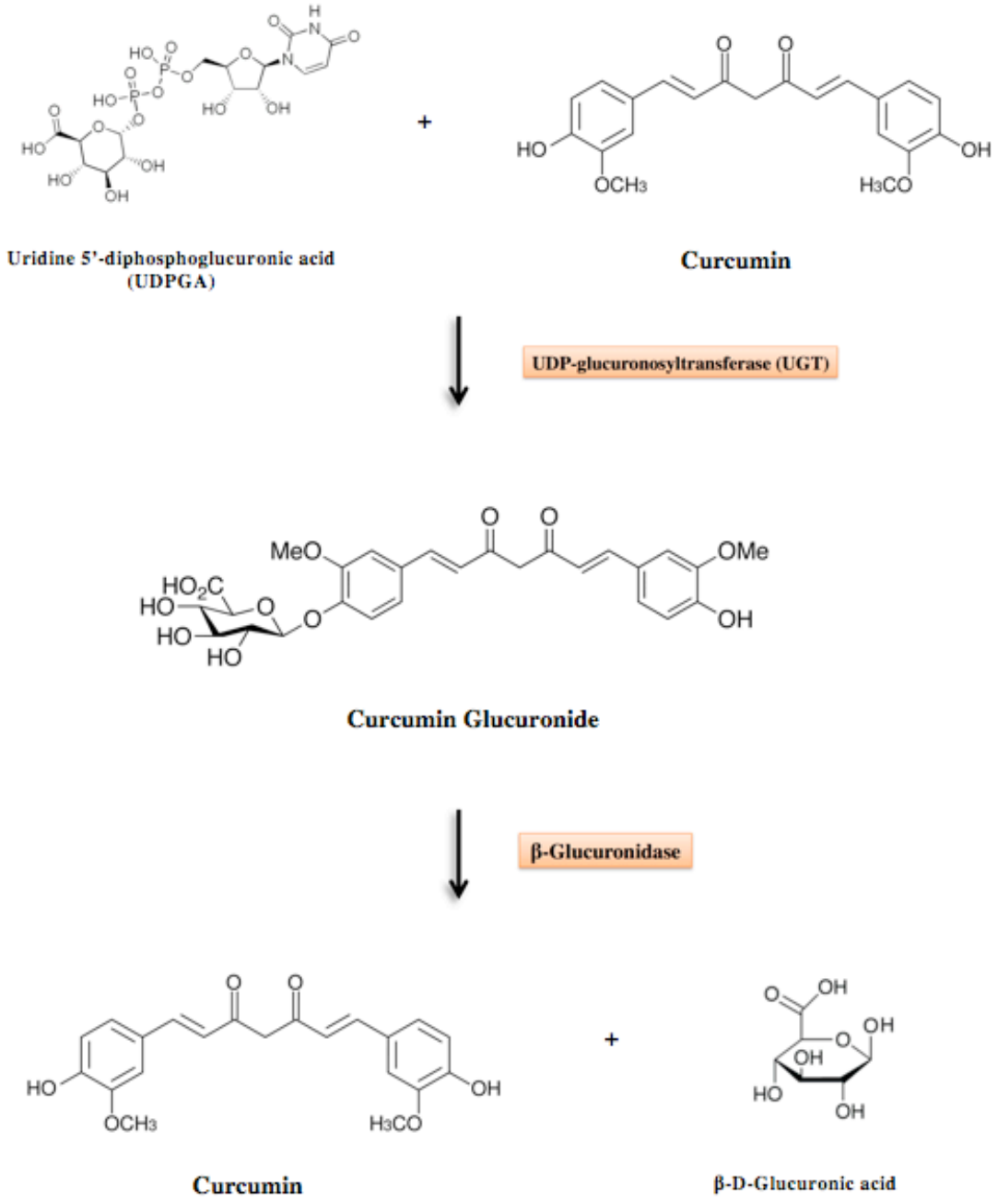

Figure 1.3. Curcumin metabolism to curcumin glucuronide by UDP-glucuronosyltransferase, and subsequent hydrolysis of curcumin glucuronide to curcumin by β-glucuronidase.

1.13 Literature Reports of β-Glucuronidase Expression, Activity, and Prodrug Activation

Several reports point to the elevated levels of β-glucuronidase in inflammatory and disease pathology. β-glucuronidase expression and activity was shown to be highly concentrated in regions of necrosis in lung cancer surgery specimens, as determined by enzyme histochemistry (EHC) and TdT reaction experiments [121]. Within these necrotic regions, cellular debris from dead cells were seen to bear markers for the presence of human monocytes and/or granulocytes, and so it is most likely that these immune response cells liberate β-glucuronidase. Enzyme activity from disintegrating cells, however, was only marginal. Additionally, a strong correlation was observed between the regions of high local β-glucuronidase concentration and areas of abundant and rapid DNA degradation, as seen by immunohistochemistry of human tumor xenografts and TdT reaction products [121]. From these observations, it was concluded that the inflammatory response and immune cells that are present within the necrotic regions of tumors largely contribute to β-glucuronidase activity.

There has also been evidence for a strong correlation between the β-glucuronidase content or expression that is present within tissue and the levels of enzyme activity observed. One study looked at the β-glucuronidase contents in healthy human pancreas, chronic pancreatitis, and pancreatic adenocarcinoma samples and how the enzyme levels in the tissue homogenates measure to their respective specific activities. It was found that there is a direct correlation between enzyme expression levels and specific activity; tissues with minimal β-glucuronidase levels (i.e., normal pancreatic tissue) had the lowest activity, while tissues with high β-glucuronidase content (i.e., pancreatitis and pancreatic

adenocarcinoma tissue) had the greatest specific activities [122]. Enzyme activity was determined by monitoring the levels of 4-methylumbelliferyl-β-D-glucuronide (MUG) conversion to parent compound 4-methylumbelliferone (MU) by HPLC analysis in these studies.

Several epidemiological studies have reported *in vitro* and *in vivo* β-glucuronidase mediated activation of both exogenously and endogenously generated prodrugs. An example of an exogenously generated prodrug is HMR 1826 (N-[4-β-Glucuronyl-3-nitrobenzyloxycarbonyl]doxorubicin), a derivative of doxorubicin with a bound glucuronic acid moiety that exhibits a much lower systemic toxicity profile as compared to doxorubicin. As for an endogenously generated metabolite prodrug, SN-38-glucuronide (SN-38G) is a prime example. SN-38G is an inactive metabolite of SN-38, a potent topoisomerase I inhibitor. Irinotecan (CPT-11) is a clinically important prodrug that is used to treat advanced colorectal and lung cancer [123]. CPT-11 is hydrolyzed by carboxyesterases to yield the active metabolite SN-38, which can be further metabolized to inactive SN-38G by various glucuronosyltransferases (UGTs). *In vitro* and *in vivo* studies have been performed with both HMR 1826 and CPT-11 to evaluate the accumulation levels and efficacy of doxorubicin and SN-38, respectively, based on the activation potential of β-glucuronidase.

When administering a prodrug for a therapeutic regimen, the main goal is to reduce systemic toxicity by improving the drug targeting and accumulated drug concentration at the site of action. Evidence of this was shown when normal lung and bronchial carcinoma tissue resected from human patients and tissues were perfused with either free drug doxorubicin or HMR 1826 [124]. Final tissue concentrations of

doxorubicin in normal lung and tumor were determined after 2.5 hours of perfusion with either 5 μg/mL doxorubicin or 400 μg/mL HMR 1826 by HPLC. While doxorubicin levels were not significantly different between the form of drug administered in normal lung tissue – most likely due to marginal β-glucuronidase activity – the concentrations of doxorubicin were markedly different in tumor. Tumor tissue perfused with HMR 1826 had a mean doxorubicin concentration of 14.04 ± 12.9 ug/g, while perfusion with free doxorubicin gave a final mean doxorubicin concentration of 1.78 ± 3.11 ug/g [124]. The increased concentration of active drug in the tumor when administered in the prodrug form shows the potential of activation selectivity based on the action of β-glucuronidase.

β-glucuronidase activity is just as important in activating endogenously generated prodrugs. It has been shown that significant levels of active SN-38 are formed from SN-38G in both liver and human neuroblastoma NB1691 xenograft tumor tissue collected from female SCID mice [123]. Mice were dosed intravenously with CPT-11 at 10 mg/kg, and following activation to SN-38 and successive metabolism to SN-38G, β-glucuronidase activity was determined by monitoring the rate of SN-38G to SN-38 conversion. Not only was there significant β-glucuronidase activity found in both liver and tumor homogenates, but it was also observed that the β-glucuronidase activity was not saturable over the SN-38G concentration range of 0.12 – 50 μM, as determined by the linearity of the SN-38G concentration versus SN-38 production profiles for both tumor and liver homogenates.

In another set of studies that correlate *in vitro* cell cytotoxicity experiments with *in vivo* efficacy in animal xenografts, the importance of prodrug activation by β-glucuronidase is reiterated. Studies were performed with parent EJ human bladder

carcinoma cells (EJ) and EJ cells expressing membrane-tethered β-glucuronidase (EJ/mβG) implanted in female SCID mice [125]. β-glucuronidase activity assays showed significant activity in incubation with both cultured EJ/mβG cells and EJ/mβG tumor homogenates, whereas minimal activity was seen with parent EJ cells and EJ tumor homogenates. In subsequent *in vivo* efficacy studies with human xenografts of both EJ and EJ/mβG tumors, the EJ/mβG tumor-bearing mice group receiving two daily intravenous doses of CPT-11 at 10 mg/kg showed the treatment to be most efficacious, as compared to other groups that were either EJ tumor-bearing receiving CPT-11 treatments or EJ/mβG tumor-bearing receiving PBS control treatments [125]. Efficacy was determined based on average tumor volumes at the end of the treatment study, with the EJ/mβG tumor-bearing mice receiving CPT-11 treatment having the lowest tumor volumes after 14 days of daily treatment. These studies further show that β-glucuronidase play an essential role in activating glucuronidated prodrugs.

β-glucuronidase not only exhibits higher specific activity with its increased levels in inflammatory and disease tissue, but enzyme kinetics studies also show that the rate of conversion is fastest in tissue having the highest β-glucuronidase content. In one study, 2 substrates of β-glucuronidase – MUG and HMR 1826 – were used to study the enzyme kinetics with the 3 types of pancreatic tissue as mentioned above [122]. With increasing serial two-fold concentrations of either drug (MUG: 0.56 – 5 mM; HMR 1826: 6.25 – 400 μM) in incubation with tissue homogenates (2.25 μg total protein/50 uL, 30 minutes, 37°C for MUG; 1.13 μg total protein/50 μL, 2 hours, 37°C for HMR 1826), the increasing conversion to parent compound or active drug occurred by either a sigmoidal velocity curve or Michaelis-Menten-like kinetics. V_{max} for prodrug activation was highest

in pancreatic cancer tissue homogenate as compared to pancreatitis and healthy tissue for both drugs, indicating that the V_{max} values vary depending on the tissue type and their associated enzyme contents [122].

Activity levels of β-glucuronidase are dependent on reaction pH conditions as well as on temperature. In studies with human lung cancer and healthy lung tissue homogenate involving HMR 1826, it has been documented that enzymatic activity is about 15 times higher at pH 5.0 (1582 ± 190.2 nmol doxorubicin formed/hour/mg protein) than at physiological pH of 7.4 (100.0 ± 2.6 nmol doxorubicin/hour/mg protein). A nearly 5-fold increase in β-glucuronidase activity was seen at reaction pH 6.5, the pH of tumor tissue (466.8 ± 98.1 nmol doxorubicin/hour/mg protein) as compared to reaction at pH 7.5, which corresponds to extracellular tissue in healthy lung tissue (100.0 ± 2.6 nmol doxorubicin/hour/mg protein). Enzyme kinetic studies show V_{max} of β-glucuronidase activity to be an estimated 2-3 times greater in a reaction environment of pH 6.5 than at pH 7.5 [126].

Additionally, further studies show that temperature and pH conditions are factors that affect β-glucuronidase activity and the degree of enzymatic cleavage as well. The function of β-glucuronidase in pancreatic tissue of varying disease stages has been assessed based on reaction temperature at physiological pH [122]. Temperatures of 37°C (physiological) and 42°C (hyperthermia treatment) were used in the study. Their experiment results showed that increased β-glucuronidase cleavage of both MUG and HMR 1826 occurred at elevated temperatures (42°C) as compared to normal physiological temperatures. Enhanced release of parent compound MU and doxorubicin was observed at 42°C, and a linear correlation between temperature and levels of β-

glucuronidase activity and therefore parent drug released was even observed from 37°C to 57°C. Thus, hyperthermia treatment may be beneficial in terms of increased enzyme activity to enhance drug targeting and accumulation levels at the site of action. Overall, it can be concluded from these studies that temperature and pH conditions of the β-glucuronidase hydrolysis reaction has a significant effect on the activation of prodrugs, and that the acidic tumor microenvironment in the extracellular matrix plays a role in increasing the activity of β-glucuronidase.

Considering the correlation between β-glucuronidase expression with specific activity and the effect of pH conditions on enzyme activity, glucuronidated prodrugs are not only activated at greater enzyme levels due to increased β-glucuronidase expression, but the acidic microenvironment within the extracellular matrix of the tumor also serves to promote increased activity. In healthy normal tissue, marginal levels of β-glucuronidase plus physiological pH conditions yield minimal levels of enzymatic activity. In inflammatory and tumor tissue, however, increased levels of β-glucuronidase coupled with a lower pH in the tumor microenvironment work in tandem to increase specific activity levels.

Prodrug activation by β-glucuronidase alone is not only an effective means of prodrug delivery in itself, but there has also been evidence of glucuronide prodrug antitumor activity synergizing with targeting the tumor microenvironment for anti-angiogenesis. One study reported the use of a novel cell-impermeable, inactive glucuronide prodrug 9-aminocamptothecin glucuronide (9ACG) with antiangiogenic monoclonal antibody DC101 having a synergistic effect in limiting tumor cell growth and xenograft tumor growth [127]. These studies also showed the importance that immunity

plays in potentiating such synergy – treatments of 9ACG resulted in potent antitumor activity in human tumor xenografts of colon adenocarcinoma LS174T cells in Balb/c *nu/nu* nude mice immunodeficient in T-cells, whereas the same treatments in NOD/SCID mice deficient in immune cells such as macrophages and neutrophils bearing the same xenografted tumors showed minimal antitumor response. This is again suggestive of these immune cells playing a crucial role in liberating and activating β-glucuronidase in the extracellular matrix. When antiangiogenic DC101 was simultaneously administered with 9ACG, antitumor activity was further enhanced and survival of mice bearing resistant human tumor xenografts was prolonged, most likely due to the increased neutrophil infiltration and tumor vessel normalization that is associated with DC101 administration. These results show that not only is β-glucuronidase a key player in prodrug activation, but the activity can be further enhanced with the co-administration of other drugs that may alter the tumor microenvironment to induce greater immune cell infiltration.

1.14 Self-Microemulsifying Drug Delivery System (SMEDDS)

Oral drug administration is the primary route of administration for approximately 85% of all drugs sold in the United States and Europe [128]. Drugs can be divided into four classes according to the Biopharmaceutical Classification System (BCS) based on drug solubility and permeability:

Class I:	High Permeability and High Solubility
Class II:	High Permeability and Low Solubility
Class III:	Low Permeability and High Solubility
Class IV:	Low Permeability and Low Solubility

Curcumin is classified as a class IV drug that exhibits both low solubility and low permeability. Low solubility causes poor drug dissolution and low permeability leads to poor absorption through the gut wall. These factors, combined with the extensive first-pass metabolism of curcumin, contribute to its low systemic bioavailability.

Self-microemulsifying drug delivery systems (SMEDDS) have been utilized in previous studies to improve the oral bioavailability of hydrophobic compounds that have low solubility. SMEDDS typically consist of optically isotropic (i.e., has only one refractive index) mixtures of oil, surfactant, and co-surfactant that upon addition to aqueous media, form stable oil-in-water microemulsions. Microemulsions are transparent or translucent, isotropic colloidal dispersions that have low viscosity and are thermodynamically stable. SMEDDS present solubilized drugs in stable oil-in-water nanoemulsions of small droplet sizes (< 50 nm), which can be formed either by adding SMEDDS to an aqueous phase prior to dosing or with aqueous GI fluids upon administration [129]. Microemulsions improve the drug absorption by essentially improving drug dissolution [130-131].

Depending on the composition ratios of aqueous phase, surfactant, co-surfactant, and oil, a microemulsion can exist as one of three types: (1) water-in-oil (w/o) system, which consists of an aqueous phase dispersed in a continuous oil phase; (2) oil-in-water (o/w), where oil is the dispersed phase and water is the continuous phase; and (3) an oil

and water bi-continuous microemulsion in which the amount of oil and water present are equivalent [132]. Differences between microemulsions and emulsions are that while microemulsions form droplet sizes of less than 50 nm, are translucent, and form spontaneously, emulsions have larger droplet sizes (>200 nm), are opaque and turbid in appearance, and require external energy input to formulate. The translucency of a microemulsion is due to light being able to penetrate through without being scattered because of the smaller dispersed phase droplet sizes. Two major advantages of using microemulsions over emulsions in improving drug dissolution rate are that microemulsions are thermodynamically stable once formed and that an external force is not required for formation.

Microemulsion systems for pharmaceutical purposes are composed of surfactants, co-surfactants, and lipids that are generally regarded as safe (GRAS) by the FDA. Oils and lipids serve primarily to dissolve the drug and enhance drug absorption in the GI tract. Surfactants lower the interfacial tension between the two immiscible oil and aqueous phases, while co-surfactants are weaker surfactants that enhance the ability of the surfactant to further decrease surface tension. Lipids that are widely used in microemulsions include both natural oils, such as triglycerides (vegetable oils – palm, peanut, corn, olive), and synthetic oils, including ethyl oleate, isopropyl palmitate, Captex® 300, and Captex® 355 [133]. Commonly used surfactants are zwitterionic and nonionic, including hydrogenated castor oils and sucrose esters [134]. For co-surfactants, ethanol and mono- and di-glycerides are the most commonly employed in microemulsion formulations [135-136].

Examples of the clinical application of SMEDDS to improve drug bioavailability and commercially available microemulsions include ritonavir (Norvir®), saquinavir (Fortovase®), and cyclosporine (Sandimmune® and Sandimmune Neoral®). Cyclosporin A (CsA), a potent immunosuppressant widely used in organ transplantation to prevent rejection, is a prime example of a successful marketed drug microemulsion formulation to enhance bioavailability. Cyclosporine is highly lipophilic and has very poor solubility, and therefore has low bioavailability when orally administered. Patient-to-patient oral bioavailability was also highly variable because of such properties. Development of cyclosporine in a microemulsion formulation has shown positive results in dose proportion pharmacokinetic studies in greatly improving bioavailability and lowering inter-patient variability [137]. Despite such success with Cyclosporin A, however, large-scale commercialization of using the microemulsion formulation approach to enhance the oral bioavailability of lipophilic, low soluble drugs proves to be difficult. This is due to variability in the improvement of oral bioavailability from drug to drug, potential precipitation of the hydrophilic drug in a continuous aqeuous phase, and surfactant and co-surfactant use limitations.

Due to previous reports of success in microemulsions enhancing the bioavailability of low dissolution drugs, we chose this approach to increase drug absorption and therefore systemic bioavailability of curcumin. Studies in this thesis examining curcumin accumulation and efficacy, as well as parent drug and metabolite pharmacokinetics, utilized a curcumin SMEDDS formulation for oral administration.

1.15 Clinical Overview of Breast Cancer

The preventive and therapeutic effects of curcumin are wide ranging on a great number of inflammatory diseases including cancer; however, the focus of this thesis is to investigate the chemopreventive potential of curcumin against breast cancer. Breast cancer is the most common cancer among American women besides lung cancer, and in 2015, it is estimated that approximately 30% of new cancer diagnoses in women will be breast cancers – 231,840 new cases being invasive, and 60,290 new cases being non-invasive (*in situ* carcinoma). About 1 in 8 women (~12%) will develop invasive breast cancer in her lifetime, and as of this year, more than 2.8 million women in the U.S. have a history of breast cancer, which includes women who are either currently undergoing or have finished treatment [138-139]. Caucasian women are at a slightly higher risk for breast cancer than African-American women, though in women under 45, the disease is more prevalent in African-American women than Caucasian women. Overall statistics show African-American women having a higher mortality rate from breast cancer than any other ethnicity. Death rates have been decreasing since 1989 due most likely to advances in treatment, earlier detection, and increased awareness. Less than 15% of women diagnosed with breast cancer have a family member who has also had breast cancer, though a woman's risk of breast cancer doubles if an immediate relative such as a mother, sister, or daughter had been diagnosed [140].

The disease is caused by genetic mutations that are a result of environmental factors and lifestyle such as diet, exercise, and stress levels, rather than by inherited genetic predisposition – 85% of breast cancer patients have no family history of breast cancer. The exception, however, is the 5-10% of breast cancer cases that are linked to

inherited gene mutation, such as mutations of the BRCA1 and BRCA2 genes, which increases the lifetime risk of developing breast cancer to 45-65%. Ovarian cancer risk is also increased with mutations in these genes [141, 142]. Prognosis and treatment options are largely dependent on breast cancer type and stage at the time of diagnosis. In general, the 5-year relative survival rate is >90% when the disease is diagnosed in the initial stages (0 or I), but drops significantly when it is diagnosed in the more advanced invasive/metastatic stages (III and IV), which has a much lower survival rate at 5-years post-diagnosis (<20%) [143-145].

Breast cancer is the uncontrolled growth of breast epithelial cells, often referring to a malignant tumor that has formed from cells of the breast. A tumor can be either benign, which is non-invasive and therefore considered non-cancerous, or malignant, which is the invasive form that poses the danger of spreading to other parts of the body. Breast cancer most commonly originates in either the lobules, which are the milk-producing glands, or the ducts, the channels that carry milk from the lobules to the nipple. It is less common for breast cancer to begin in stromal tissue, which are the fatty and fibrous connective tissues that provide structure, support, and protection. Typical human mammary glands comprise of approximately 20 milk-secreting lobules, which are made up of milk-producing epithelial cells and myoepithelial cells. Development and function of the lobules and ducts is highly dependent on the hormonal levels of estrogen and progesterone [146]. As time passes, cancer cells have the potential to breach the basement membrane that is containing them *in situ*, intravasate into systemic circulation, and invade nearby healthy breast tissue or lymph nodes, which are small organs that serve to filter out foreign substances. Once in the lymph nodes, cancer cells can follow

circulation to other parts of the body, where extravasation and colonization at distant metastatic sites can occur [147].

The stage of breast cancer is a reference to the degree of how far the cancer cells have advanced beyond the primary tumor. Four characteristics determine cancer stage: cancer size, whether the cancer is invasive or non-invasive, whether cancer is present in the lymph nodes, and whether metastasis has occurred. Breast cancer stage can also be described as local (stages 0, I – cancer is confined within the breast), regional (stages I, II, III – lymph nodes are involved), or distant (stages III, IV – cancer has spread to other parts of the body) [148]. The following are the stages of breast cancer:

Stage 0: The cancer has been diagnosed early enough where it is still in its initial stages of developing in the breast ducts and has remained there – often termed *in situ*.

Stage I: Breast cancer cells start to become invasive, penetrating into either healthy fatty breast tissue or the lymph nodes.

Stage II: The cancer has either grown, spread, or both. Tumor size remains small, if there is one at all. There may be no cancer in the lymph nodes, or it may have spread to as many as three glands.

Stage III: Breast cancer is considered advanced at this point, but was diagnosed before it spread to bones and distant organs.

Stage IV: Cancer cells have metastasized to distant sites in the body, with the most common being in bones, lungs, liver, and brain.

Another important aspect of breast cancer that is highly considered in prognosis and treatment options is molecular subtype [149, 150]. While cancer subtype is now a major determinant of the appropriate therapeutic regimens in the clinic, breast cancer research in recent years have also actively focused on developing new therapies based on molecular subtype. The disease is divided into four major subtypes: luminal A, luminal B, triple negative/basal-like, and HER-2+ (Table 1.1).

Table 1.1: Breast Cancer Subtypes and Prevalence

Subtype	These tumors tend to be*	Prevalence (approximate)
Luminal A	ER+ and/or PR+, HER2-, low Ki67	40%
Luminal B	ER+ and/or PR+, HER2+ (or HER2- with high Ki67)	20%
Triple negative/basal-like	ER-, PR-, HER2-	15-20%
HER2 type	ER-, PR-, HER2+	10-15%

*These are the most common profiles for each subtype. However, not all tumors within each subtype will have all these features.

ER+ = estrogen receptor-positive

ER- = estrogen receptor-negative

PR+ = progesterone receptor-positive

PR- = progesterone receptor-negative

HER2+ = HER2/neu receptor-positive

HER2- = HER2/neu receptor-negative **[151-156]**

Prognosis and decisions for treatment options are primarily based on tumor stage and cancer subtype – that is, based on hormone (estrogen/progesterone) receptor status and HER-2/*neu* status. Tumors overexpressing estrogen and progesterone receptors (ER+ and PR+, respectively) are most often treated with hormone-based therapies [157]. Examples include Tamoxifen, Toremifene (Fareston®), and Fulvestrant (Faslodex®), which all act to block estrogen from binding to estrogen receptors in breast cancer cells and thereby inhibit cell growth and division [158]. HER-2+ type tumors, or tumors that are of cells overexpressing the human epidermal growth factor receptor 2 on their surface, are often treated with tyrosine kinase inhibitors (TKIs) along with other chemotherapeutic agents such as docetaxel, doxorubicin, cyclophosphamide, carboplatin, and paclitaxel [159, 160]. Trastuzumab (Herceptin®) is a monoclonal antibody that is widely used for treatment of HER-2+ breast cancer. Triple negative subtype, so called because it overexpresses neither hormone receptors nor HER-2 receptor, is rather difficult to treat, but has nonetheless proven to be responsive to radiation and chemotherapeutic treatments. Other less common subtypes include normal breast-like, apocrine molecular type, and claudin-low type. Breast cancers that do not fall into any of the above-listed subtype categories are often termed unclassified.

1.16 Models for Studying Breast Cancer *In Vivo*

Breast cancer is not one single disease, but rather a multitude of breast diseases that have diverse histopathological features, genetic variations, and a wide range of prognostic outcomes [161]. Due to the complexity of this heterogeneic disease, our knowledge of breast cancer biology and its effective treatment is limited by the

availability of experimental model systems that mimic the typical stages of tumor development in humans. Despite this challenge, significant advances in knowledge have been made with xenograft and transgenic models. Both orthotopic xenograft and genetically engineered mouse (GEM) models have their strengths and limitations in contributing to the better understanding of breast cancer. Orthotopic human tumor xenografts best predict drug effects and response in human tumors, while transgenic models are best used for investigating the role of specific genes in tumorigenesis in an immunocompetent environment.

1.16.1 Xenograft Models

Human tumor xenograft models have been widely employed to investigate the malignant transformation of tumorigenesis – invasion and metastasis – and response to therapy based on specific tumor type [162]. In xenograft models, human tumor cells are transplanted directly either under the skin (subcutaneous) or into the type of organ of tumor origin (orthotopic) in immunocompromised mice. Xenografts of cells from one species into a different species (i.e., human cells into a mouse) require the host species to be immunocompromised so as to not reject the cells from another species.

Immunocomprised mice that are used in xenografts include athymic nude mice and severely compromised immunodeficient (SCID) mice, as well as other types of immunocompromised mice, such as nonobese diabetic/severely compromised immunodeficient (NOD/SCID) mice. Athymic nude mice lack a thymus and therefore are unable to produce T cells. In animals homozygous for the SCID mutation, T and B cell

lymphocyte development is impaired, and in NOD/SCID mice, natural killer (NK) cell function is deficient in addition to lacking T and B cells [163].

Direct injection of breast cancer cells into the mammary glands of mice is termed as an orthotopic xenograft. Cells can also be injected intravenously by tail vein injection to study the effects of cell colonization and treatment at common metastasis sites, such as the lungs, brain, liver, lymph nodes, and bones. Studies that investigate the treatment effects on primary tumor would benefit most from subcutaneous or orthotopic xenografts; for metastatic studies involving characterization of circulating tumor cells and treatment of metastatic tumors, intravenous injection of cells would be the preferred route of inoculation due to the direct administration of cells into the systemic circulation.

A wide array of breast cancer cell lines is available for both *in vitro* and *in vivo* studies. These cell lines range greatly in terms of genetic profile, and are representative of the heterogeneity of human patient tumors [164, 165]. Cell lines are characterized based on their syngeneity to type of species (i.e., mouse or human), cell type (i.e., epithelial), tissue (i.e., mammary or breast), morphology (i.e., epithelial), and sub-type (i.e., ER/PR+, HER-2 overexpressed, or triple negative in the case of breast cancer). Selecting cell lines for their specific properties and phenotypes is important in understanding the functionalities and treatment responses to that specific group or subtype of disease.

A major disadvantage to xenograft models is that mice are immunocompromised and therefore the tumor microenvironment is not a true representation of patient tumors, where the immune system plays a crucial role in tumorigenesis. Tumor cells are already tumorigenic prior to injection, and so the initiation stages and treatment options at these stages cannot be examined. Furthermore, there are genetic differences between the cells

cultured *in vitro* for xenograft as compared to cells that are of the primary tumor in the clinic, and so results from treating xenografted tumors may be different than the results of that same treatment in the clinic [161].

Direct transplantation of primary human tumor cells into immunocomprimised mice (patient-derived xenografts; PDX), however, offers several advantages. Direct orthotopic xenografts can predict response of the tumor cells to specific drugs in a human patient, as well as provide a realistic representation of the complex heterogeneity of tumor cells in the mouse model. Moreover, these models can rapidly predict a human tumor response to a given therapeutic regime based on the observed results.

1.16.2 Transgenic Models

Transgenic models are widely employed for studying human diseases and their treatments. GEM contribute extensively to understanding the genes involved in the promotion and progression of breast cancer. Transgenic models are produced by either overexpressing an oncogene or suppressing a tumor suppressor gene, allowing for the study of specific treatments for certain genotypes [161]. One key advantage of such models is that treatments can be studied from the initiation stage of tumorigenesis, unlike in xenograft models. Gene expression specific to the mammary tissue can be generated using mouse mammary tumor virus long terminal repeat (MMTV-LTR) and whey acidic protein (WAP) promoters [166]. Oncogenes such as *Erbb2*, *Myc*, *Ccnd1* (encoding cyclin D1), polyoma virus middle T (PyMT), and *Hras*, and tumor suppressor genes such as *Trp53*, *Brca1*, and *Pten* (phosphatase and tensin homologue) have been modified to create various transgenic models specific to breast cancer [166-169].

There are several advantages and disadvantages to using transgenic models for studying the treatment effects of breast cancer. The advantages of working with GEM include: (1) many genetic backgrounds and specific abnormalities can be analyzed by using several strains of mice; (2) tumorigenesis can be monitored from the initial stages of development and so a variety of therapeutic approaches can be studied at each stage; (3) mutations closely relate to those found in human tumors; and (4) the tumor is present in an immunocompetent environment, which mimics a realistic tumor microenvironment. Disadvantages to these models are: (1) only a limited number of genes are targeted in GEM and so the complex heterogeneity of human tumors cells and the microenvironment is not mirrored; (2) development of such models are expensive and the time required for experimental work is much longer; (3) tumor development is highly variable; and (4) since GEM are still mouse tumors, it is difficult to predict the outcomes of a similar treatment on human tumors, and so the translation of response from mouse to the clinic may be limited [170].

1.16.2.1 Balb-*neu*T

To incorporate a more realistic mouse model that closely mimics what occurs clinically with HER-2+ breast cancer, the Balb-*neu*T transgenic mouse model was employed for both *in vitro* and *in vivo* studies in this thesis. The Balb-*neu*T model is a genetically engineered mouse model that overexpresses an activated form of the rat HER-2/*neu* oncogene driven under the transcriptional control of the mouse mammary tumor virus (MMTV) promoter/enhancer. The mutated gene encodes a single point mutation at position 664 in the transmembrane domain of p185/*neu* in which a valine residue is

replaced with glutamic acid. This point mutation promotes both the homo- and heterodimerization of p185/*neu* and transforms the HER-2/*neu* proto-oncogene into a dominant transforming oncogene. Early onset of HER-2/*neu* transgene expression in the mammary epithelium of female Balb/c mice was associated with development of tumors in the entire mammary epithelium. Both the developmental stages of tumorigenesis and tumor histology of the model closely resemble that found in HER-2+ breast cancer in human patients.

In the Balb-*neu*T model, autochthonous mammary tumors that originate in the lobules of the mammary gland begin forming from a single cell and develop over several months. At 3-4 weeks of age, female Balb-*neu*T mice exhibit hyperplasia in the terminal lobular buds. Microvessels then increase in both number and density at age 4-6 weeks due to correspondingly higher levels of pro-angiogenic factors such as VEGF and FGF [171]. By 8-12 weeks, *in situ* carcinoma is established and by 16 weeks of age, the disease progresses to invasive lobular carcinoma in which the tumor is no longer locally confined, and can potentially metastasize to other regions of the body. At least one palpable tumor can be detected by 16-20 weeks; by 28 weeks, all ten mammary glands have palpable tumors.

In addition to tumorigenesis being primarily driven by the overexpression of HER-2/*neu* oncogene, inflammation also plays a major role in this model. Pro-inflammatory cytokines such as TNF-α and interleukins (i.e., IL-1β) were found to be increasingly overexpressed in Balb-*neu*T mice that were advancing from *in situ* carcinoma to invasive lobular carcinoma (12-16 weeks of age). These cytokines are important in activating the NF-κB pathway, in which activated NF-κB regulates gene

expression within the nucleus to promote inflammation [172]. Vasculature and microvessel growth factors within the tumor microenvironment of female Balb-*neu*T mice also decrease at the invasive lobular carcinoma stage (16 weeks) as compared to those in the initial hyperplastic stage of tumorigenesis. This is indicative of angiogenesis being most important in the onset of tumor development, and that the formation of new blood vessels decreases at later stages of the disease.

1.17 Innovation

The tumor-specific enzymatic activation hypothesis is highly innovative, because it explains, for the first time, how relatively non-toxic, dietary molecules can help reduce the occurrence of cancer despite their poor oral bioavailability. This hypothesis also points to an attractive strategy to target chemopreventive agents specifically to the tumor site following oral administration. That is, approaches that can improve plasma concentrations of the glucuronide metabolite will allow for tumor-targeted delivery of the active parent compound. A number of clinical trials have been conducted with very high oral doses of curcumin (up to 12 g/dose) [67]. Such trials have generally been considered as failures because these high doses failed to achieve effective plasma concentrations of curcumin [173]. The prodrug hypothesis would suggest that these studies should evaluate plasma concentration of curcumin glucuronide as an indicator of efficacy rather than that of curcumin.

Because many other natural chemopreventive agents undergo glucuronidation [6], the research presented in this thesis here will provide a model for studies with other dietary agents for chemoprevention. Also, since upregulation of β-glucuronidase activity

is observed generally during inflammation [174], this research is expected to impact a wide array of inflammatory diseases.

1.18 Statement of Problem and Hypothesis

Curcumin has been shown to modulate multiple oncogenic signaling pathways [175]. Epidemiological studies attribute low incidence of certain types of cancers in specific populations to the chemopreventive and antioxidant properties of diets rich in curcumin [176, 177]. In general, the numerous therapeutic effects of curcumin make it a strong candidate for cancer chemoprevention; the polyphenol, however, has poor bioavailability after oral dosing [72, 87]. This raises an interesting question: *how does dietary curcumin exhibit chemopreventive activity despite not being absorbed into the systemic circulation in its active form?* The objective of this thesis project is to investigate the mechanisms behind this 'bioavailability paradox'.

Overexpression of β-glucuronidase and increased enzyme activity in the tumor tissue in comparison to its relatively minimal activity in normal cells could potentially explain the bioavailability paradox with curcumin and other chemopreventive agents. ***We propose that curcumin glucuronide is an inflammation-responsive natural prodrug that gets converted back to curcumin 'on-demand'***. In the absence of inflammation, curcumin would undergo extensive glucuronidation, and the inactive glucuronides will be excreted rapidly through renal clearance. However, in the presence of tissue inflammation (a common feature of many pathologies including cancer), β-glucuronidase is upregulated. This enables the regeneration of the active parent compound at the site of inflammation. Curcumin is a highly lipophilic molecule capable of tissue accumulation

[26]. Thus, prolonged dietary consumption of curcumin can result in a slow but significant accumulation of curcumin at sites of inflammation, enabling its chemopreventive activity. This hypothesis also explains how large oral doses of curcumin do not cause toxicity – water-soluble glucuronide cannot cross membrane barriers and is cleared rapidly from the body.

1.19 Research Objectives

The specific aims and objectives of this research project were the following:

1. Determine the relationship between disease stage/tumor subtype and β-glucuronidase activity in human and mouse mammary tumors
2. Investigate the role of β-glucuronidase activity in the chemopreventive efficacy of oral curcumin
3. Evaluate the pharmacokinetics of curcumin and curcumin glucuronide in wild-type and tumor-bearing mouse models

Chapter II

Materials and Methods

2.1 Materials

Curcumin powder from *Curcuma longa* (Turmeric), high purity (analytical grade) curcumin (≥94% curcumin content), 4-Nitrophenyl β-D-glucuronide (≥98%), 4-nitrophenol, D-saccharic acid 1,4-lactone (saccharolactone), β-glucuronidase (*Helix pomatia)*, and anhydrous dimethyl sulfoxide (≥99.9%) were purchased from Sigma-Aldrich (St. Louis, MO). Acetonitrile and methanol were purchased from Fisher Scientific (Pittsburgh, PA). Anti-β-glucuronidase antibody (ARP44234_T100) was purchased from Aviva Systems Biology (San Diego, CA). HRP-linked anti-rabbit IgG was purchased from Cell Signaling Technology (Beverly, MA). Anti-β-actin was purchased from Sigma-Aldrich. An activity-based near-infrared glucuronide trapping probe for imaging β-glucuronidase expression and activity *in vivo* was kindly provided by Dr. Yu-Ling Leu (Department of Pharmacy, Chia Nan University of Pharmacy and Science, Tainan, Taiwan).

2.2 Cell Lines

MDA-MB-231 and MDA-MB-231 LM2 human mammary adenocarcinoma cells, stably transfected with luciferase, were purchased from Caliper Life Sciences. 4T1 mouse mammary gland tumor cells (ATCC CRL-2539), JC mouse mammary adenocarcinoma cells (ATCC CRL-2116), MCF-7 human mammary adenocarcinoma cells (ATCC HTB-22), and SkBr3 human mammary adenocarcinoma cells (ATCC HTB-30) were purchased from the American Type Culture Collection. TuBo mouse mammary gland tumor cells, derived from a spontaneous mammary tumor which arose in a Balb-*neu*T transgenic mouse expressing a transforming rat *neu*, were kindly provided by Dr. Wei-Zen Wei

(Barbara Ann Karmanos Cancer Institute, Wayne State University, Detroit, MI). MDA-MB-231, MDA-MB-231 LM2, 4T1, and JC cells were cultured at 37°C in a humidified atmosphere containing 5% CO_2 with RPMI 1640 (Corning Cellgro, Manassas, VA) supplemented with 10% FBS and 1% penicillin/streptomycin. MCF-7 cells were cultured with Eagle's Minimum Essential Medium (MEM) (Corning Cellgro, Manassas, VA) supplemented with 10% FBS and 1% penicillin/streptomycin. TuBo and SkBr3 cells were cultured with Dulbecco's modified Eagle medium (DMEM) (Corning Cellgro, Manassas, VA) supplemented with 10% FBS and 1% penicillin/streptomycin.

2.3 Animals

In vivo studies were conducted in wild-type Balb/c, transgenic Balb-*neu*T, and athymic immunocompromised nude mice (National Cancer Institute). Balb-*neu*T and Balb/c mice were bred as described previously [178, 179]. Genotyping using tail snips collected at 1-3 weeks of age was performed by Transnetyx Inc. (Cordova, TN). All animals were 8 to 12 weeks old at the time of the experiment. All mice were maintained under a 12-hour light/dark cycle, given access to food and water *ad libitum*, and were maintained under a temperature-controlled environment. All studies and protocols were approved by the Institutional Animal Care and Use Committee of the University of Minnesota.

2.4 Self-Microemulsifying Drug Delivery System (SMEDDS)

The SMEDDS formulation chosen for all studies was Cremophor® EL – Carbitol^{TM} – Captex® 355 (surfactant, co-surfactant, oil) at a 6:3:1 ratio. Cremophor®

EL and Carbitol™ were initially mixed in a 2:1 w/w, surfactant-to-cosurfactant ratio, followed by mixing with Captex® 355 at a 10:1 w/w, surfactant-to-oil ratio. The resulting formulation was the 'Blank SMEDDS' formulation. 30 mg of curcumin from *Curcuma longa* was solubilized in 1 gram of Blank SMEDDS to generate the 'Curcumin SMEDDS' formulation used in the oral dosing studies.

2.5 β-Glucuronidase Activity Assays

Enzymatic activity assay in various cell lines consisted of intact, viable cells and cell lysates that were prepared by the freeze-thaw method, with freezing being at -80°C for 1 hour. Intact MDA-MB-231 cells were cultured in hypoxic conditions (< 5% O_2) for 96 hours prior to the assay. For orthotopic tumor models, tumor cells were injected into mammary fat pad #4 and tumors were allowed to grow to 100, 400, 700 and 1200 mm^3 in separate cohorts of mice. When the desired volume was reached, mice were euthanized and the tumor tissues were collected and processed for β-glucuronidase assay. In female wild-type Balb/c and transgenic Balb-*neu*T mice, mammary tissue and spontaneously forming tumors were collected at 3 weeks (normal), 6 weeks (atypical mammary hyperplasia), 10 weeks (carcinoma *in situ*), 16 weeks (invasive lobular carcinoma), and 23 weeks (metastases) of age, with each age group representing the various stages of tumorigenesis. All tissues were stored at -80°C. Tumors were homogenized in distilled water using a handheld tissue homogenizer (Omni International, Kennesaw, GA). To measure enzymatic activity, the conversion rate of 4-Nitrophenyl β-D-glucuronide (NPG) to 4-Nitrophenol (NP) was monitored (Figure 2.1). Intact cells and cell lysates were incubated with NPG for 2 hours at 37°C, and intact MDA-MB-231 cells subjected to

hypoxia were incubated with NPG for 1 and 3 hours at 37°C. Tumor homogenates with an initial NPG concentration of 20 µg/mL were incubated in a water bath at 37°C and samples were collected at 0, 1, 2, 3, and 4 hours. Ice cold acetonitrile (4:1 v/v) was added to the samples to stop enzymatic activity at each time point. Samples were centrifuged for 8 minutes at 14,000 rpm, and NPG and NP concentrations in the supernatant were determined by HPLC.

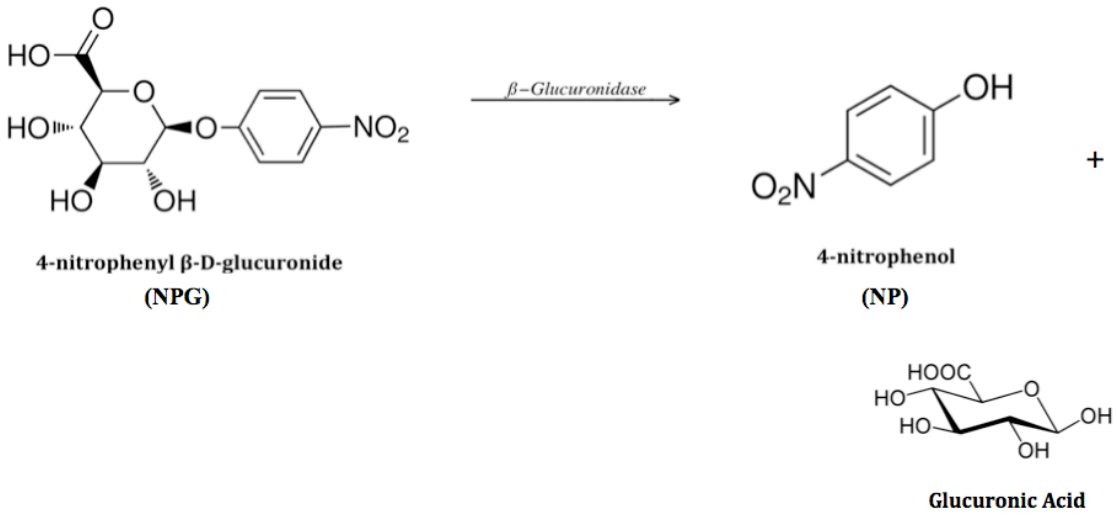

4-nitrophenyl β-D-glucuronide (NPG)

4-nitrophenol (NP)

Glucuronic Acid

Figure 2.1. 4-Nitrophenyl β-D-Glucuronide (NPG) Conversion to 4-Nitrophenol (NP) by β-Glucuronidase.

2.6 *In Vivo* Chemopreventive Efficacy of Curcumin Formulations

Female virgin Balb/c *nu/nu* and athymic nude mice (National Cancer Institute) were used in these studies. Mice were randomized into three groups of six animals each. In the first group, mice were orally dosed (100 μL) with 100 mg/kg of curcumin SMEDDS formulation. The second group of mice was dosed with 100 μL of blank SMEDDS formulation, and the third group of mice remained untreated. Oral gavage treatments began one day prior to injection of tumor cells. Tumor cells were suspended in cell growth medium (10^6 cells/0.1 mL/mouse) and injected into the fourth mammary fat pad of the mice. Tumor size was measured using Vernier calipers and mice were weighed on alternate days throughout the study. Volume was calculated using the formula $V = (L \times W^2)/2$, where length (L) and width (W) of the tumor are the longest and shortest diameters, respectively. Mice were euthanized at the end of the study, and a portion of the tumor tissue collected was fixed with 10% phosphate-buffered formalin for histology while the other portion was frozen at −80°C. Formalin-fixed tissues were switched to 70% ethanol after 24 hours.

2.7 Curcumin and Curcumin Glucuronide Pharmacokinetics in Tumor-Bearing and Wild-Type Mice

The pharmacokinetics of curcumin and curcumin glucuronide was evaluated in Balb/c mice bearing 4T1 or TuBo tumor, following either oral dosing of curcumin SMEDDS or intravenous (tail vein) injection of curcumin glucuronide. 4T1 and TuBo models were selected for their high and low specific activity levels of β-glucuronidase, respectively (see data section). For the oral dosing study, mice were randomized into two

groups of fifteen animals each. The first group of mice was injected with 4T1 tumor cells (10^6 cells/0.1 mL/mouse) suspended in cell growth medium into the fourth mammary fat pad. The second group received TuBo tumor cell injections in the same manner. Tumors were grown to a volume of 400 mm^3 in size, at which mice were administered a single oral dose of curcumin SMEDDS (100 mg/kg curcumin). Animals were euthanized at 0.5, 1, 2, 4, and 8 hours (n = 3 per time point) post oral administration, and plasma, tumor, lung, liver, and kidneys were collected.

For intravenous dosing of curcumin glucuronide, mice were randomized into two groups of twenty-one mice. Mice were injected with 4T1 tumor cells in one group and TuBo cells in the other group as described above. Tumors were grown to a volume of 400 mm^3 in size, at which mice were administered a single intravenous dose of curcumin glucuronide (2 mg/kg) by tail vein injection. Animals were euthanized at 0.25, 0.5, 1, 2, 4, 8, and 24 hours (n = 3-5 per time point per group) post intravenous administration, and plasma, tumor, lung, liver, and kidneys were collected. All plasma and tissues were stored at -80°C until further processing.

For curcumin and curcumin glucuronide analysis, tissue samples were homogenized in 2 mL of distilled water using a handheld homogenizer (Omni International, Kennesaw, GA) and then lyophilized for 48 hours (Labconco, Kansas City, MO). Curcumin and curcumin glucuronide were extracted from dried tissues with 2 mL methanol for ~18 hours at room temperature on a rotary extractor. Acetonitrile was added to thawed plasma (1:4 v/v, plasma to acetonitrile) without prior processing. Tissues samples were centrifuged at 4,000 rpm for 10 minutes, and tissue supernatant and plasma samples were dried under nitrogen stream. Curcumin and curcumin glucuronide were

reconstituted with 0.3 mL acetonitrile. Samples were centrifuged at 14,000 rpm for 8 minutes to rid samples of tissue debris, and final supernatant was analyzed by LC-MS/MS to determine drug concentrations.

Curcumin and curcumin glucuronide pharmacokinetics was also evaluated in wild-type Balb/c mice following curcumin glucuronide tail vein intravenous injection. Our aim in using wild-type Balb/c mice was to investigate curcumin and curcumin glucuronide levels in lung and liver tissue in a non-tumor bearing mouse model. Mice were administered a single intravenous dose of curcumin glucuronide by tail vein injection at 2 mg/kg. Animals were euthanized at 0.25, 0.5, 1, 2, 4, 8, and 24 hours (n = 3-4 per time point) post intravenous administration, and plasma, mammary gland, lung, and liver were collected. All plasma and tissue were stored at -80°C until processing. Curcumin and curcumin glucuronide concentrations were analyzed by LC-MS/MS.

Stability of curcumin and curcumin glucuronide during the extraction and the efficiency of extraction were determined by spiking tissues and plasma from untreated animals with 2 μg of each compound dissolved in DMSO prior to lyophilizing, followed by extraction and analysis of curcumin and curcumin glucuronide as described above. Extraction efficiency was calculated as a percent of curcumin and curcumin glucuronide recovered from the spiked tissues. Calculated extraction efficiencies in plasma, mammary tumor, lung and liver are displayed in Tables 2.1 and 2.2.

Table 2.1. Extraction Efficiencies of Curcumin from Plasma, Tumor, Lung, and Liver.

Extraction Efficiency of Curcumin	
Plasma	**89%**
Tumor	**30%**
Lung	**32%**
Liver	**18%**

Table 2.2. Extraction Efficiencies of Curcumin Glucuronide from Plasma, Tumor, Lung, and Liver.

Extraction Efficiency of Curcumin Glucuronide	
Plasma	**36%**
Tumor	**23%**
Lung	**12%**
Liver	**5%**

2.8 Curcumin Accumulation in Transgenic and Orthotopic Models

Mammary tumors from female virgin transgenic Balb-*neu*T mice and Balb/c mice bearing orthotopic JC, TuBo, 4T1 or no tumors were used to evaluate the accumulation of curcumin in tumor. JC and TuBo tumors were collected from the month-long oral dosing efficacy studies and used for these studies. The 4T1 model was selected for its high specific activity levels of β-glucuronidase (see data section). The first group of mice was injected with 4T1 tumor cells (10^6 cells/0.1 mL/mouse) suspended in cell growth medium into the fourth mammary fat pad. The second group did not receive cell injections and served as the control group (n = 5-6 per group). Both groups of mice were dosed with oral curcumin SMEDDS (100 μL) at 100 mg/kg once the tumor-bearing mice reached tumor volumes of 400 mm^3. Daily oral dosing of the curcumin SMEDDS formulation was administered for 14 consecutive days. On the last day of the study, mice were euthanized at 1 hour post-dose, plasma and tumors were collected and stored at -80°C until further processing. To extract drug from plasma, acetonitrile was first added to thawed plasma (1:4 v/v, plasma to acetonitrile) to precipitate proteins. Plasma samples were centrifuged at 14,000 rpm for 8 minutes, and the supernatant was used directly for LC-MS/MS analysis. For other tissues, samples were weighed and homogenized in 2 mL of distilled water using a handheld homogenizer (Omni International, Kennesaw, GA), followed by lyophilization for 48 hours (Labconco, Kansas City, MO). Methanol was used to extract curcumin from dried tissues for ~18 hrs at room temperature on a rotary extractor. Tissues samples were centrifuged twice, first at 4,000 rpm for 10 minutes and then at 14,000 rpm for 8 minutes to eliminate any tissue debris from samples. Final supernatant was used directly for LC-MS/MS analysis of curcumin.

2.9 Cell Cytotoxicity Studies

Cells were seeded in 96-well plates at a seeding density of 5,000 per well/100 μL medium and incubated in 5% CO_2 at 37°C. Following attachment, cells were treated with 0.1 to 25 μmol/L curcumin dissolved in the growth medium (using 0.1% DMSO) for 72 hours. Fresh medium containing curcumin was added every day. Cell viability was measured using MTS assay. The formazan product formed was quantified by measuring the absorbance at 490 nm using a microplate reader (ELx800, BioTek Instruments). The mean absorbance for each treatment was determined and then expressed as percent viability relative to control (0.1% DMSO-treated group). IC50 values were calculated using GraphPad Prism software version 5.01 (GraphPad Software, Inc., La Jolla, CA).

2.10 Western Blotting

Tumors were homogenized in distilled water using a handheld tissue homogenizer (Omni International, Kennesaw, GA). Samples were incubated at 4°C overnight, followed by centrifugation at 14,000 rpm for 8 minutes at 4°C. Protein concentrations in the supernatant were analyzed by bicinchoninic acid (BCA) assay (Thermo Scientific), with bovine serum albumin as the standard. Protein samples (50 μg) were loaded onto 4% - 15% SDS-PAGE gel (Bio-Rad Laboratories) and, after electrophoresis, transferred onto a nitrocellulose membrane (Whatman) using a Criterion blotter (Bio-Rad Laboratories). The membrane was blocked with 5% non-fat dry milk in PBS-Tween 20 (PBST), pH 7.4, for 1 hour and incubated with primary antibodies against β-glucuronidase (Aviva Systems Biology, San Diego, CA) or β-actin (Sigma-Aldrich) in 5% non-fat dry milk in PBST overnight at 4°C. After three 10-minute washes with 0.1% PBST, the membrane

was incubated with secondary anti-rabbit IgG conjugated with horseradish peroxidase (Cell Signaling) in 5% non-fat dry milk in PBST for 1 hour and then washed thrice again with 0.1% PBST. The transferred proteins and band intensities were visualized using SuperSignal West Pico Chemiluminescent Substrate (Thermo Scientific). For densitometric quantification, immunoblots were digitized on a flat bed scanner and the signal intensities of the visualized bands were quantified using ImageJ and OriginPro 8.1 (Northampton, MA) software. β-actin served as a loading control. Relative normalized expression was calculated by dividing the signal intensity of each band by the staining intensity of β-actin in the corresponding lane.

2.11 *In Vivo* Fluorescence Imaging of β-Glucuronidase Activity

Athymic immunocompromised nude mice (National Cancer Institute) bearing MDA-MB-231 LM2 (also referred to as LM2) were used to correlate the levels of β-glucuronidase activity according to stage of tumorigenesis. LM2 cells, a derivative of MDA-MB-231 human mammary adenocarcinoma cells, were selected for their ability to metastasize to lung tissue *in vivo* [186]. Tumor cells were suspended in cell growth medium (10^6 cells/0.1 mL/mouse) and injected into the fourth mammary fat pad of virgin female mice. Tumor size was monitored on alternate days throughout the study. Fluorescence imaging was carried out on a Caliper LifeScience (Hopkinton, MA) IVIS® Spectrum Instrument when tumor volume reached 100, 400, 700, and 1200 mm^3. Mice were intravenously injected with 100 μg of NIR-TrapG/mouse in 100 μL of 1X DPBS at 24 hours prior to imaging. NIR-TrapG, an activity-based NIR-fluorescent difluoromethylphenol-glucuronide probe [180], has λ_{ex} = 710 nm and λ_{em} = 780 nm. Data

was analyzed using LivingImage® software. Quantification of the fluorescence was performed using ImageJ software (Bethesda, MD).

2.12 Immunohistochemistry to Evaluate β-Glucuronidase Expression

Immunohistochemistry studies with a human breast carcinoma tissue microarray (BRC-961, US Biomax, Rockville, MD) were performed to validate the clinical relevance of β-glucuronidase overexpression in chemoprevention by curcumin. BRC-961 consists of 96 sample cores representing normal, non-malignant human breast tissue and breast carcinoma tissue that range in disease stage (normal tissue, benign tumor, hyperplasia, in situ carcinoma, malignant tumor) and sub-type (HER-2+, ER/PR+, triple negative). Sample cores were stained with anti-β-glucuronidase antibody (Aviva Systems Biology, San Diego, CA), and β-glucuronidase positive staining was detected with EDTA. Stained sample cores were evaluated under an optical microscope at x400 magnification, and staining intensity of each core was quantified using ImageJ software (Bethesda, MD). Percentage of sample core stained was correlated directly with β-glucuronidase expression.

2.13 Immunohistochemistry to Evaluate Curcumin Effects on Ki-67, CD-31, and Cleaved Caspase-3 Levels

Female athymic nude mice bearing MDA-MB-231 xenografted tumors were orally dosed once daily for two months with blank SMEDDS, curcumin SMEDDS, or remained untreated as described above. Mice were sacrificed when tumor volumes reached 1200 mm^3 and mammary tissue was collected. Tumor samples were fixed in 10%

phosphate-buffered formalin for 24 hours and subsequently transferred to 70% ethanol. Tissue processing and staining for Ki-67, CD-31, and cleaved caspase-3 were carried out by the Comparative Pathology Shared Resource at the University of Minnesota. All the samples were received by the Comparative Pathology Shared Resource laboratory in 70% v/v ethanol/water, and processed accordingly for routine histology and embedded in paraffin. Samples were cut into 4 μm sections, and after deparaffinization, sections were stained with antibodies against Ki-67, CD-31, and cleaved caspase-3. Abnormal tissue areas (lobular hyperplasia, carcinoma *in situ*, and invasive carcinoma) were measured in 40x magnification photographs using ImageJ software (Bethesda, MD). Ki-67, CD-31, and cleaved caspase-3 staining were quantified by taking 15 unique 400x images per tissue and using ImageJ software to measure the staining intensity of each image. Results are presented as average percent of tissue stained for each biomarker, and staining intensity was correlated directly with levels of Ki-67, CD-31, and cleaved caspase-3 expression. Staining in the central necrotic region of the tumor was excluded from analysis.

2.14 HPLC Analysis

All HPLC analyses were performed using a Beckman Coulter HPLC system attached to UV-PDA and fluorescence (Jasco, Easton) detectors. Sample injection volume was 50 μL for all analytes.

4-nitrophenol (NP) and 4-nitrophenyl β-D-glucuronide (NPG). The mobile phase consisted of 10 mM ammonium acetate buffer adjusted to pH 4.0 using glacial acetic acid (A) and acetonitrile (B) running at a flow rate of 1.0 mL/min. The composition of the

mobile phase was 45:55 v/v, A:B. Compounds were separated using the Scherzo SM C-18 column (Imtakt). NPG (λ_{max} = 302 nm) eluted at 3.9 min and NP (λ_{max} = 314 nm) eluted at 3.2 min. Total run time was 6 minutes. NPG and NP produced linear standard plots over the concentration range of 0.625 – 20 μg/mL with $R^2 > 0.998$ (Figure 2.3).

Curcumin. The mobile phase consisted of 10 mM ammonium acetate buffer adjusted to pH 4.0 using glacial acetic acid (A) and acetonitrile (B) running at a flow rate of 1.0 mL/min. Composition varied as such: 0 min. 20% B, 0-2 min. 20-70% B, 2-4 min. 70% B, 4-8 min. 70-20% B, 8-9 min. 20% B. The column used was Eclipse XDB C-18 (150 x 4.6 mm, 5 μm) with an Agilent Zorbax cartridge guard column (C-18, 12.5 x 4.6 mm). Analytical grade curcumin (retention time, 7.8 min) was detected using a UV-Vis detector (excitation λ_{max} = 430 nm). Curcumin produced a linear standard plot over the concentration range of 0.015 – 1 μg/mL with $R^2 > 0.999$ (Figure 2.2).

2.15 LC-MS/MS Analysis

All LC-MS/MS analyses were performed using an Agilent Technologies 1200 series system with negative ESI connected to a TSQ Quantum system (Agilent Technologies, coupled to Finnigan TSQ Quantum Discovery Max triple quadrupole detector, Thermo Electron). Sample injection volume was 5 μL for all analytes.

Curcumin and curcumin glucuronide. The mobile phase consisted of (A) 0.1% formic acid and (B) acetonitrile. Separation was achieved on an Agilent XDB-C18 column (50 mm x 4.5 mm internal diamater, 1.8 μm particle size), fitted with an Agilent Zorbax cartridge guard column (C-18, 12.5 x 4.6 mm). Linear gradient flow (0.5 mL/min) with a total run time of 9 min was used: 0-0.5 min: 25% B, 0.5-2.9 min: 25-

100% B, 2.9-4.9 min: 100% B, 4.9-5.5 min: 100-25% B, 5.5-9 min: 25%. Samples were analyzed in positive ion mode. Analytical grade curcumin and curcumin glucuronide were monitored using single reaction monitoring of the 369.1 to 176.0 and 545.2 to 368.1 transitions, respectively. Retention times of curcumin glucuronide and curcumin under these conditions were 4.25 and 5.03 minutes, respectively. The chromatographic data were acquired and analyzed using Xcaliber software (Thermo Scientific). Curcumin produced a linear standard plot over the concentration range of 0.005 – 2.5 μg/mL with $R^2 > 0.996$ (Figure 2.4), and curcumin glucuronide produced a linear standard plot over the concentration range of 0.005 – 10 μg/mL with $R^2 > 0.992$ (Figure 2.5).

2.16 Determination of Pharmacokinetic Parameters

Non-compartmental analysis of the drug concentrations was performed using Phoenix WinNonlin software version 6.3 (Pharsight, St. Louis, MO). Pharmacokinetic parameters for curcumin and curcumin glucuronide disposition were obtained from the concentration-time profiles of plasma and tumor tissue in both the TuBo and 4T1 models. The area under the concentration-time curve ($AUC_{0-\infty}$) for plasma and tumor were calculated using the trapezoidal method. The terminal half-life ($t_{1/2}$) was determined by using the following equation:

$$t_{1/2} = \frac{0.693}{k}$$

The terminal rate constant (k) was calculated using Phoenix WinNonlin 6.3.

2.17 Statistical Analysis

Statistical analyses of observed differences between two groups were performed using Student's two-sample t-test. Comparisons between more than two groups were performed using ANOVA followed by Newman-Keuls' testing, with a probability level of $p < 0.05$ being considered statistically significant.

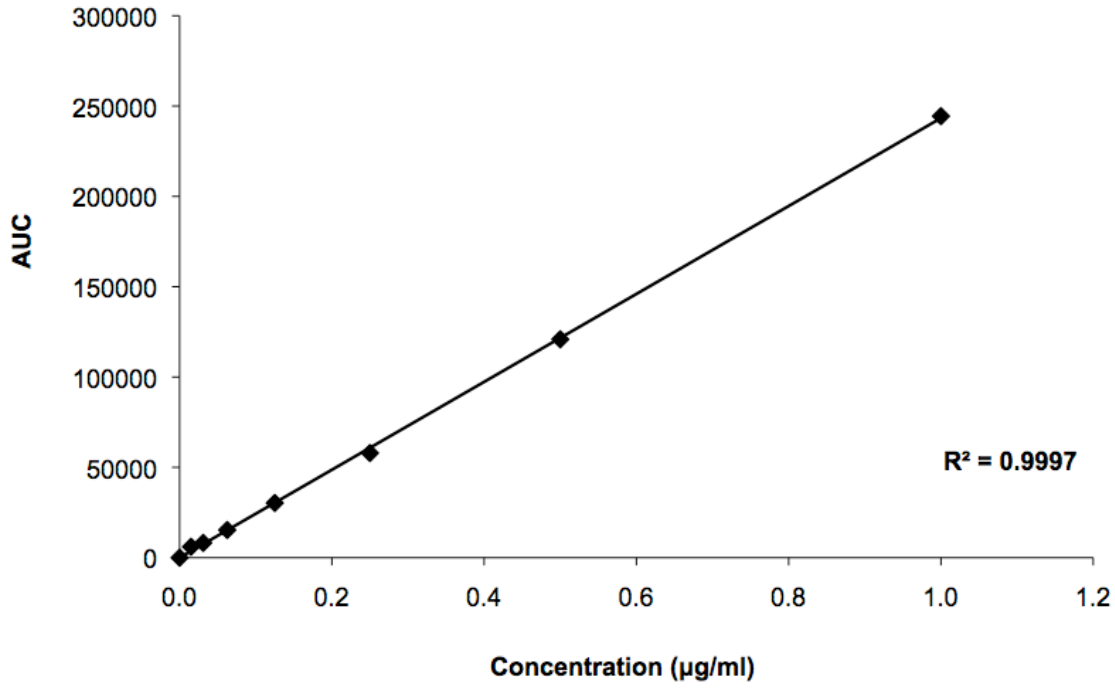

Figure 2.2. Standard Curve for the Quantification of Curcumin by HPLC Analysis.

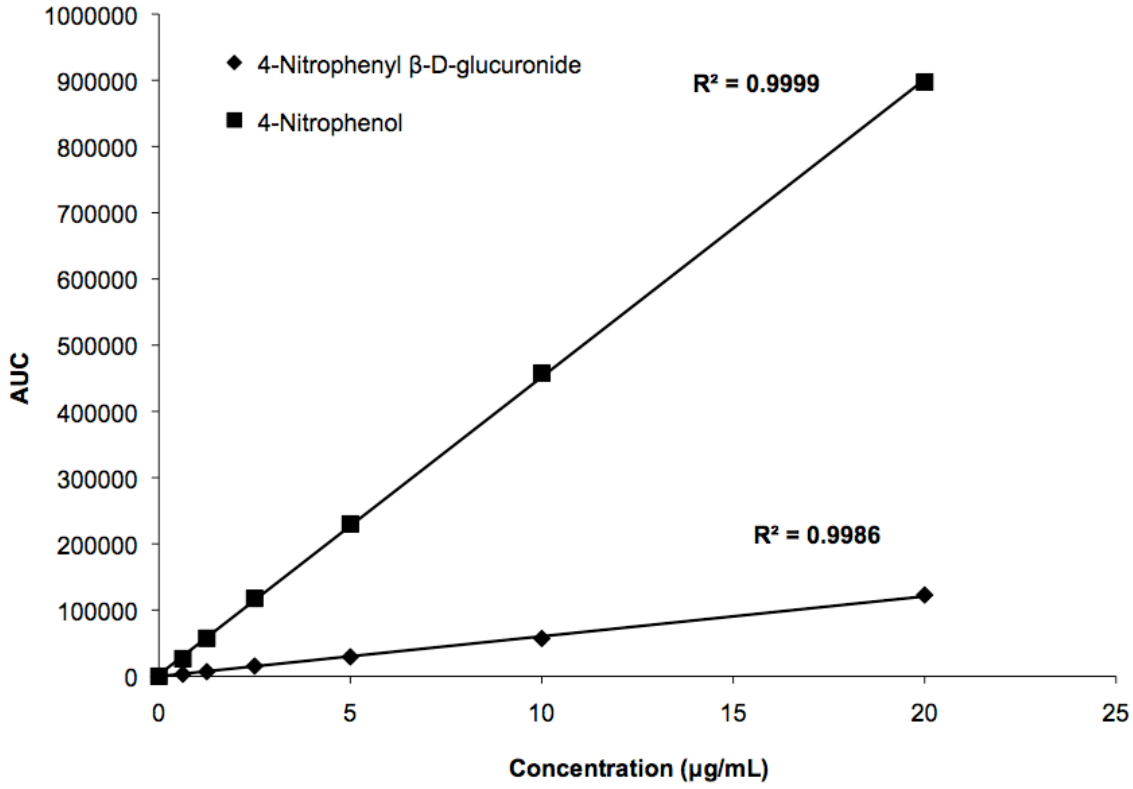

Figure 2.3. Standard Curve for the Quantification of 4-Nitrophenyl β-D-Glucuronide and 4-Nitrophenol by HPLC Analysis.

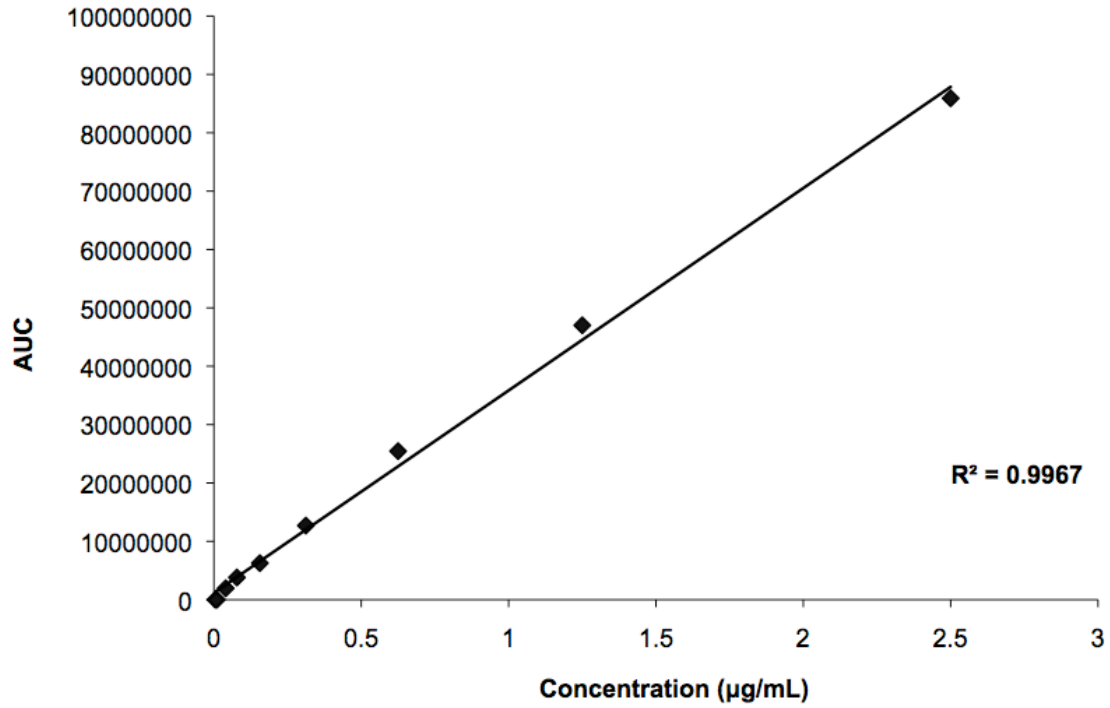

Figure 2.4. Standard Curve for the Quantification of Curcumin by LC-MS/MS Analysis.

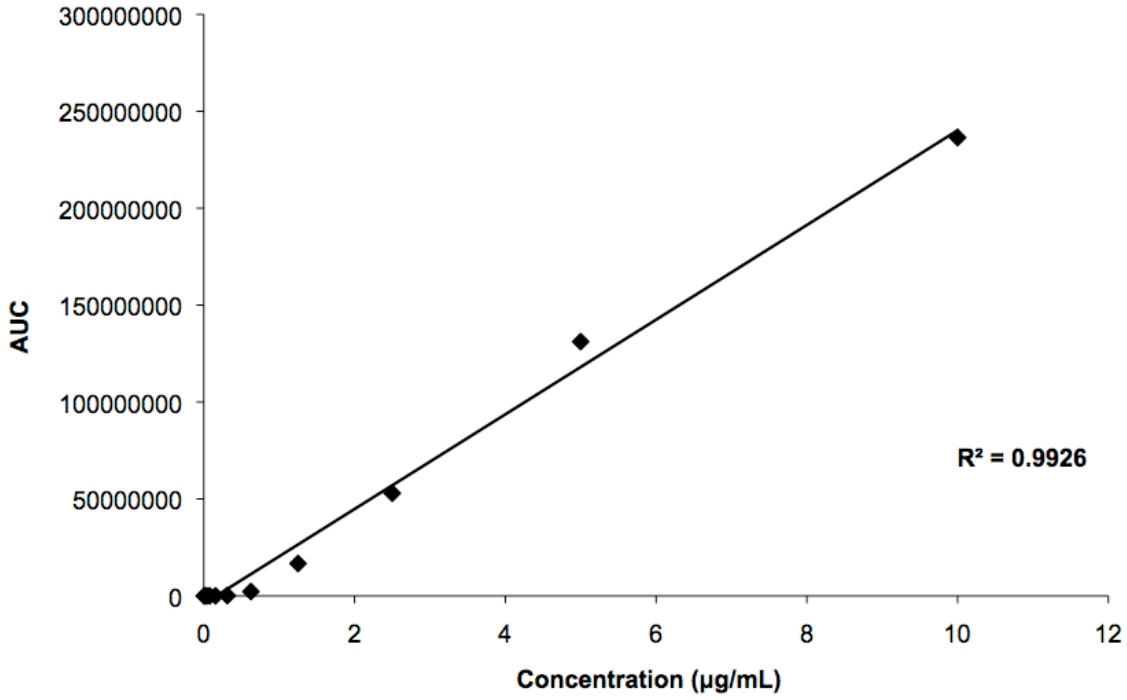

Figure 2.5. Standard Curve for the Quantification of Curcumin Glucuronide by LC-MS/MS Analysis.

Chapter III

Experimental Results

3.1 β-Glucuronidase Expression According to Breast Cancer Stage and Subtype in Human Breast Carcinoma Tissue

β-glucuronidase expression was determined by immunohistochemistry in human breast carcinoma tissue that varied in both breast cancer stage and subtype. Representative images of the microarray sample cores stained for β-glucuronidase expression are shown in Figure 3.1. Qualitative analysis showed that HER-2+ subtype sample cores had the highest levels of staining, followed by triple negative subtype. Sample cores consisting of normal, healthy breast tissue revealed barely detectable levels of staining for β-glucuronidase expression. Based on the results from the quantitative analysis of enzyme expression levels according to subtype, triple positive subtype had the lowest β-glucuronidase expression at 2.82 ± 1.14% of the sample core stained. ER/PR+ subtype showed slightly higher enzyme levels (5.58 ± 1.45%) than triple positive subtype levels. Triple negative and HER-2+ subtypes had the highest β-glucuronidase expression levels on average at 11.89 ± 2.96% and 17.25 ± 4.78%, respectively (Figure 3.2).

Expression of β-glucuronidase was also studied according to breast cancer stage of tumorigenesis. Results are displayed as enzyme expression by stage, and within each stage, the individual subtypes. As the microarray was limited in the number of samples in the earlier stages of breast cancer (i.e., normal, benign, hyperplasia, *in situ*), the results convey only the few sample cores that were represented in each of these stages. The most represented stage on the microarray was the malignant (invasive carcinoma/metastatic) stage. According to results, the β-glucuronidase expression levels increased as the stage advanced, regardless of the subtype. For triple positive subtype, enzyme expression increased from normal (0.59 ± 0.09% of sample core stained) to carcinoma *in situ* (5.87 ±

1.87%) and malignant (5.40 ± 2.30%; $P<0.05$). In ER/PR+ sample cores, β-glucuronidase levels increased from normal (2.67 ± 1.07%) and hyperplasia (3.07 ± 1.18%) to malignant stage (9.91 ± 2.68; $P<0.05$). Enzyme levels were shown to be the highest in the most advanced malignant stage, with expression levels according to subtype following a similar trend as when just the subtype was analyzed alone: triple positive (5.40 ± 2.30%) < ER/PR+ (9.91 ± 2.68%) < triple negative (11.89 ± 2.96%) < HER-2+ (16.13 ± 4.59%). Once again, HER-2+ subtype showed the highest expression level as compared to other subtypes (Figure 3.3).

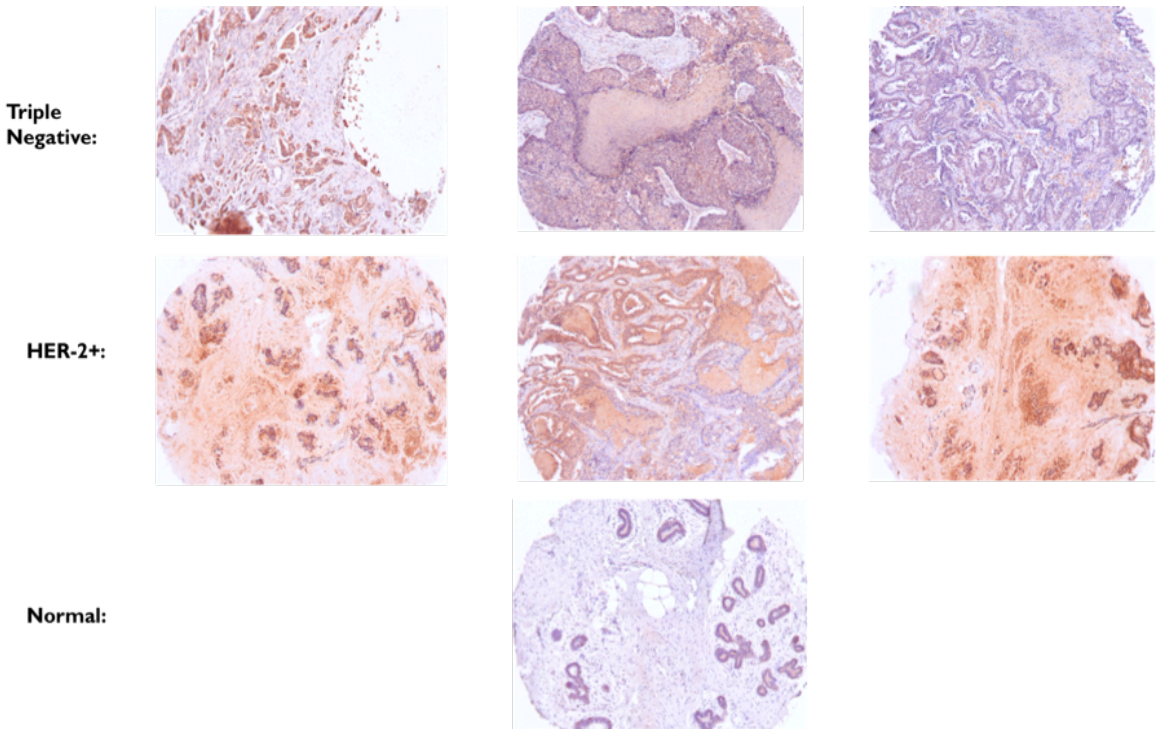

Figure 3.1. Representative images from immunohistochemistry on primary human breast tumor tissue stained for β-glucuronidase expression in normal tissue, triple negative type, and HER-2+ type breast cancer. Sample cores are from the BRC-961 microarray from US Biomax, Inc.

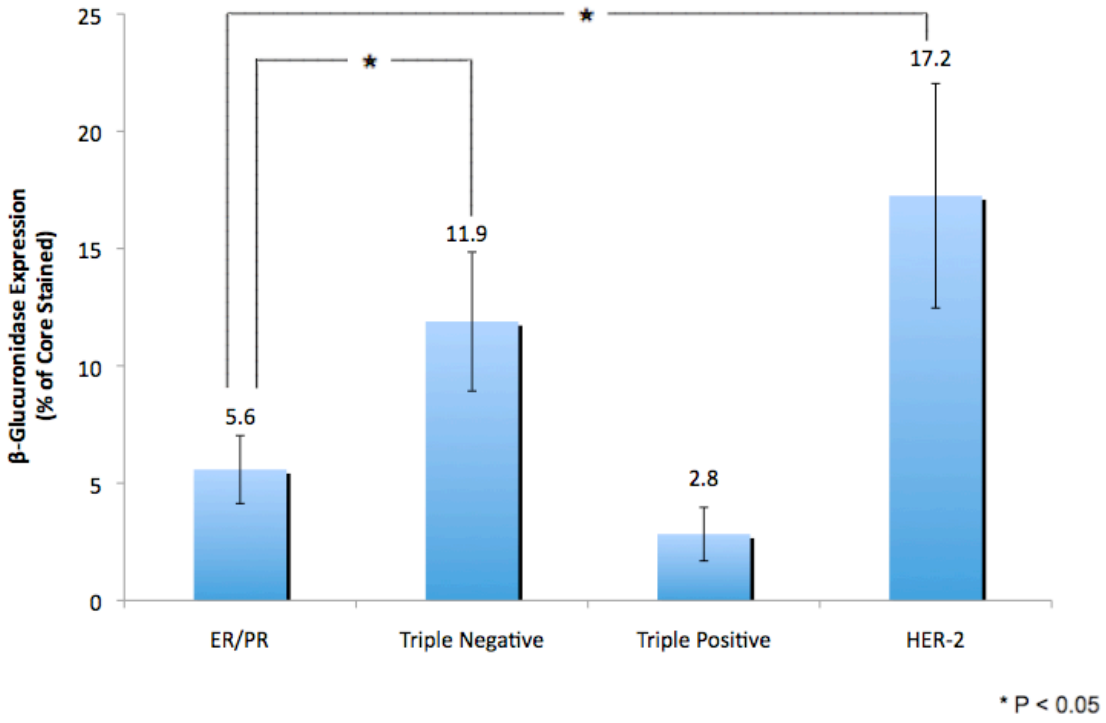

Figure 3.2. Levels of β-glucuronidase expression (percentage of core stained) in sample cores of primary human breast tumor tissue from BRC-961 microarray. β-glucuronidase expression was quantified according to subtype of breast cancer. Data shown are Mean ± SE. * P<0.05

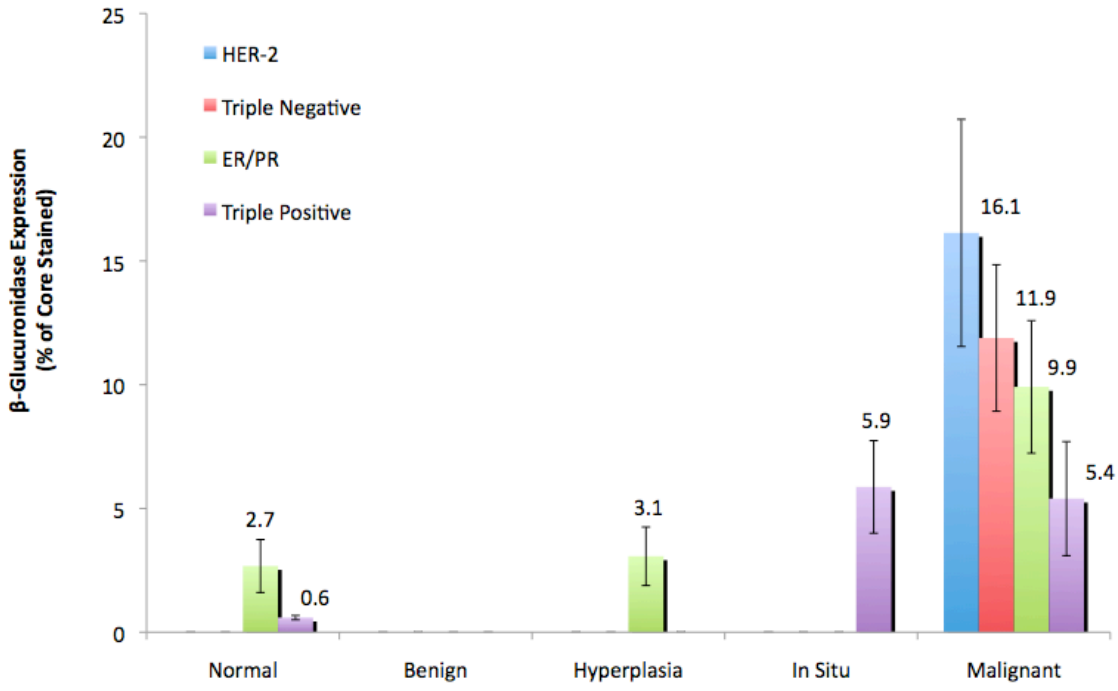

Figure 3.3. Levels of β-glucuronidase expression (percentage of core stained) in sample cores of primary human breast tumor tissue from BRC-961 microarray. β-glucuronidase expression was quantified according to stage of breast cancer. Each stage was quantified based on breast cancer subtype. Data shown are Mean ± SE.

3.2 Normalized β-Glucuronidase Expression in HER-2+ Balb-*neu*T Model

The presence of β-glucuronidase protein in mammary tumor tissue of transgenic Balb-*neu*T mice was determined by Western blotting. Mammary tissue and tumors were collected at 3, 8, 12, 16, and 23 weeks of age to represent each stage of tumorigenesis, ranging from hyperplasia (3 weeks) to metastasis (23 weeks). These studies showed that mammary tissue during the earlier stages of tumorigenesis (3, 8, 12 weeks of age) showed lower levels of β-glucuronidase than at the more advanced stages of invasive carcinoma and metastasis (16, 23 weeks). The normalized protein level at 23 weeks of age was found to be, on average, 2.6- and 4.6-fold greater than at 8 and 12 weeks, respectively (Figures 3.4 and 3.5).

3.3 Specific Activity of β-Glucuronidase in HER-2+ Transgenic Balb-*neu*T and Wild-Type Balb/c Models According to Stage of Tumorigenesis

To investigate the hypothesis that β-glucuronidase is overexpressed in the mammary tumors as compared to healthy tissue, mammary tissues from wild-type Balb/c mice and that from transgenic Balb-*neu*T mice bearing mammary tumors were studied. Tissue from both the wild-type and transgenic strains were extracted from mice at various ages to represent the progressive stages of tumorigenesis (n = 3 per stage): 3 weeks (hyperplasia), 8 and 12 weeks (carcinoma *in situ)*, 16 weeks (invasive carcinoma), and 23 (metastasis) weeks of age.

In the Balb-*neu*T model, the initial stages of tumorigenesis exhibit low levels of β-glucuronidase specific activity. At 3 and 8 weeks of age, mammary tissue yielded 2.58 ± 0.72 and 2.97 ± 0.32 nmol NP formed/hr/mg protein, respectively. By 12 weeks,

mammary tumors are further developed and had a specific activity of 5.72 ± 0.90 nmol NP formed/hr/mg protein. At 16 weeks, activity levels dropped slightly to 4.31 ± 0.49 nmol NP formed/hr/mg protein before increasing to 10.71 ± 0.78 nmol NP formed/hr/mg protein at 23 weeks of age (Figure 3.6).

β-glucuronidase specific activity levels in the mammary tissue from the wild-type Balb/c model were minimal as compared to that from the Balb-*neu*T model. Whereas the specific activity increased with age and tumor progression in the Balb-*neu*T model, the levels in the Balb/c model were relatively constant: ~1 nmol NP formed/hr/mg protein from 3 weeks to 23 weeks of age. The highest activity was observed to be at 16 weeks in Balb/c (1.45 ± 0.86 nmol NP formed/hr/mg protein), which was lower than the lowest activity in the transgenic model at 3 weeks (2.58 ± 0.72 nmol NP formed/hr/mg protein) (Figure 3.6).

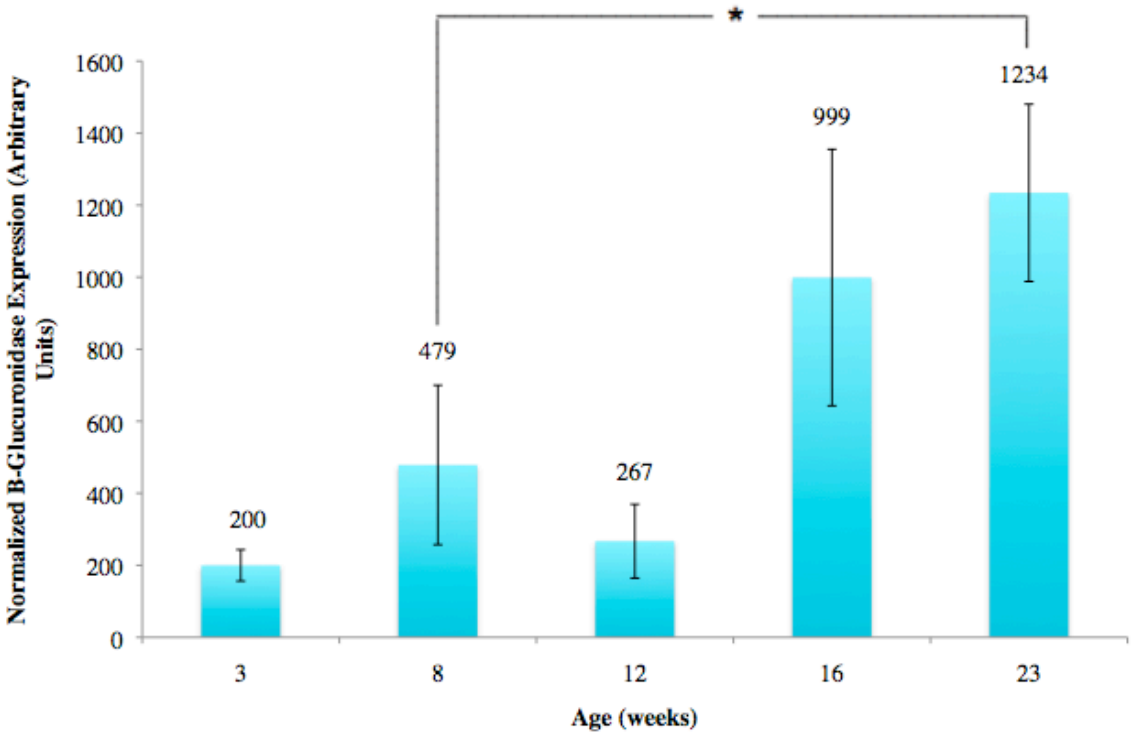

Figure 3.4. β-glucuronidase expression normalized to total protein in HER-2+ Balb-*neu*T mammary tumor tissue at different stages of tumorigenesis, as determined by Western blotting. Data shown are Mean ± SE, n = 3. * $P<0.05$

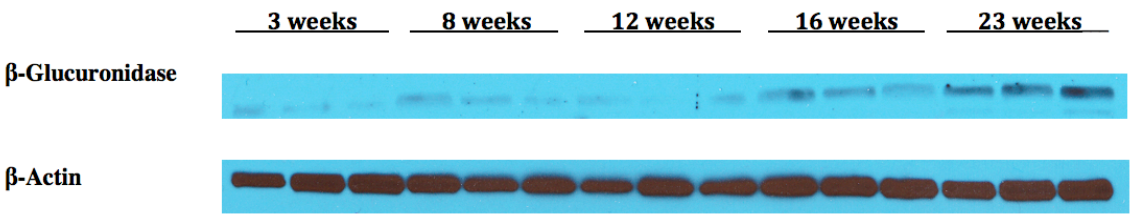

Figure 3.5. β-Glucuronidase expression according to age of mice, which corresponds to each stage of tumorigenesis. Mammary tumor samples from different age groups of female transgenic Balb-*neu*T mice were analyzed for enzyme expression by Western blotting. β-Actin served as the protein loading control.

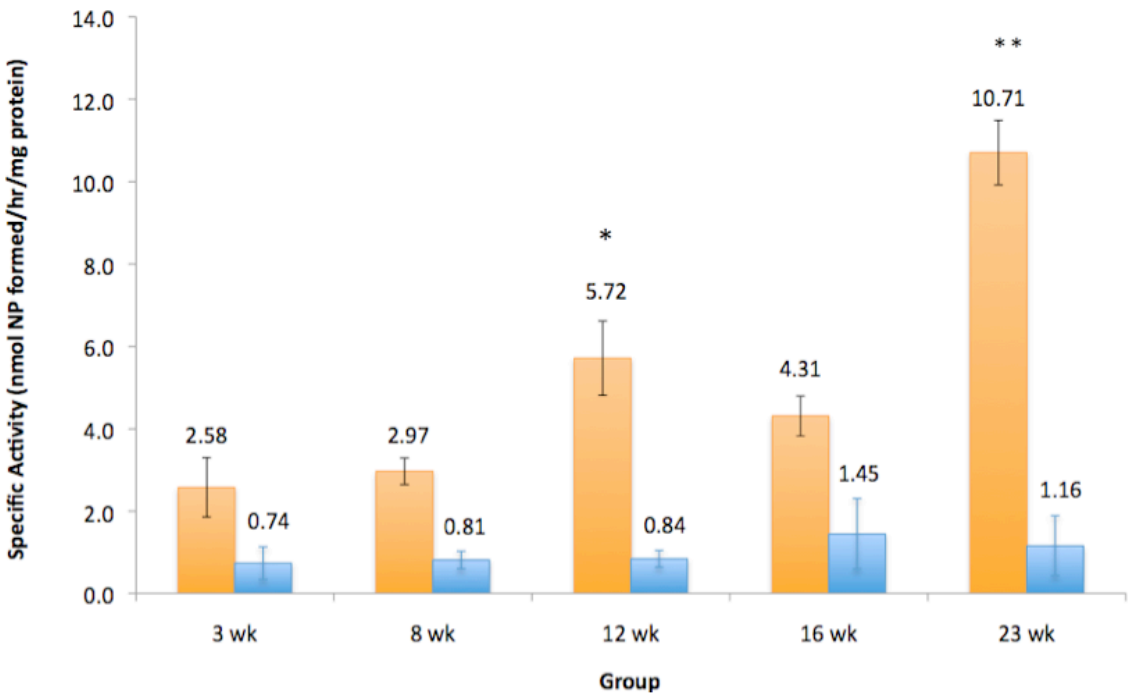

Figure 3.6. Specific activity (nmol NP formed/hr/mg protein) of β-glucuronidase in HER-2+ transgenic Balb-*neu*T mammary tumor tissue (orange) and wild-type Balb/c healthy mammary tissue (blue). Mammary tissue from wild-type female Balb/c mice and mammary tumors from female Balb-*neu*T mice were collected at 3, 8, 12, 16, and 23 weeks of age to represent each stage of tumorigenesis. Tissues collected were processed for enzyme activity assays. β-glucuronidase activity was determined by monitoring the conversion rate of 4-nitrophenyl β-D-glucuronide (NPG) to the parent compound 4-nitrophenol (NP) for 4 hours of incubation at 37°C. NPG and NP concentrations were determined by HPLC. Data shown are Mean ± SE, n = 3. * $P<0.05$, compared to specific activity in Balb-*neu*T mammary tumor tissue at age groups 3 and 8 weeks; ** $P<0.05$, compared to specific activity in Balb-*neu*T mammary tumor tissue at age groups 3 – 16 weeks, ANOVA.

3.4 β-Glucuronidase Activity is Present in Tumor Tissue but Absent in Plasma from HER-2+ Balb-*neu*T Model

To determine whether β-glucuronidase activity is present in plasma – which may potentially account for some levels of the active drug being present in the systemic circulation – enzyme activity assays were conducted with plasma and compared to tumor tissue homogenate data. In the mammary tumor tissue, the amount of NPG decreased by 12% on average per hour, and after 3 hours of incubation, 61.11 ± 3.62% NPG remained in the sample homogenate. Such a significant rate of NPG conversion is indicative of high levels of β-glucuronidase present within the tumor. On the contrary, no significant conversion of NPG to NP was seen in plasma samples even at the end of 4 hours (Figure 3.7).

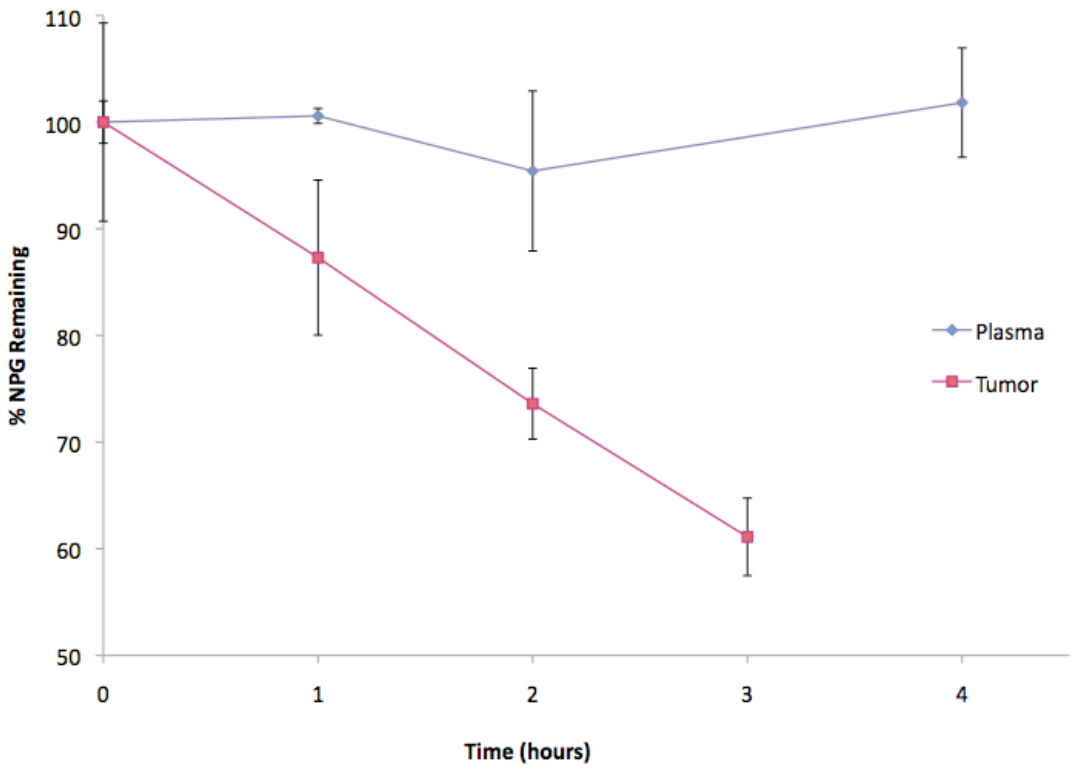

Figure 3.7. β-Glucuronidase activity is present in tumor tissue but absent in plasma from HER-2+ Balb-*neu*T model. Enzyme activity was determined by monitoring the conversion rate of 4-nitrophenyl β-D-glucuronide (NPG) to the parent compound 4-nitrophenol (NP) for 3-4 hours of incubation at 37°C. NPG and NP concentrations were determined by HPLC. Data shown are Mean ± SD, n = 3.

3.5 β-Glucuronidase Activity in HER-2+ Balb-*neu*T Mammary Tumor Tissue is Inhibited by Saccharolactone (GUSB Inhibitor)

To ensure that β-glucuronidase is specifically responsible for cleaving the glucuronide moeity from NPG and that the decreasing levels of NPG in the enzyme activity assays is not a result of spontaneous degradation or other enzymes, saccharolactone, a known inhibitor of β-glucuronidase, was used as a control. In Balb-*neu*T mammary tumor homogenate without saccharolactone, the amount of NPG decreased by 12% on average with each additional hour; after 3 hours of incubation, 61 ± 3% NPG remained in the homogenate. With the addition of saccharolactone, however, the conversion rate was much lower than without the inhibitor. Tumor homogenate incubated with saccharolactone had an average NPG activation rate of only 2% per hour. After 4 hours, 94.53 ± 2.82% NPG remained in tumor tissue homogenate containing the inhibitor (Figure 3.8). This study confirmed that conversion of NPG to NP was specifically catalyzed by β-glucuronidase.

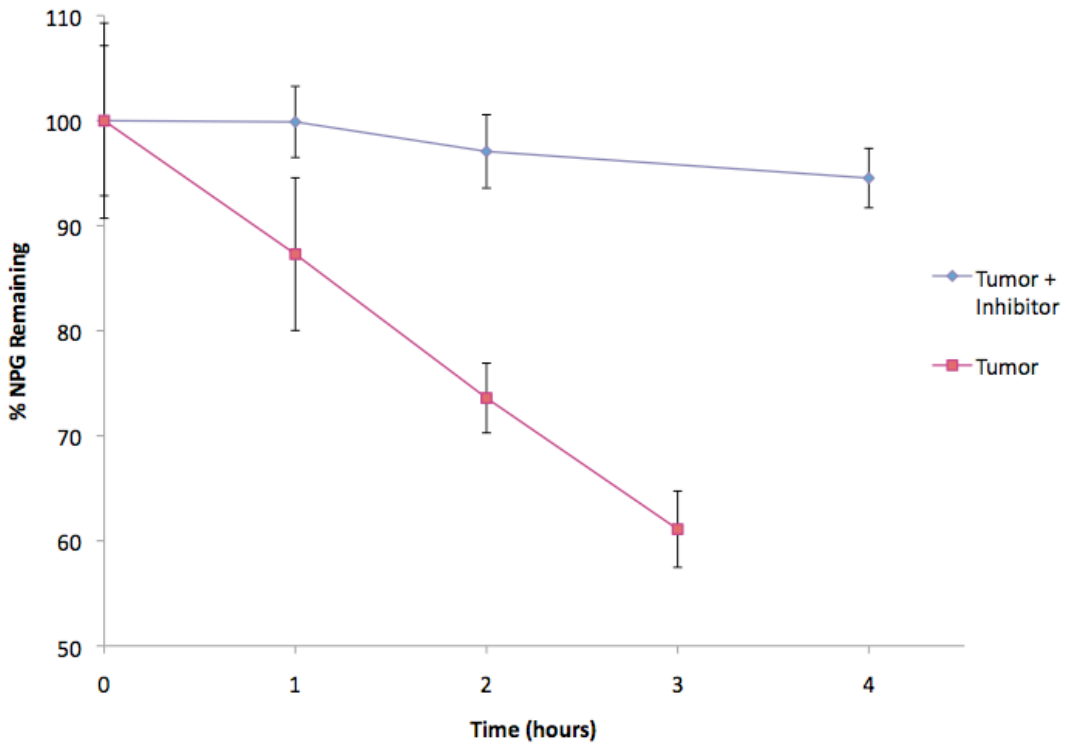

Figure 3.8. β-Glucuronidase activity in HER-2+ mammary tumor tissue from the Balb-*neu*T mouse model is inhibited by Saccharolactone (GUSB Inhibitor). Enzyme activity was determined by monitoring the conversion rate of 4-nitrophenyl β-D-glucuronide (NPG) to the parent compound 4-nitrophenol (NP) for 3-4 hours of incubation at 37°C. NPG and NP concentrations were determined by HPLC. Data shown are Mean ± SD, n = 3.

3.6 NIR-TrapG: *In Vivo* β-Glucuronidase Activity Imaging in LM2 Model

β-glucuronidase activity *in vivo* was investigated using an activity-based near-infrared fluorescent difluoromethylphenol-glucuronide probe (NIR-TrapG). This probe in the glucuronidated state has no fluorescence, but becomes fluorescent upon activation by β-glucuronidase. The fluorescence detected can in turn be used to identify regions where significant β-glucuronidase activity occurs. The goal of this study was to use this probe to longitudinally interrogate for regions of high β-glucuronidase activity using live animal imaging.

According to the resulting data of fluorescence imaging and its quantification, significant fluorescent signals were present in not only the tumor, but in the liver region as well. Data was presented as average image area of fluorescence, given in the units $Pixels^2$. LM2 tumors on average yielded fluorescent signals that increased correspondingly with tumor size. Tumor volumes of 100, 400, 700, and 1200 mm^3 showed average fluorescent image areas of 10 ± 0.4 $pixels^2$, 78 ± 2 $pixels^2$, 423 ± 49 $pixels^2$, and 1056 ± 28 $pixels^2$, respectively (Figures 3.9 and 3.10). The increase in fluorescence in tumor was linear with respect to tumor growth. In the case of the liver, while the fluorescent signal did increase with tumor volume, the elevation of fluorescence levels did not correspond to tumor volume increase as closely as in the case of tumor fluorescence. A sudden increase in signals in the liver region was observed from 400 mm^3 (212 ± 8 $pixels^2$) to 700 mm^3 (943 ± 168 $pixels^2$). Liver fluorescent signals did not increase significantly as tumors grew to 1200 mm^3 (1084 ± 242 $pixels^2$).

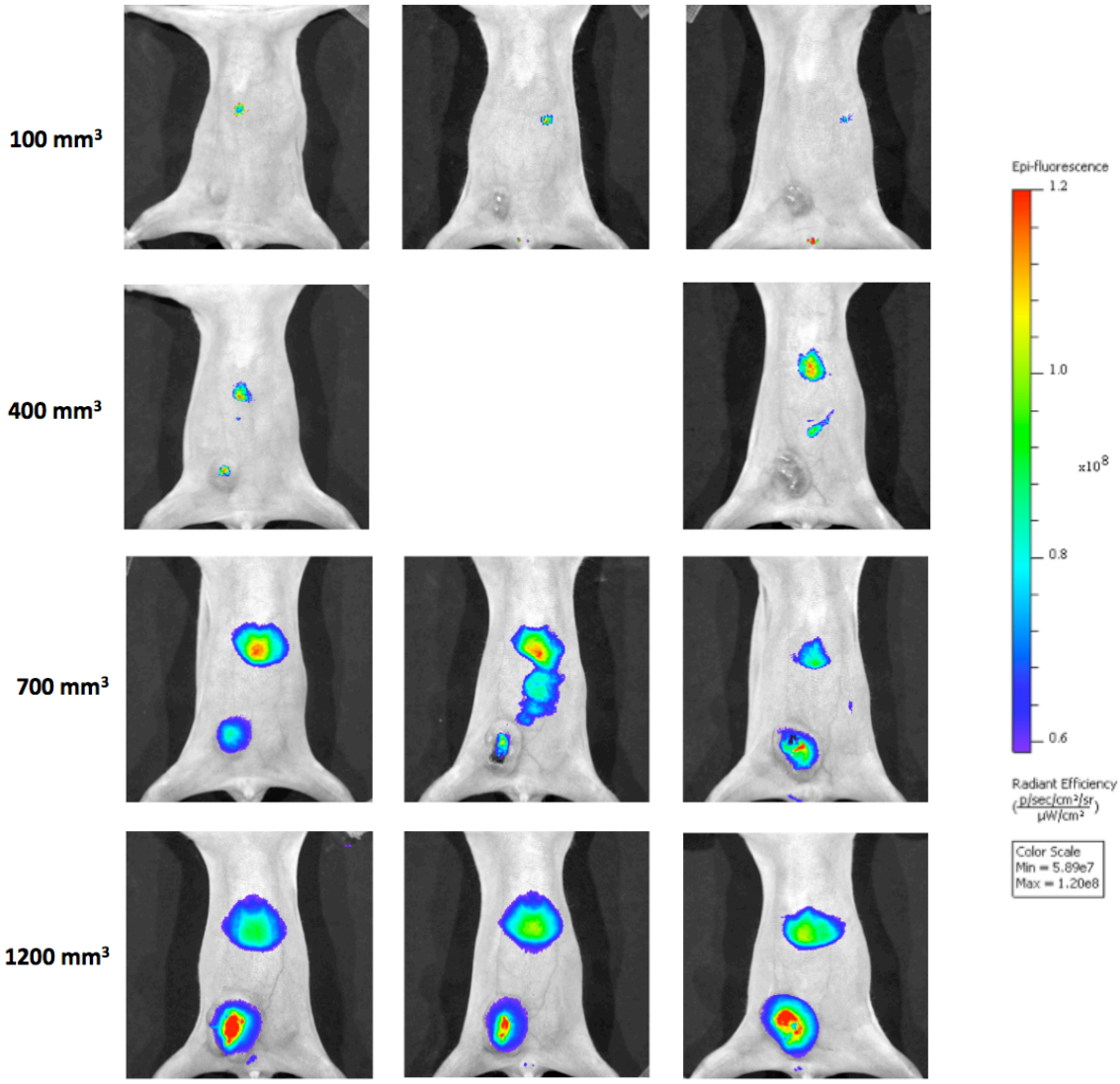

Figure 3.9. Fluorescent probe imaging displaying *in vivo* β-glucuronidase activity in LM2 tumor model. Immunocompromised athymic nude mice were injected orthotopically with LM2 cells at 500,000 cells/mouse and tumors were grown to 100, 400, 700 and 1200 mm^3. At each volume, mice were administered NIR-TrapG (100 µg), a glucuronidated probe that becomes fluorescent upon activation by β-glucuronidase, and animals were imaged for fluorescence at 24 hours post-dose.

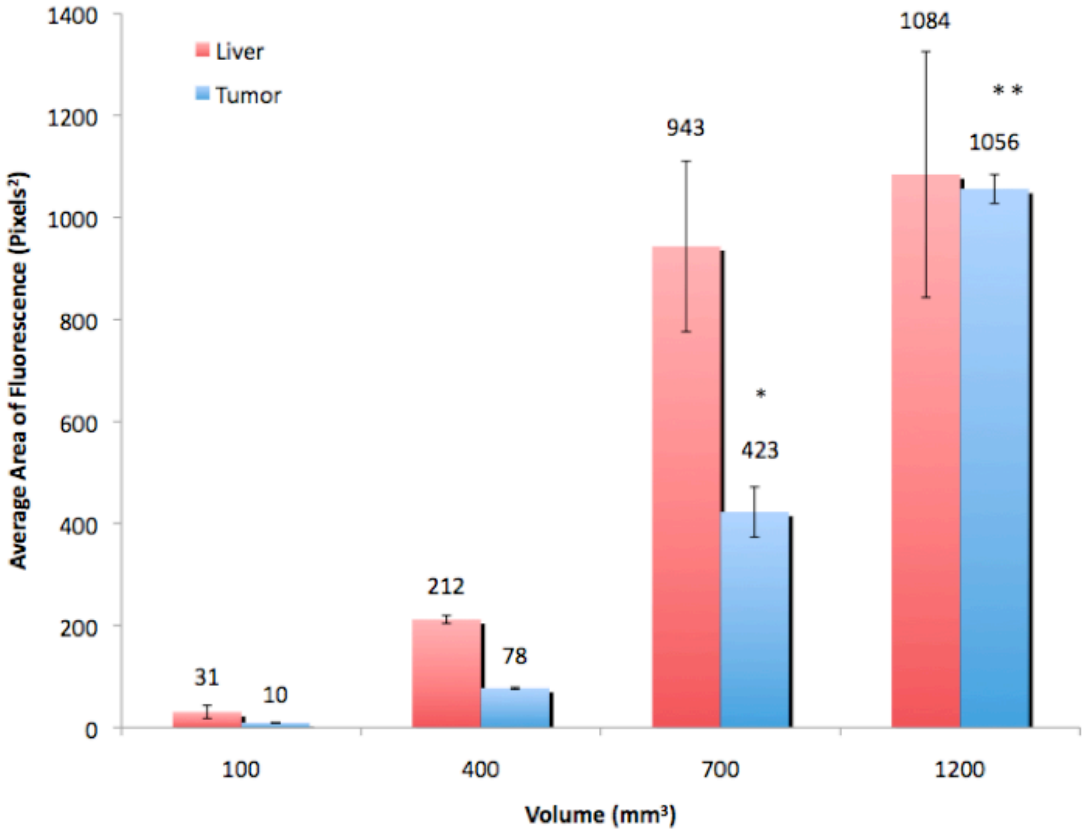

Figure 3.10. Average image area of fluorescence (Pixels^2) in liver and tumor of LM2 tumor model. Immunocompromised athymic nude mice were injected orthotopically with LM2 cells at 500,000 cells/mouse and tumors were grown to 100, 400, 700 and 1200 mm^3. At each volume, mice were administered NIR-TrapG (100 µg), a glucuronidated probe that becomes fluorescent upon activation by β-glucuronidase, and animals were imaged for fluorescence at 24 hours post-dose. Data shown are Mean ± SE, n = 3.

* P<0.05, compared to fluorescence in tumor at 400 mm^3; ** P<0.05, compared to fluorescence in tumor at 700 mm^3, ANOVA.

3.7 Specific Activity of β-Glucuronidase in Mammary Tumor Models: JC, TuBo, MDA-MB-231, 4T1

Different breast cancer subtypes and cell lines are known to vary in aggression. Four mammary tumor models were used for these studies: JC (triple negative, syngeneic to Balb/c), TuBo (HER-2+, syngeneic to Balb/c), MDA-MB-231 (triple negative, human adenocarcinoma), and 4T1 (triple negative, syngeneic to Balb/c). Mammary tissue from wild-type Balb/c mice and tumors from the orthotopic models were collected at 100, 400, 700, and 1200 mm^3 to measure β-glucuronidase specific activity levels.

Results show that β-glucuronidase specific activity increased with tumor size up to 400 mm^3 for all models (Figure 3.11). At 400 mm^3 and above, specific activity levels did not increase further with tumor volume growth. Wild-type Balb/c mammary tissue had β-glucuronidase specific activity levels ranging from 0.74 ± 0.40 to 1.16 ± 0.73 nmol NP formed/hr/mg protein. TuBo tumors showed the lowest levels of β-glucuronidase activity in comparison to the other 3 models. At 100 mm^3, activity levels were at 0.31 ± 0.09 nmol NP formed/hr/mg protein and at 1200 mm^3, levels increased to 1.47 ± 0.03 nmol NP formed/hr/mg protein. These activity levels, however, were much lower than the other 3 triple negative models. In MDA-MB-231, JC, and 4T1 tumors at 100 mm^3, specific activities were 2.70 ± 0.32, 2.85 ± 0.43, and 2.06 ± 0.08 nmol NP formed/hr/mg protein, respectively. Levels increased to 4.33 ± 0.77 nmol NP formed/hr/mg protein for MDA-MB-231, 5.10 ± 0.65 nmol NP formed/hr/mg protein for JC, and 5.17 ± 0.74 nmol NP formed/hr/mg protein for 4T1. The 4T1 model exhibited the highest β-glucuronidase specific activity, which may be due to its aggressiveness in terms of cell growth,

proliferation, tumor formation, and increased infiltration of inflammatory cells such as macrophages and neutrophils [114].

Lungs are a common site for breast cancer metastasis. There is strong potential for the presence of β-glucuronidase activity in metastatic lesions as well as in primary tumors. Due to the aggressiveness of the 4T1 model and high β-glucuronidase specific activity, lungs from Balb/c mice bearing 4T1 tumors in the later stages (>1200 mm^3) and from wild-type Balb/c mice of the same age were collected and analyzed for enzyme activity levels. Lungs extracted from 4T1 tumor bearing mice had significantly greater β-glucuronidase activity than those from wild-type Balb/c mice (1.97 ± 0.17 versus 1.26 ± 0.14 nmol NP formed/hr/mg protein; $P<0.05$) (Figure 3.12). These results support the proposition that metastatic sites may also overexpress β-glucuronidase, suggesting that distant metastatic sites may also be capable of glucuronide prodrug activation.

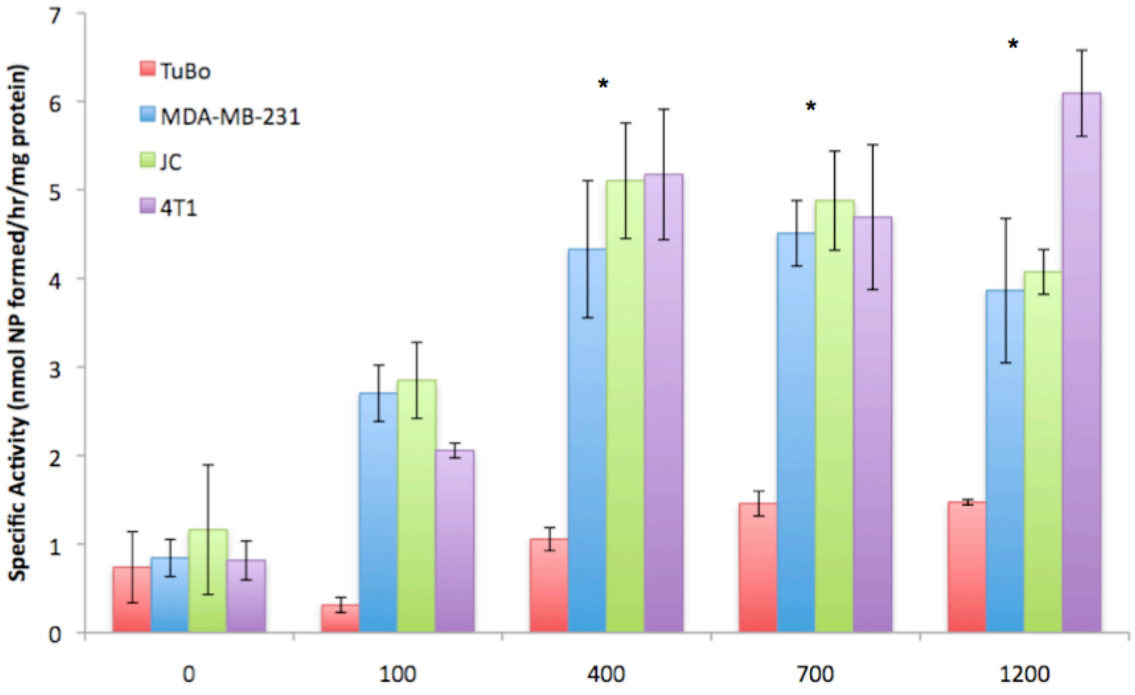

Figure 3.11. Specific activity (nmol NP formed/hr/mg protein) of β-glucuronidase in 4 mammary tumor models. Female Balb/c mice were injected orthotopically with JC, TuBo, 4T1, and MDA-MB-231 cells at 1,000,000 cells/mouse and tumors were grown to 100, 400, 700 and 1200 mm^3. At each volume, tumors were collected and processed for enzyme activity assays. β-glucuronidase activity was determined by monitoring the conversion rate of 4-nitrophenyl β-D-glucuronide (NPG) to the parent compound 4-nitrophenol (NP) for 4 hours of incubation at 37°C. NPG and NP concentrations were determined by HPLC. Data shown are Mean ± SE, n = 3. * $P<0.05$, compared to specific activities at 0 mm^3 and 100 mm^3, ANOVA.

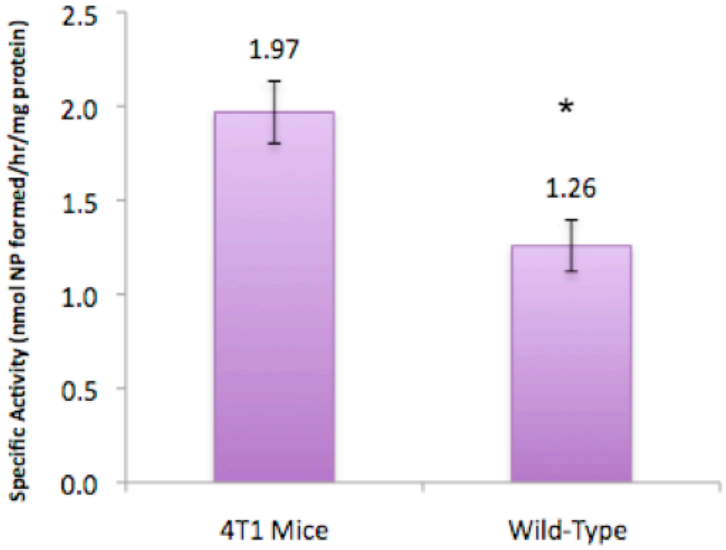

Figure 3.12. Specific activity (nmol NP formed/hr/mg protein) of β-glucuronidase in lungs from 4T1 model. Female Balb/c mice were injected orthotopically with 4T1 cells at 1,000,000 cells/mouse and tumors were grown to 1200 mm^3. Lungs were collected and processed for enzyme activity assays. β-glucuronidase activity was determined by monitoring the conversion rate of 4-nitrophenyl β-D-glucuronide (NPG) to the parent compound 4-nitrophenol (NP) for 4 hours of incubation at 37°C. NPG and NP concentrations were determined by HPLC. Data shown are Mean ± SE, n = 3. * $P<0.05$, ANOVA.

3.8 Chemopreventive Efficacy of Oral Curcumin in Mammary Tumor Models: JC, TuBo, MDA-MB-231, 4T1

The chemopreventive efficacy of orally dosed curcumin in a microemulsion formulation was evaluated in four different mammary tumor models: JC, TuBo, MDA-MB-231, and 4T1. Tumor bearing mice were orally administered curcumin in a self-microemulsifying drug delivery system (SMEDDS) formulation at 100 mg/kg daily beginning one day prior to cell injection, and the once daily dosing lasted until the end of the study. All the tumor models, except for TuBo, showed reduced tumor growth rate with the curcumin microemulsion treatment. At the end of a month-long study with TuBo, tumor volumes across all three treatment groups were similar. While the curcumin SMEDDS treated group (582 ± 69 mm^3) had an average tumor volume lower than that of the blank SMEDDS (815 ± 101 mm^3) and the untreated (748 ± 69 mm^3) groups, the difference between the groups was not statistically significant (Figure 3.14).

In the other three models, the curcumin SMEDDS treated group had statistically significant lower tumor growth rates than the blank SMEDDS and untreated groups. In the JC model, the curcumin SMEDDS group (515 ± 89 mm^3) had a lower average tumor volume at the end of the month-long study when compared to the blank SMEDDS (932 ± 79 mm^3) and untreated (856 ± 116 mm^3) groups ($P<0.05$) (Figure 3.13). Similar was the case with the 4T1 model, where the curcumin SMEDDS treated group (1199 ± 180 mm^3) had a significantly lower volume at the end of the study than the blank SMEDDS treated group (1886 ± 126 mm^3) ($P<0.05$) (Figure 3.15). However, the difference was not statistically significant when the curcumin treated group was compared with the untreated group, which had a final average volume of 1487 ± 186 mm^3. This lack of significance

between the curcumin treated and untreated groups, as well as the overall higher volumes of the 4T1 tumors in all the three treatment groups at one month post-inoculation, could be attributed to the aggressive nature of the 4T1 model.

The MDA-MB-231 model proved to be the most responsive to oral curcumin treatment, as shown by the significantly lower tumor volume of the curcumin SMEDDS treated group at the end of a 2-month long efficacy study as compared to the other control treatment groups (Figure 3.16). This data is quite notable, as efficacy is shown in a human tumor xenograft model. At 2 months, the mean tumor volume in the curcumin SMEDDS treatment group was 41.9% lower than that of the blank SMEDDS treated group (819 ± 147 mm^3 versus 1951 ± 148 mm^3, respectively).

The weights of mice in each of the three experimental treatment groups were monitored throughout the study to assess potential systemic toxicity effects due to drug and microemulsion treatment. Both the blank and curcumin SMEDDS treatments did not cause any gross toxicity, as the body weights were either relatively constant (TuBo model) or increased slightly (4T1 and MDA-MB-231 models) throughout the course of the study (Figures 3.17). JC was the only one model in which average weights slightly decreased, but since the decrease was <10% from the beginning to the end of the study, the treatments were still deemed safe.

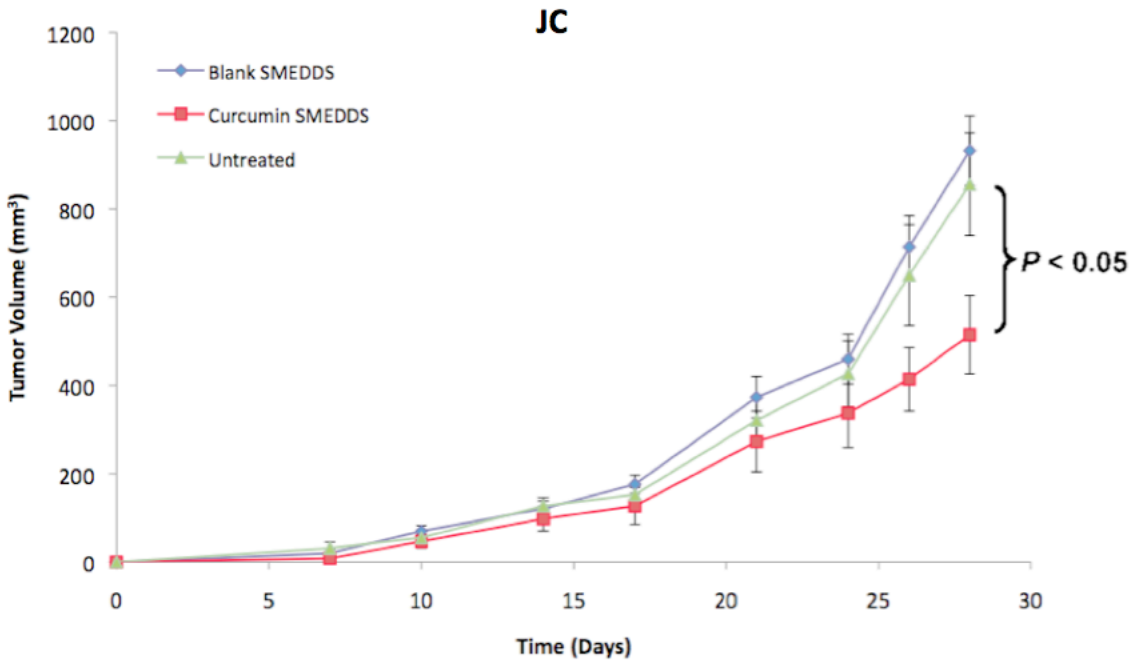

Figure 3.13. Oral dosing of curcumin SMEDDS formulation inhibits JC tumor growth rate. Female Balb/c mice were injected orthotopically with JC cells at 1,000,000 cells/mouse and dosed orally with curcumin daily at 100 mg/kg (n=6 per group: curcumin SMEDDS, blank SMEDDS, untreated). Treatments began 1 day prior to injection of tumor cells. Points, mean (n=6); bars, SE. P<0.05, ANOVA.

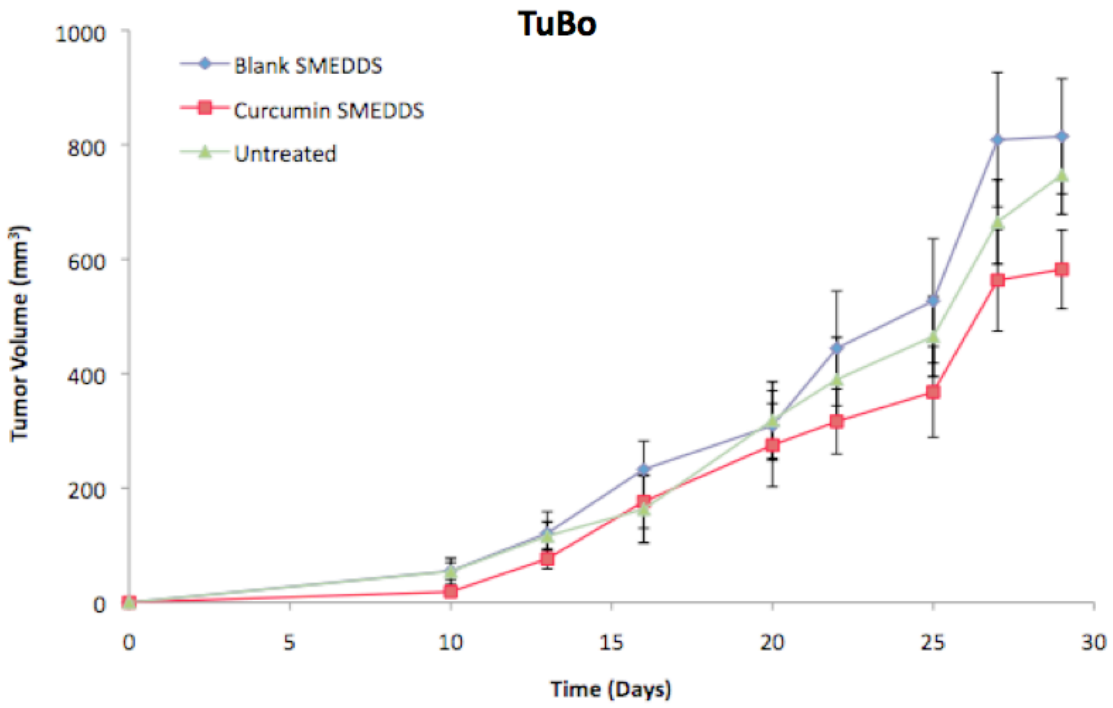

Figure 3.14. Oral dosing of curcumin SMEDDS formulation has no significant effect on TuBo tumor growth rate. Female Balb/c mice were injected orthotopically with TuBo cells at 1,000,000 cells/mouse and dosed orally with curcumin daily at 100 mg/kg (n=6 per group: curcumin SMEDDS, blank SMEDDS, untreated). Treatments began 1 day prior to injection of tumor cells. Points, mean (n=6); bars, SE.

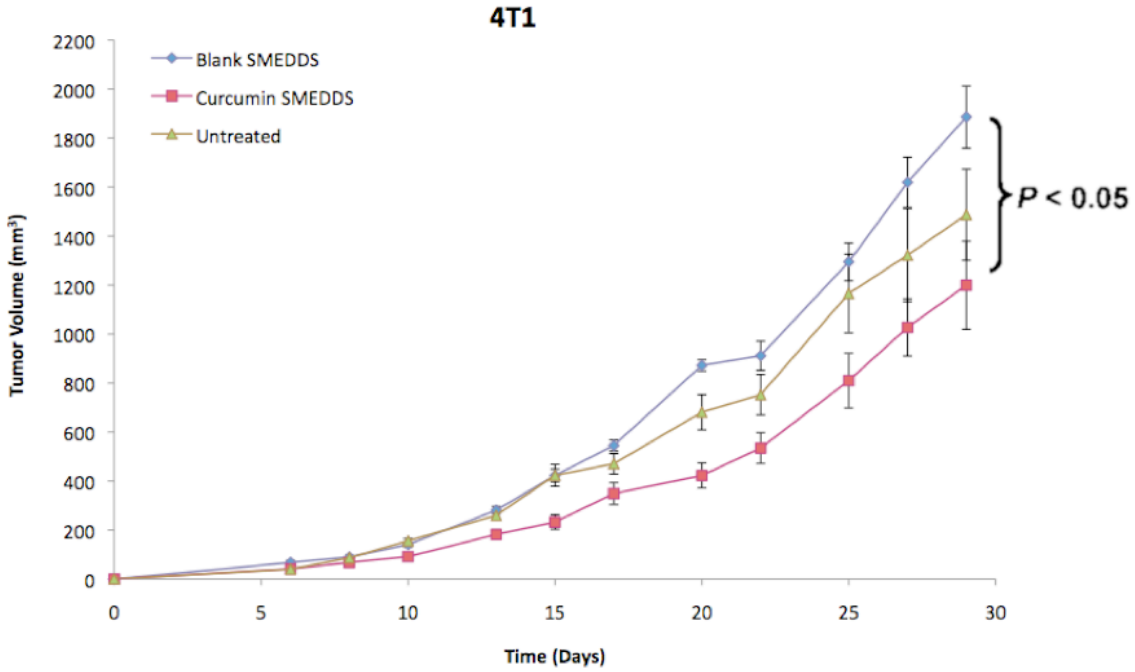

Figure 3.15. Oral dosing of curcumin SMEDDS formulation has no significant effect on 4T1 tumor growth rate. Female Balb/c mice were injected orthotopically with 4T1 cells at 1,000,000 cells/mouse and dosed orally with curcumin daily at 100 mg/kg (n=6 per group: curcumin SMEDDS, blank SMEDDS, untreated). Treatments began 1 day prior to injection of tumor cells. Points, mean (n=6); bars, SE. $P<0.05$, ANOVA.

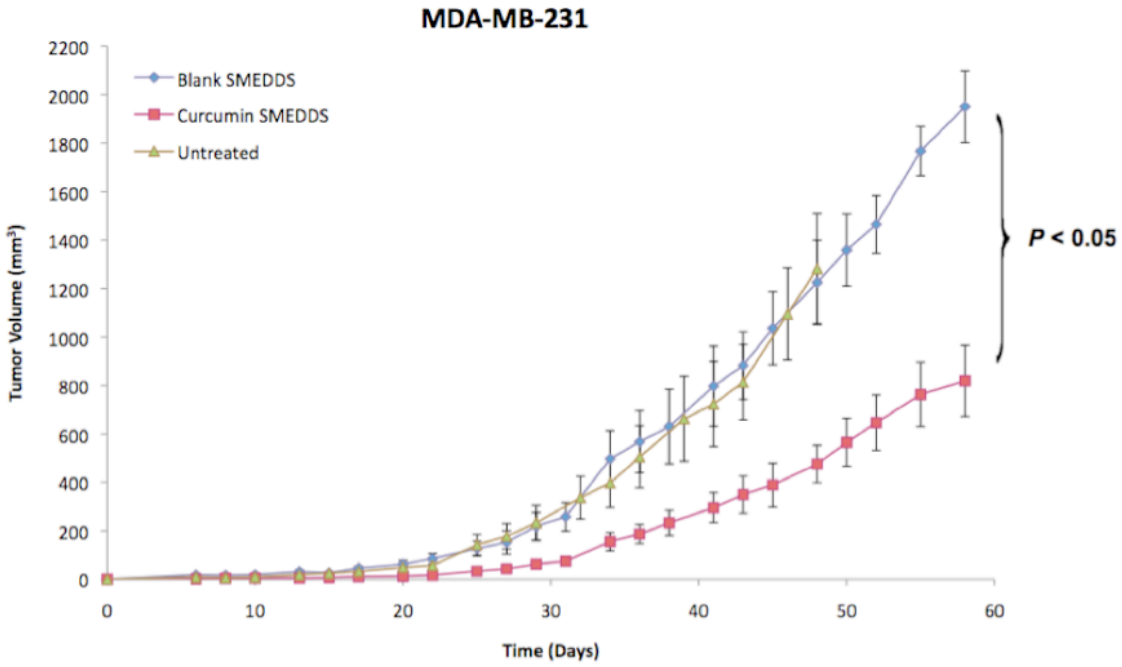

Figure 3.16. Oral dosing of curcumin SMEDDS formulation inhibits MDA-MB-231 tumor growth rate. Female athymic nude mice were injected orthotopically with MDA-MB-231 cells at 1,000,000 cells/mouse and dosed orally with curcumin daily at 100 mg/kg (n=6 per group: curcumin SMEDDS, blank SMEDDS, untreated). Treatments began 1 day prior to injection of tumor cells. Points, mean (n=6); bars, SE. P<0.05, ANOVA.

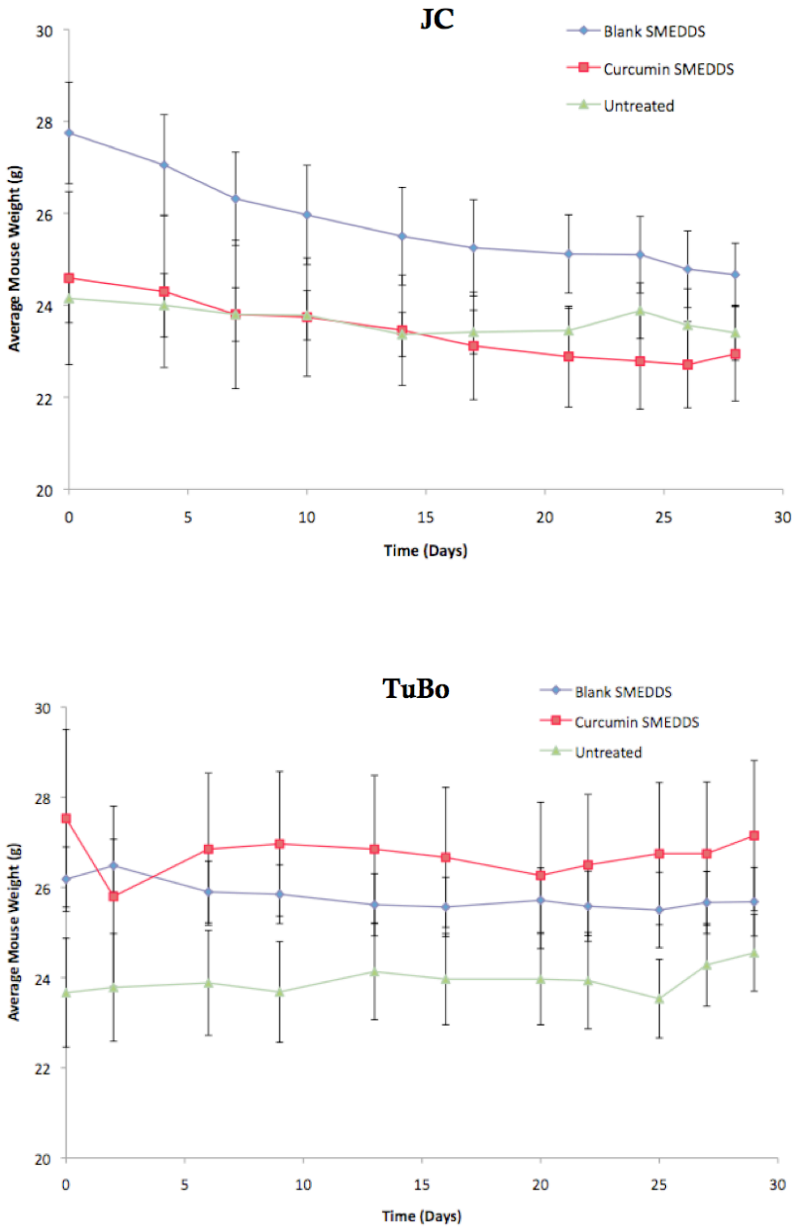

Figure 3.17.a. Average mouse weights of mice from chemopreventive efficacy studies. Female Balb/c mice were injected orthotopically with JC and TuBo cells at 1,000,000 cells/mouse and dosed orally with curcumin daily at 100 mg/kg (n=6 per group: curcumin SMEDDS, blank SMEDDS, untreated). Treatments began 1 day prior to injection of tumor cells. Points, mean (n=6); bars, SE. $P<0.05$, ANOVA.

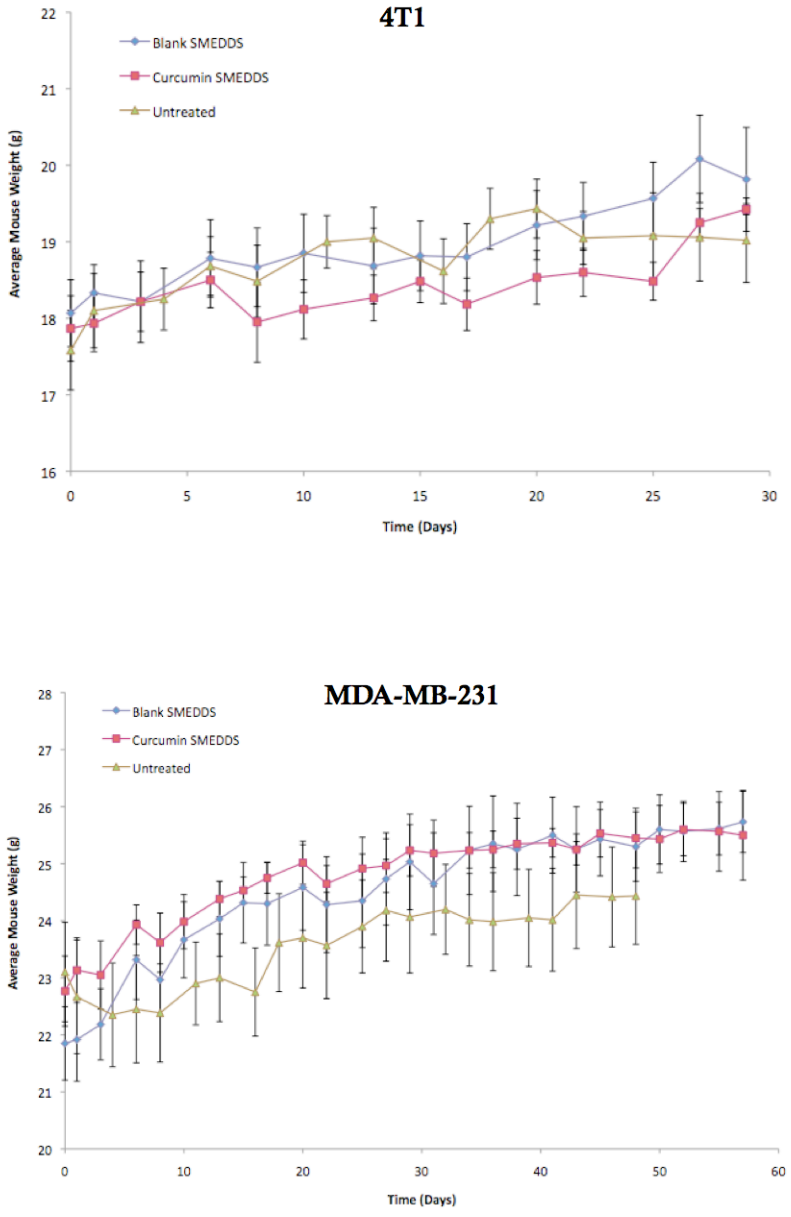

Figure 3.17.b. Average mouse weights of mice from chemopreventive efficacy studies. Female Balb/c mice were injected orthotopically with 4T1 and MDA-MB-231 cells at 1,000,000 cells/mouse and dosed orally with curcumin daily at 100 mg/kg (n=6 per group: curcumin SMEDDS, blank SMEDDS, untreated). Treatments began 1 day prior to injection of tumor cells. Points, mean (n=6); bars, SE. $P<0.05$, ANOVA.

3.9 Curcumin Cytotoxicity in JC, TuBo, MDA-MB-231, 4T1

The cytotoxic effects of curcumin were evaluated *in vitro* in four breast adenocarcinoma cell lines to determine cellular response to curcumin treatment. As shown in Figure 3.18, curcumin caused a dose-dependent cytotoxicity in all the cell lines studied. At ~14 μM curcumin treatment, JC, MDA-MB-231, and 4T1 cells are less than 10% viable, and at a doubled concentration of ~28 μM, these 3 cell lines exhibited 0% viability. TuBo cells, however, were more resistant to curcumin treatment. At a concentration of ~14 μM, 50 ± 5% of TuBo cells were viable, and at ~28 μM – a high enough concentration to completely eradicate the other three cell types *in vitro* – 20 ± 2% of TuBo cells remained viable. This resistance to curcumin treatment in TuBo cells was also reflected in IC50 values. TuBo was calculated to have the highest IC50 value of 6.40 μM, as compared to 4T1, MDA-MB-231, and JC having values of 4.71, 5.39, and 4.68 μM, respectively (Figure 3.18).

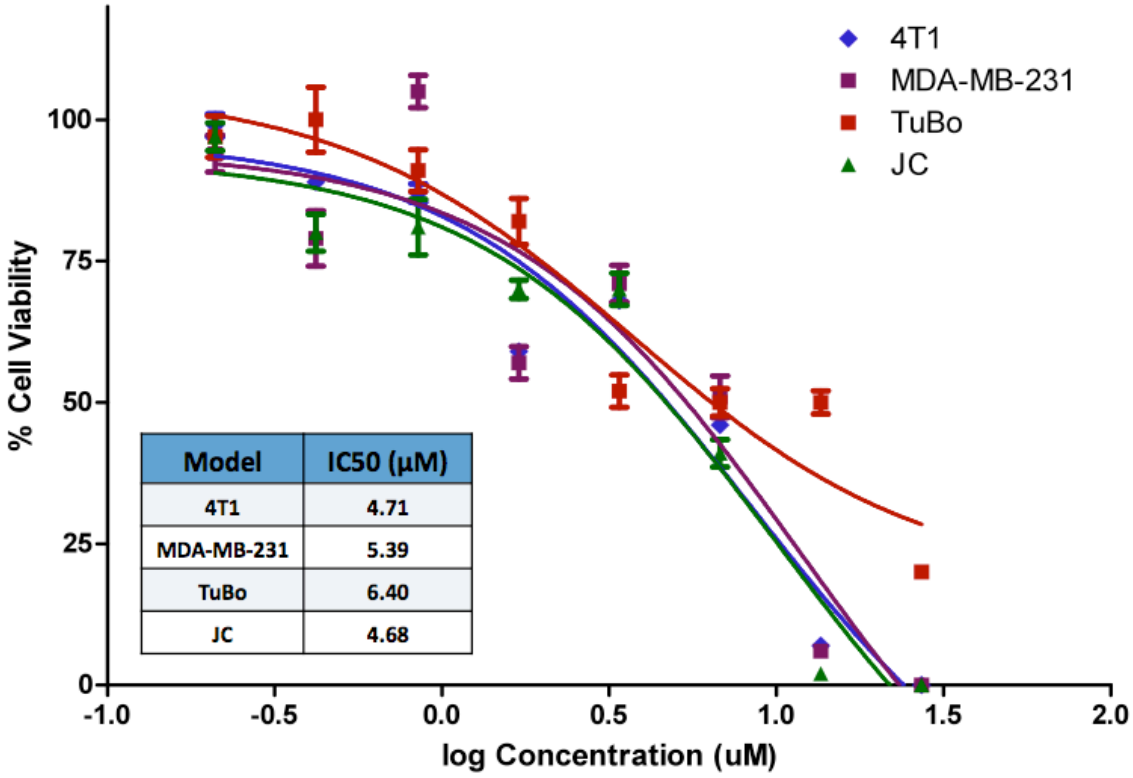

Figure 3.18. Curcumin cytotoxicity and IC50 values of various breast cancer cell lines for curcumin. Cells were treated with 0.1 – 10 µmol/L curcumin for 72 hours. Cell viability was measured using MTS assay, and the results were expressed as percent viability relative to control. Points, mean (n=6); bars, SE.

3.10 β-Glucuronidase Activity Occurs in the Extracellular Matrix

To determine whether β-glucuronidase activity occurs intracellularly or extracellularly, enzyme activity assays were performed with six breast adenocarcinoma cell lines: JC, TuBo, MDA-MB-231, MCF-7, 4T1, and SKBR3. Both intact cells and cell lysates of each cell line were studied. According to the results of the assay, all six cell lines had ~100% of NPG remaining for both intact cells and cell lysates after 2 hours of incubation at 37°C. There was no statistical difference in percent NPG remaining between incubation with the six cell lines and a negative control (PBS), indicating that negligible amounts, if any, of the NPG was converted to parent NP. To ensure that NPG conversion could be detected by this method of analysis, a positive control was included. Incubation of NPG with β-glucuronidase from *Helix pomatia* (Sigma-Aldrich) for 2 hours at 37°C resulted in 8.64 ± 2.16% and 18.00 ± 4.44% remaining by direct incubation and the freeze-thaw method, respectively (Figure 3.19).

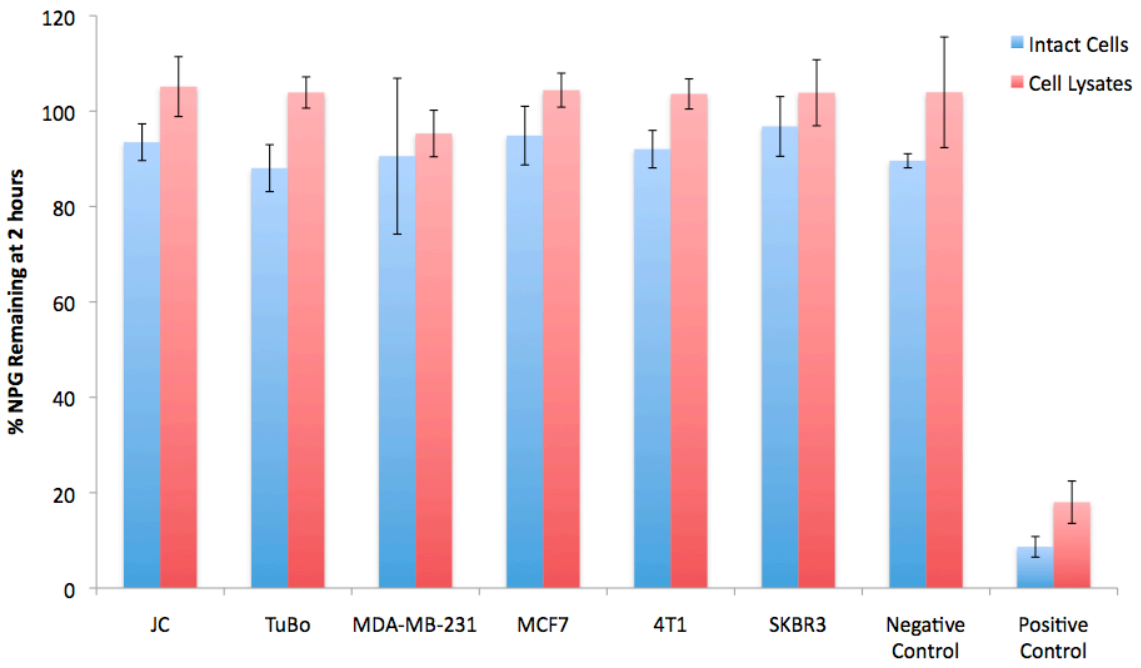

Figure 3.19. No intracellular β-Glucuronidase activity is present in intact cells and cell lysates. Enzyme activity was determined by monitoring the conversion rate of 4-nitrophenyl β-D-glucuronide (NPG) to the parent compound 4-nitrophenol (NP) in intact cells and cell lysates from 6 breast adenocarcinoma cell lines for 2 hours of incubation at 37°C. NPG and NP concentrations were determined by HPLC. Data shown are Mean ± SD, n = 6.

3.11 No Significant β-Glucuronidase Activity in MDA-MB-231 Cells in Hypoxia

Tumor hypoxia is the condition in which tumor cells are deprived of oxygen. Due to the rapid growth of tumors, the vasculature within the tumor tissue becomes highly dysregulated and therefore many regions are exposed to low oxygen levels (hypoxia) [181]. Because hypoxic microenvironments are a common phenomenon within a tumor, these conditions may affect the β-glucuronidase levels and activity of tumor cells subjected to hypoxia. β-glucuronidase activity assays were conducted on MDA-MB-231 breast adenocarcinoma cells that were subjected to hypoxic conditions in culture to determine whether a low-oxygen environment would have an effect on their β-glucuronidase activity *in vitro*. Results showed that after 1 and 3 hours of incubation with NPG, 102.29 ± 6.5% and 92.67 ± 7.02% of NPG remained, respectively (no statistical difference) (Figure 3.20). After 3 hours of incubation, no detectable amount of parent NP was observed. Thus, it was concluded that since negligible amounts of NPG were converted and that no formation of parent NP was detected after 3 hours of incubation with cells in hypoxia, low-oxygen conditions do not induce or affect β-glucuronidase activity levels in intact tumor cells.

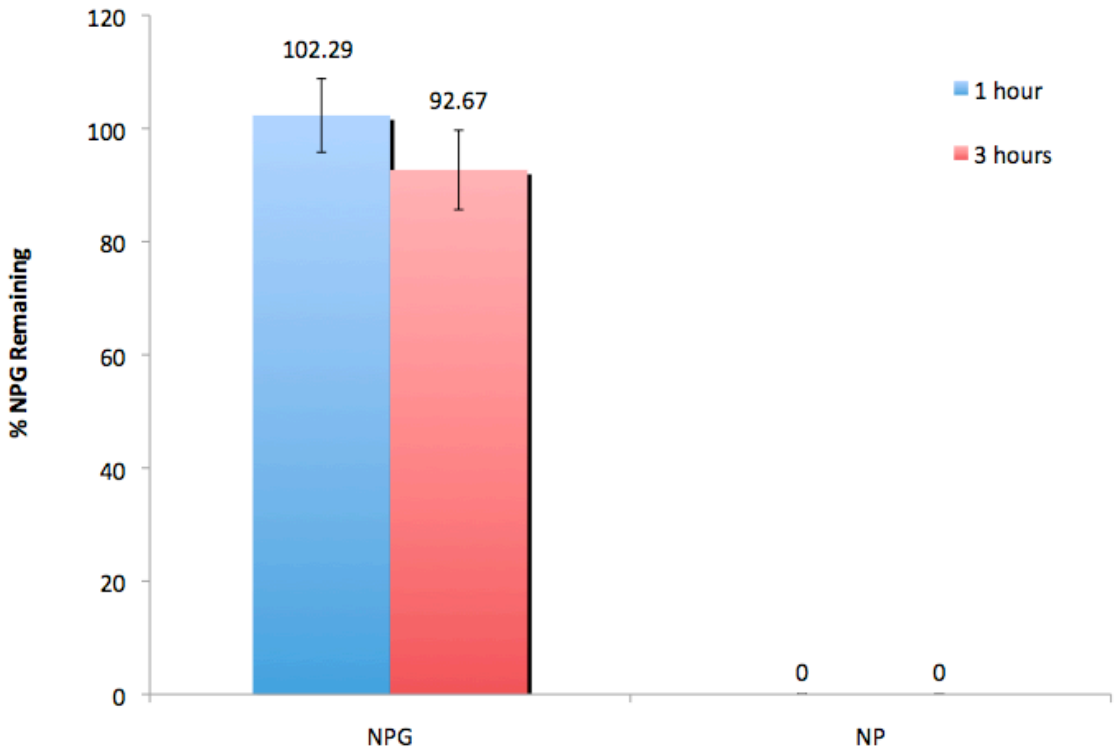

Figure 3.20. No significant β-Glucuronidase activity in MDA-MB-231 cells in hypoxia. Enzyme activity was determined by monitoring the conversion rate of 4-nitrophenyl β-D-glucuronide (NPG) to the parent compound 4-nitrophenol (NP) for 3 hours of incubation under hypoxic conditions (<5% O_2) at 37°C. NPG and NP concentrations were determined by HPLC. Data shown are Mean ± SD, n = 3.

3.12 Pharmacokinetic Study I: Curcumin SMEDDS Oral Dosing in 4T1 and TuBo Tumor-Bearing Balb/c Mice

According to our prodrug activation hypothesis, curcumin glucuronide is the predominant form of curcumin present in the plasma following oral administration of curcumin. Upon reaching the tumor microenvironment, β-glucuronidase present in the tumor extracellular matrix hydrolyzes curcumin glucuronide, yielding active curcumin at the site of action. This hypothesis was tested through evaluation of the pharmacokinetics and biodistribution of curcumin and its metabolite curcumin glucuronide. Healthy female, wild-type Balb/c mice and female mice bearing orthotopic tumors (4T1 or TuBo) were either dosed orally with curcumin SMEDDS or intravenously with curcumin glucuronide directly into the systemic circulation. 4T1 and TuBo models were chosen for these pharmacokinetic studies due to their high and low β-glucuronidase specific activities, respectively, as shown in the tumor homogenate studies. Wild-type Balb/c mice served as the control. Curcumin glucuronide was injected intravenously to study metabolite pharmacokinetics without the absorption barrier.

The first study investigated curcumin and curcumin glucuronide pharmacokinetics following a single oral dose of curcumin SMEDDS at 100 mg/kg in 4T1 (Figure 3.21) and TuBo (Figure 3.22) models. Curcumin glucuronide levels were significantly higher than that of curcumin in plasma, and the profiles of the glucuronide were similar between the two tumor models. Even though maximum concentrations were different between 4T1 (C_{max} = 62.77 μg/mL) and TuBo (C_{max} = 46.97 μg/mL), plasma concentration-time profiles were similar, and the two $AUC_{0-\infty}$ were practically identical: $AUC_{0-\infty}$ in 4T1 = 178.46 μg*hr/mL; $AUC_{0-\infty}$ in TuBo = 177.32 μg*hr/mL. The elimination half-lives were

also nearly the same for curcumin glucuronide; after non-compartmental analysis, $t_{1/2}$ was estimated to be 3.86 hours in the 4T1 model and 3.97 hours in the TuBo model. These concentration-time profiles show that, following oral curcumin delivery, the glucuronide levels in plasma are independent of the tumor model.

However, curcumin levels in the tumor tissue were different for the two tumor models. The $AUC_{0-\infty}$ and C_{max} for curcumin in the 4T1 model was significantly higher than that in the TuBo model. After non-compartmental analysis, C_{max} of curcumin in 4T1 was determined to be 104.87 ng/g, whereas in TuBo, C_{max} was 62.95 ng/g. The higher curcumin levels in 4T1 tumors were also reflected by the calculated $AUC_{0-\infty}$ values, in which $AUC_{0-\infty}$ for 4T1 was 476.47 ng*hr/g, while $AUC_{0-\infty}$ for TuBo was lower at 370.30 ng*hr/g. The average $t_{1/2}$ for curcumin elimination from the tumor was determined to be 40.53 hours for both models.

Liver concentrations of curcumin were highly variable and did not follow any type of trend. In the liver of 4T1 tumor-bearing mice, curcumin levels ranged from 0.95 ng/g to 5873.42 ng/g; in TuBo tumor-bearing mice, levels ranged from 2.34 ng/g to 2775.60 ng/g. Curcumin glucuronide concentrations were negligible in the liver for both models.

A

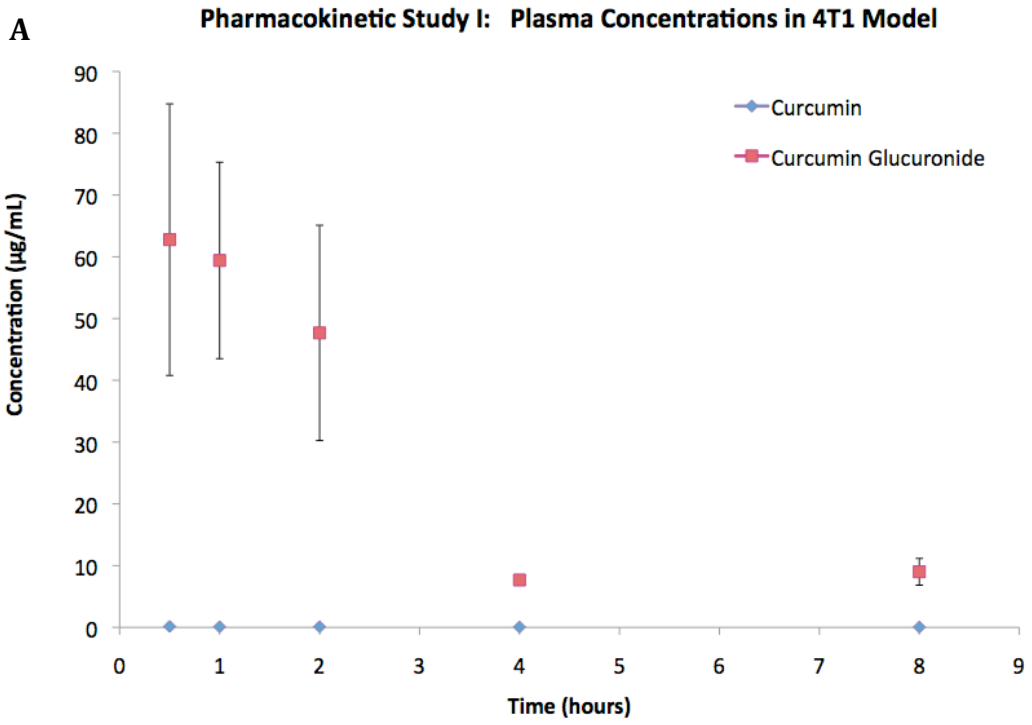
Pharmacokinetic Study I: Plasma Concentrations in 4T1 Model
Curcumin
Curcumin Glucuronide
Concentration (µg/mL)
Time (hours)
0
10
20
30
40
50
60
70
80
90
0
1
2
3
4
5
6
7
8
9

B

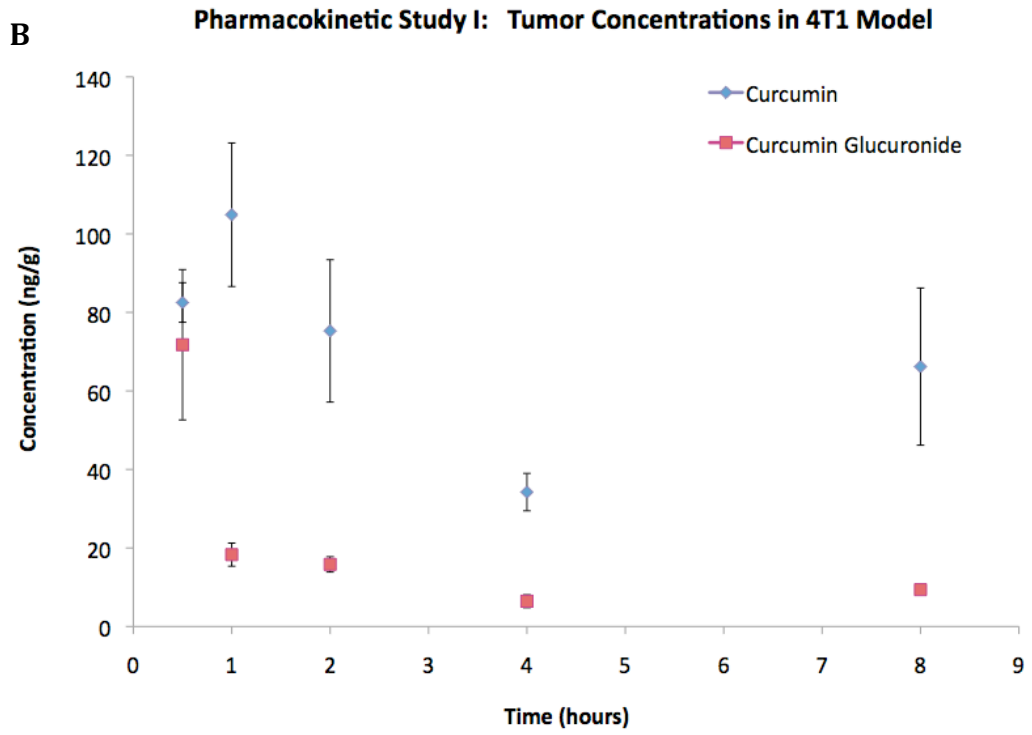
Pharmacokinetic Study I: Tumor Concentrations in 4T1 Model
Curcumin
Curcumin Glucuronide
Concentration (ng/g)
Time (hours)
0
20
40
60
80
100
120
140
0
1
2
3
4
5
6
7
8
9

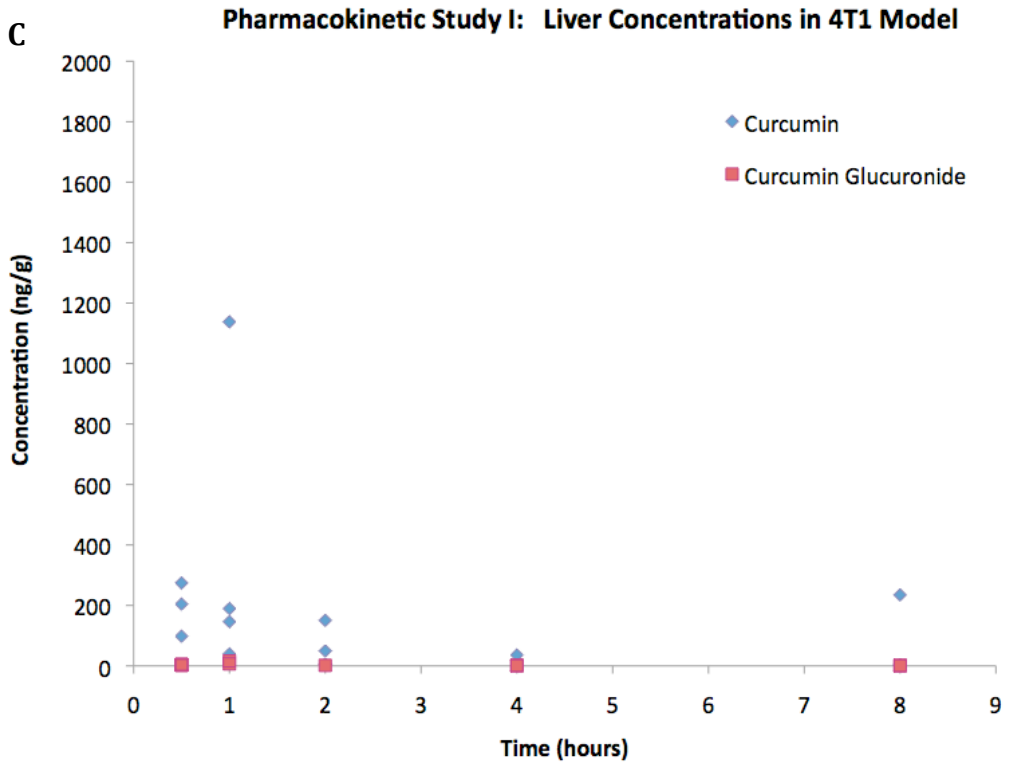

Figure 3.21. Concentration-time profiles of curcumin and its metabolite curcumin glucuronide in **(A)** plasma, **(B)** tumor, and **(C)** liver of 4T1 tumor bearing mice following a single oral dose of curcumin SMEDDS formulation (100 mg/kg). Curcumin and curcumin glucuronide concentrations were determined by LC-MS/MS. Points, mean (n = 3-4); bars, SE.

A

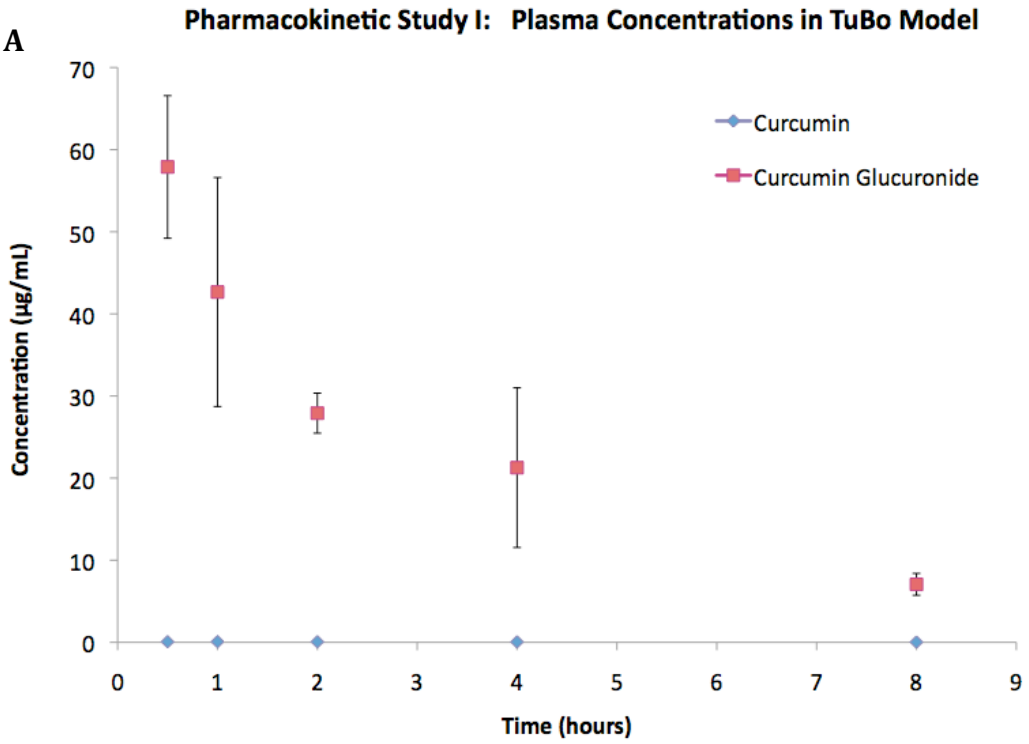
Pharmacokinetic Study I: Plasma Concentrations in TuBo Model
Curcumin
Curcumin Glucuronide
Concentration (µg/mL)
Time (hours)
0
10
20
30
40
50
60
70
0
1
2
3
4
5
6
7
8
9

B

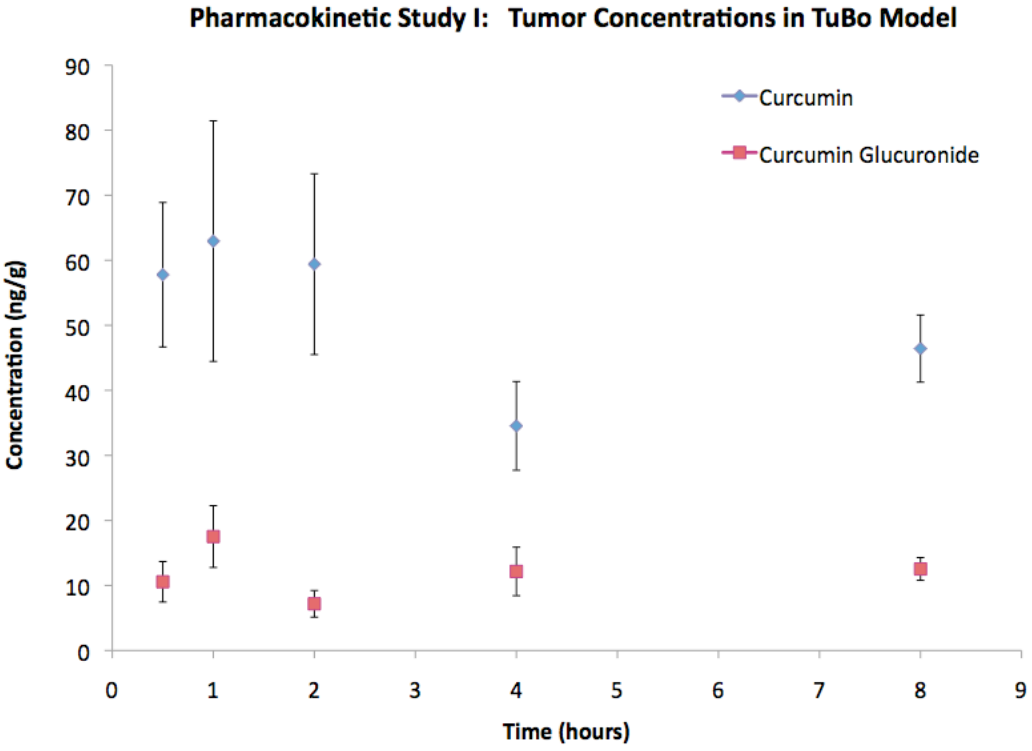
Pharmacokinetic Study I: Tumor Concentrations in TuBo Model
Curcumin
Curcumin Glucuronide
Concentration (ng/g)
Time (hours)
0
10
20
30
40
50
60
70
80
90
0
1
2
3
4
5
6
7
8
9

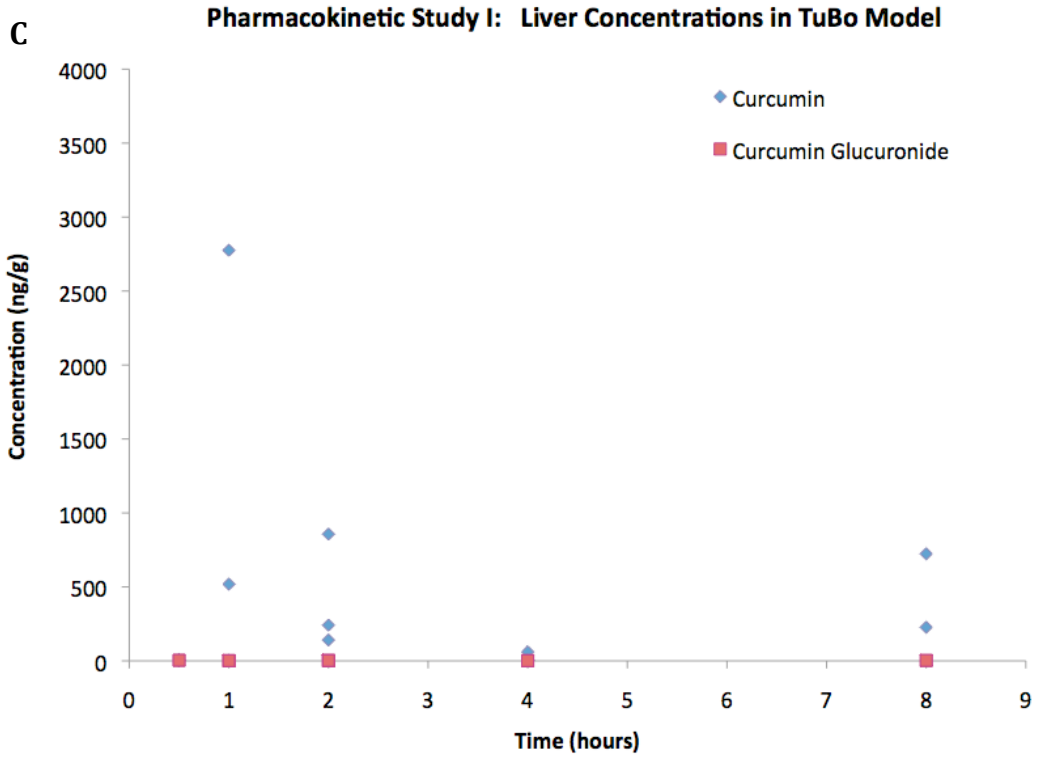

Figure 3.22. Concentration-time profiles of curcumin and its metabolite curcumin glucuronide in **(A)** plasma, **(B)** tumor, and **(C)** liver of TuBo tumor bearing mice following a single oral dose of curcumin SMEDDS formulation (100 mg/kg). Curcumin and curcumin glucuronide concentrations were determined by LC-MS/MS. Points, mean (n = 3-4); bars, SE.

3.13 Pharmacokinetic Study II: Curcumin Glucuronide Intravenous Dosing in 4T1 and TuBo Tumor-Bearing Balb/c Mice

Since curcumin glucuronide is the primary metabolite that is present in plasma following oral dosing, the pharmacokinetics of the glucuronide itself was investigated. The second study evaluated curcumin and curcumin glucuronide pharmacokinetics following a single intravenous dose of curcumin glucuronide at 2 mg/kg in both 4T1 (Figure 3.23) and TuBo (Figure 3.24) models. As in the case with oral dosing of curcumin SMEDDS, curcumin glucuronide concentrations in plasma were consistent between the two tumor models. Elimination half-lives were virtually the same – 3.93 hours in 4T1 and 3.98 hours in TuBo. T_{max} and C_{max} were almost identical as well: T_{max} = 0.25 hours for both models; C_{max} (or $C_{0.25}$) for 4T1 = 21.81 μg/mL and C_{max} for TuBo = 23.32 μg/mL. Based on non-compartmental analysis, C_o was estimated to be 48.26 μg/mL for 4T1 and 52.01 μg/mL for TuBo. $AUC_{0-\infty}$ values were 22.70 μg*hr/mL for 4T1 and 22.80 μg*hr/mL for TuBo. These results confirm that regardless of the tumor model and whether curcumin glucuronide is metabolically released into the systemic circulation or dosed directly into the systemic circulation, the metabolite exhibits similar pharmacokinetics. Curcumin levels in plasma were negligible.

Curcumin concentration levels in the tumor and lungs were similar in both 4T1 and TuBo models following an intravenous dose of the glucuronide. In the two models, curcumin levels in tumor started off low at early time points (0.25 – 4 hours) but then increased to a steady concentration that plateaued off (> 8 hours) at approximately 30 ng of curcumin per gram of tumor tissue. Similar was the case in lungs, although curcumin concentrations were initially higher (30 – 50 ng/g) at earlier time points of 0 to 2 hours,

but then steadied off after 4 hours post-intravenous dose at ~30 ng/g. Curcumin glucuronide levels in the tumor and lungs were significantly lower than that of parent curcumin.

Liver concentration levels of both curcumin and curcumin glucuronide were minimal on average as compared to plasma and other tissues. With the exception of curcumin glucuronide levels at 15 minutes post-intravenous dose for 4T1, which had a concentration of 8.35 ng/g, both compounds were found to be at concentration levels of <6 ng/g in both models.

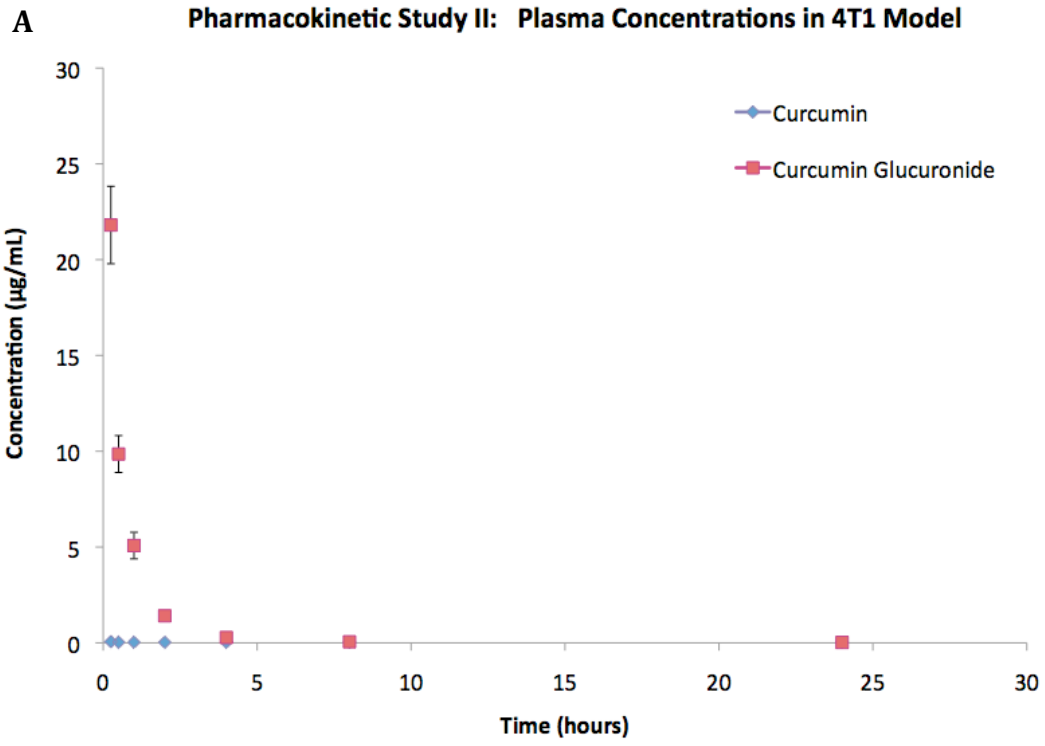

B

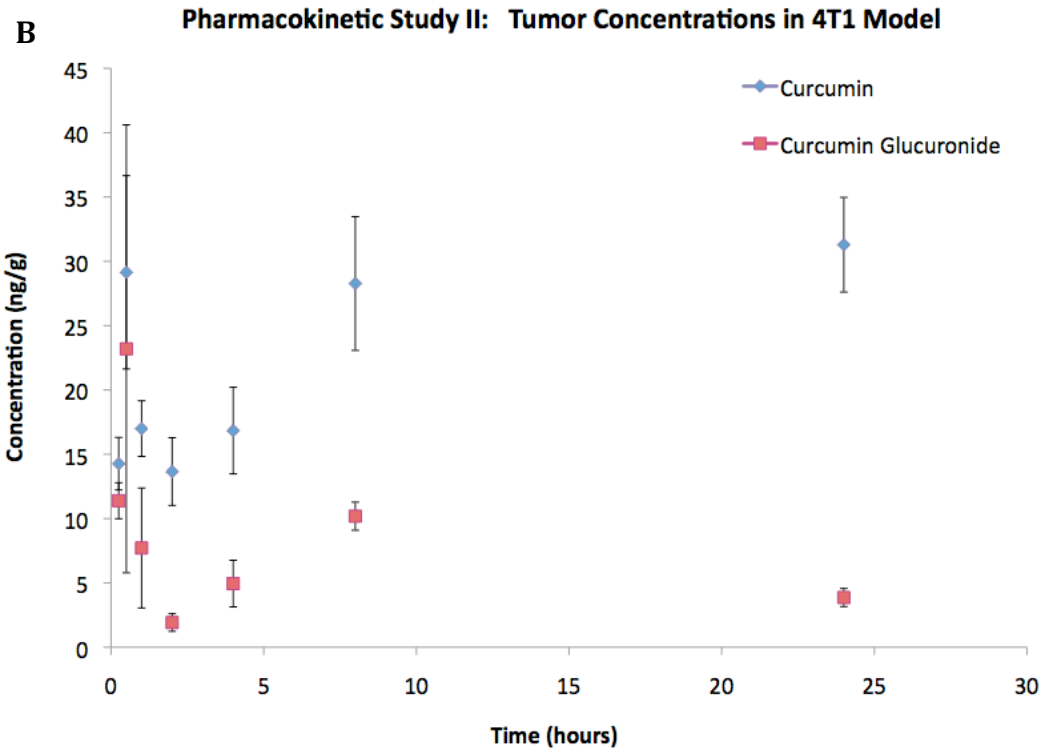
Pharmacokinetic Study II: Tumor Concentrations in 4T1 Model
Curcumin
Curcumin Glucuronide
Concentration (ng/g)
Time (hours)
0
5
10
15
20
25
30
35
40
45

C

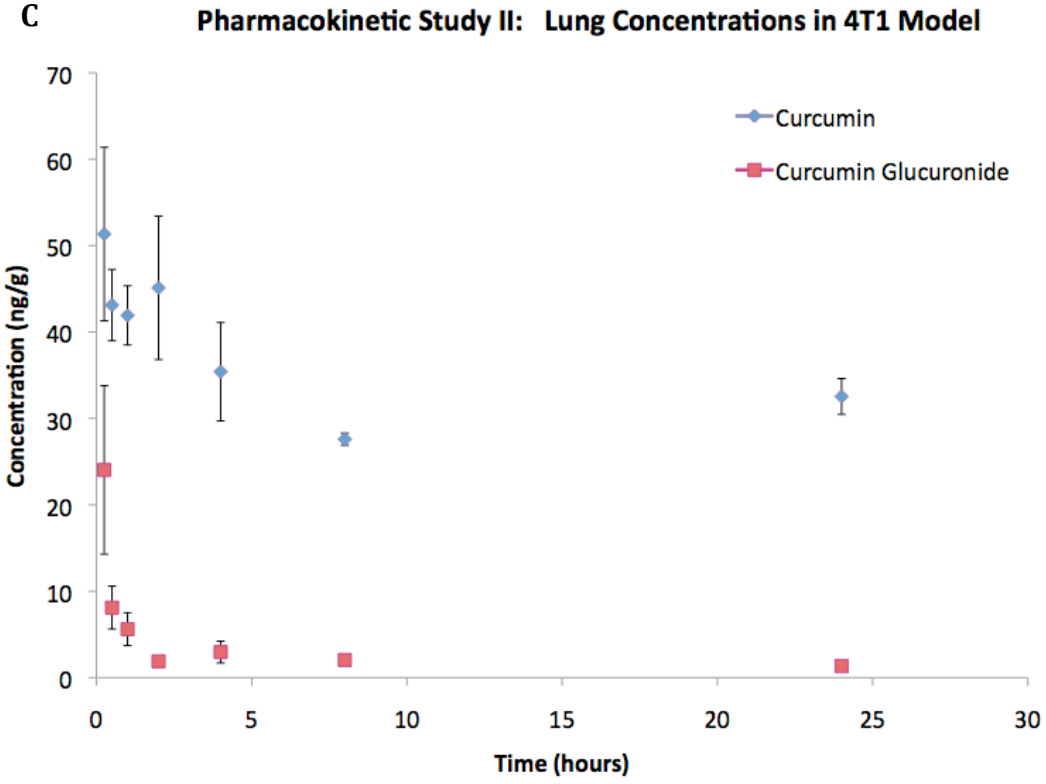
Pharmacokinetic Study II: Lung Concentrations in 4T1 Model
Curcumin
Curcumin Glucuronide
Concentration (ng/g)
Time (hours)
0
10
20
30
40
50
60
70
0
5
10
15
20
25
30

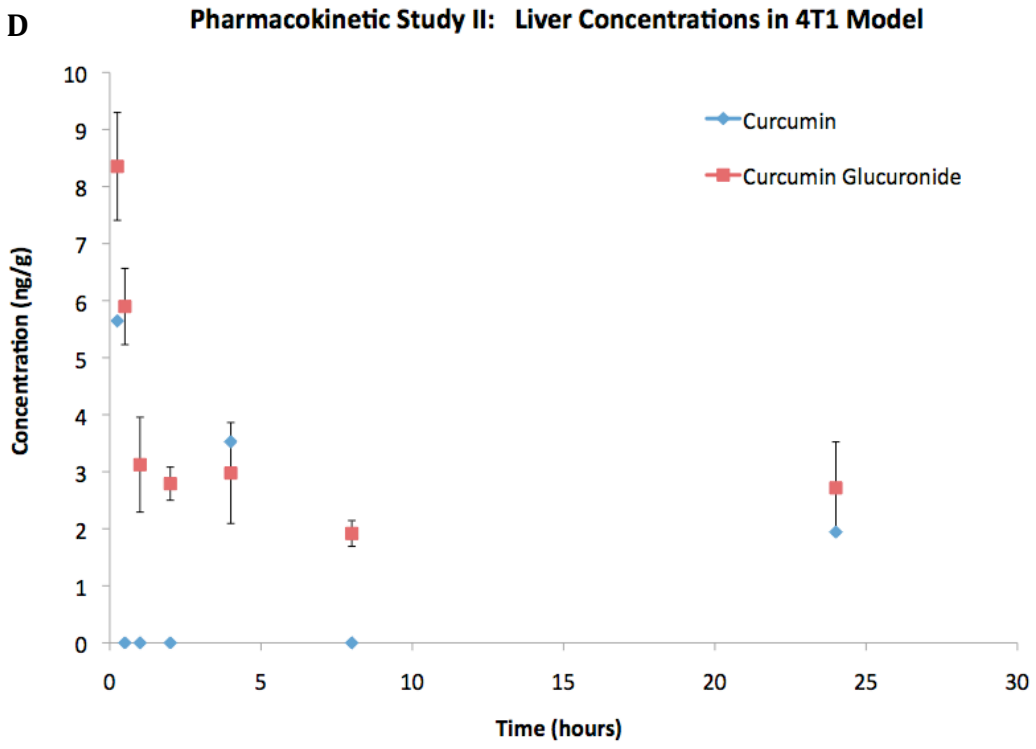

Figure 3.23. Concentration-time profiles of curcumin and its metabolite curcumin glucuronide in **(A)** plasma, **(B)** tumor, **(C)** lung, and **(D)** liver of 4T1 tumor bearing mice following a single intravenous dose of curcumin glucuronide dissolved in 80:20 DPBS:DMSO mixture (2 mg/kg). Curcumin and curcumin glucuronide concentrations were determined by LC-MS/MS. Points, mean (n = 3-4); bars, SE.

A

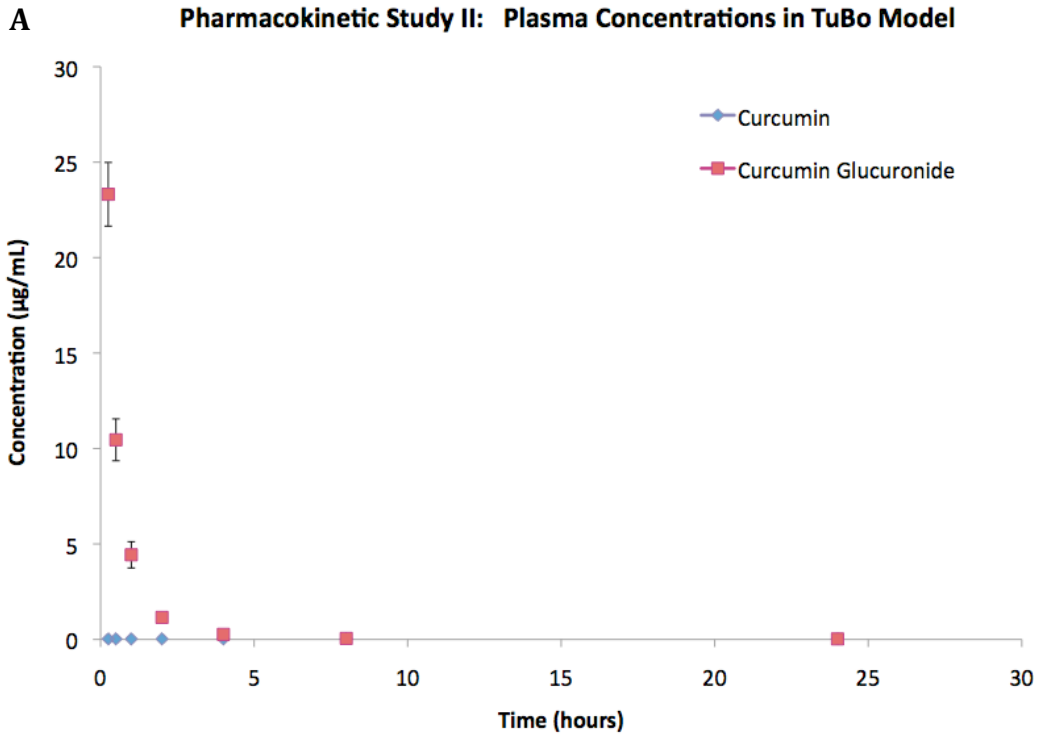
Pharmacokinetic Study II: Plasma Concentrations in TuBo Model
Curcumin
Curcumin Glucuronide
Concentration (µg/mL)
Time (hours)
0
5
10
15
20
25
30

B

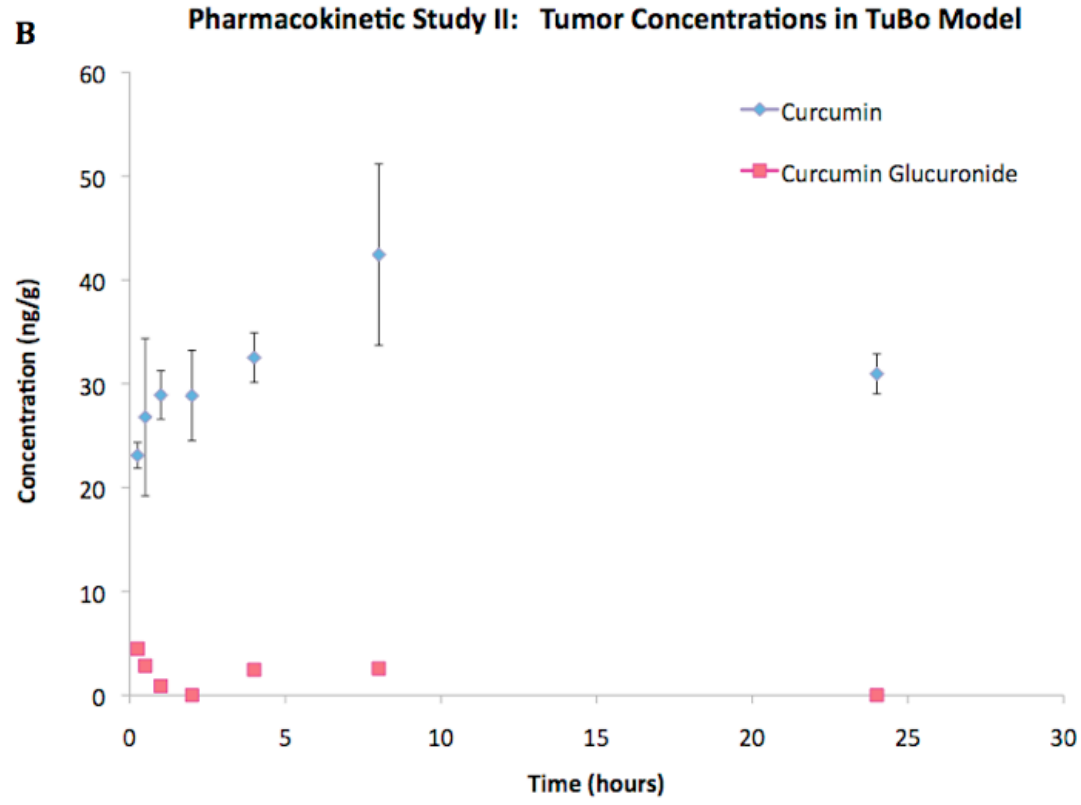
Pharmacokinetic Study II: Tumor Concentrations in TuBo Model
Curcumin
Curcumin Glucuronide
Concentration (ng/g)
Time (hours)
0
10
20
30
40
50
60
0
5
10
15
20
25
30

C

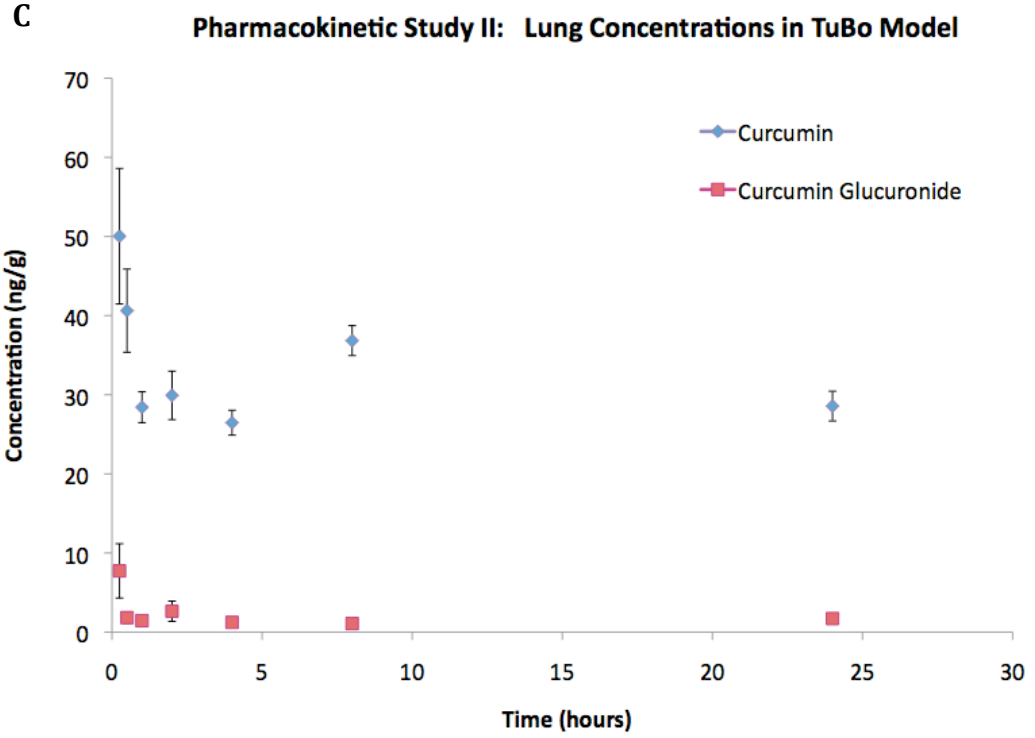
Pharmacokinetic Study II: Lung Concentrations in TuBo Model
Curcumin
Curcumin Glucuronide
Concentration (ng/g)
Time (hours)
0
10
20
30
40
50
60
70
0
5
10
15
20
25
30

D

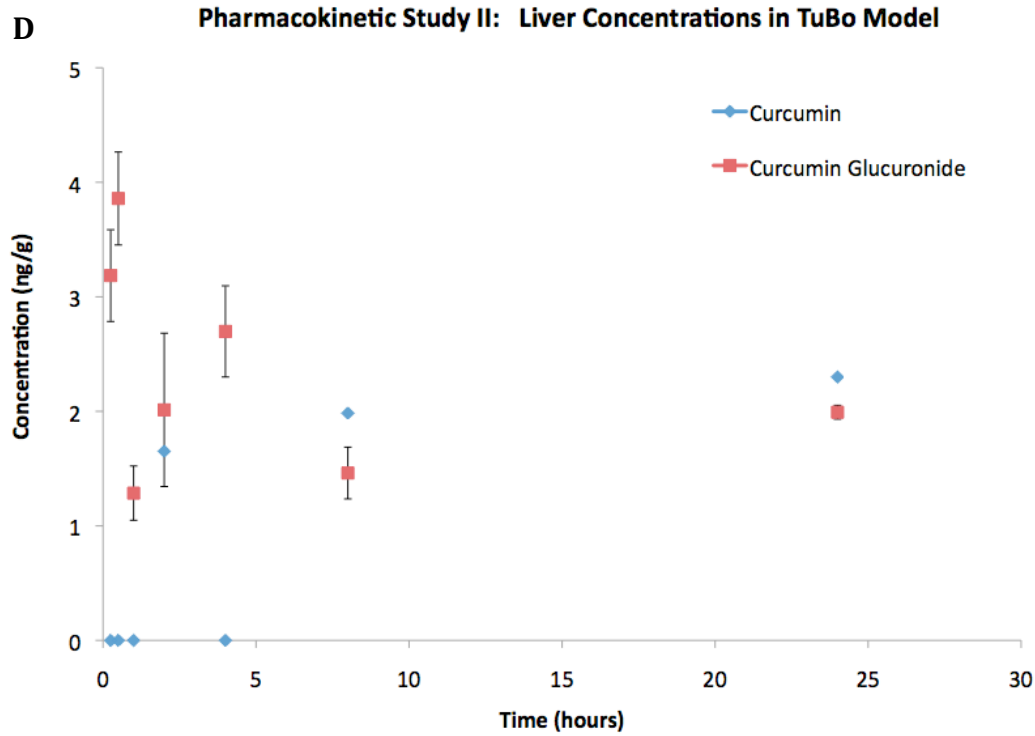
Pharmacokinetic Study II: Liver Concentrations in TuBo Model
Curcumin
Curcumin Glucuronide
Concentration (ng/g)
Time (hours)
0
1
2
3
4
5
0
5
10
15
20
25
30

Figure 3.24. Concentration-time profiles of curcumin and its metabolite curcumin glucuronide in **(A)** plasma, **(B)** tumor, **(C)** lung, and **(D)** liver of TuBo tumor bearing mice following a single intravenous dose of curcumin glucuronide dissolved in 80:20 DPBS:DMSO mixture (2 mg/kg). Curcumin and curcumin glucuronide concentrations were determined by LC-MS/MS. Points, mean (n = 3-4); bars, SE.

3.14 Pharmacokinetic Study III: Curcumin Glucuronide Intravenous Dosing in Wild-Type Balb/c Mice

To assess whether the tumor presence in an animal model would have an effect on the biodistribution of curcumin and curcumin glucuronide, a third pharmacokinetic study was conducted in which healthy, wild-type female Balb/c mice received a single intravenous dose of curcumin glucuronide at 2 mg/kg (Figure 3.25). Results showed the concentration-time profile for curcumin glucuronide in wild-type Balb/c mice to be nearly identical to the profiles of glucuronide in tumor-bearing mice. Like in the 4T1 and TuBo models, curcumin levels in plasma were minimal as compared to the curcumin glucuronide levels. These data suggest that since the pharmacokinetic profiles and parameters of curcumin glucuronide are consistent between the healthy and tumor-bearing animals, the disease status of the animal does not affect the biodistribution of curcumin glucuronide.

Curcumin levels in healthy mammary tissue of the female wild-type mice proved to be significantly lower than in the tumor of the 4T1 and TuBo models when dosed intravenously with curcumin glucuronide. In the wild-type mammary tissue, curcumin levels fall to <10 ng/g at 2 hours and beyond, as opposed to steady concentrations of ~30

ng/g in the tumor tissue in the 4T1 and TuBo models at similar time points. The lower concentration levels of curcumin in healthy mammary tissue as opposed to higher levels in tumor tissue is consistent with the comparatively lower and higher specific activity levels of β-glucuronidase in healthy and tumor-bearing mice, respectively, which strongly supports the prodrug hypothesis.

Lung and liver concentrations of curcumin in healthy mice were highly variable when dosed with curcumin glucuronide intravenously. Curcumin concentrations in lungs ranged from 1.59 ng/g to 749.21 ng/g; curcumin levels in liver ranged from 2.85 ng/g to 468.25 ng/g. While curcumin glucuronide in the lungs and liver exhibited a standard elimination curve according to the concentration-time profiles, the glucuronide levels were significantly lower than that of curcumin in both organs.

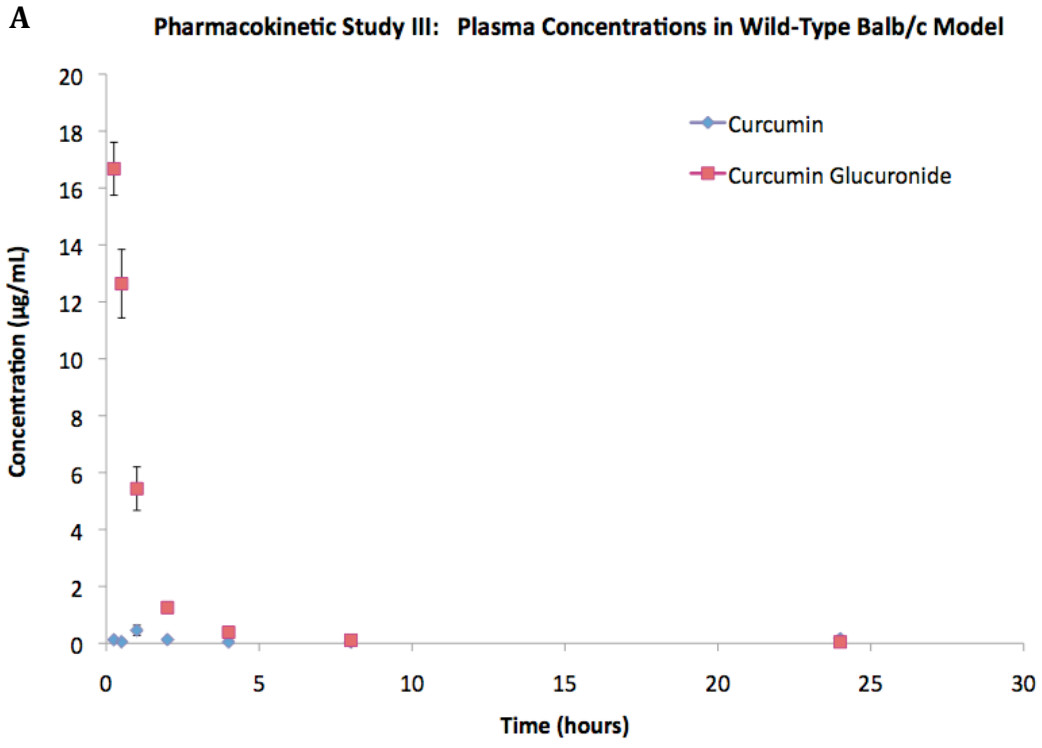

B

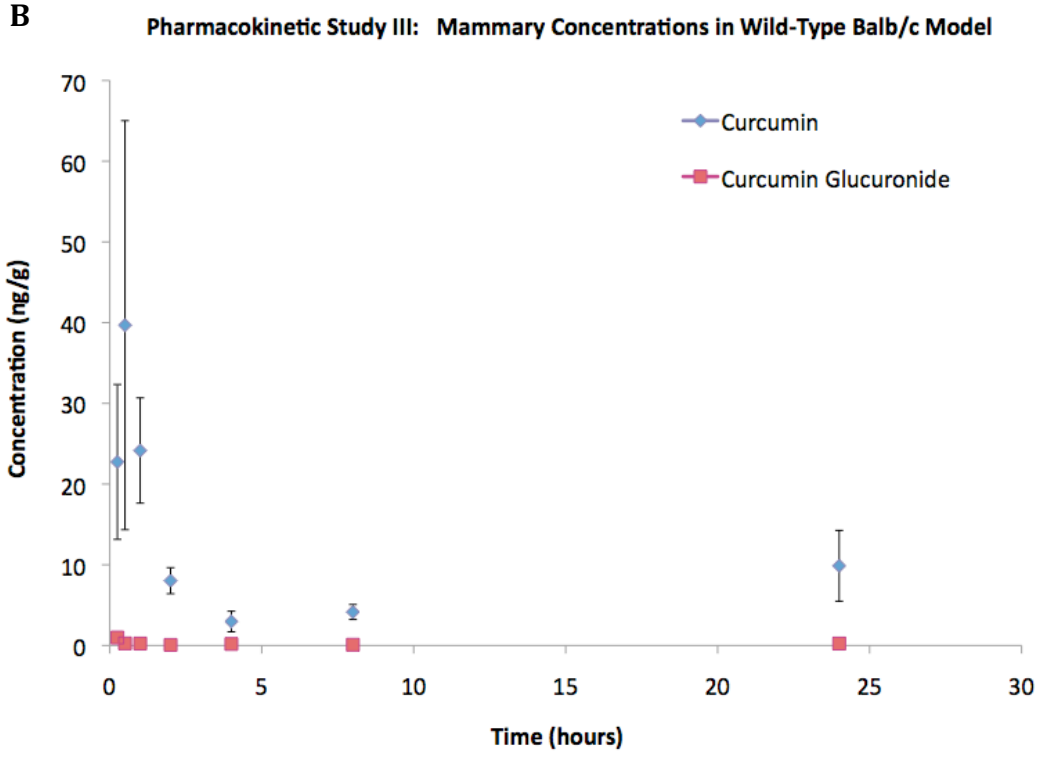
Pharmacokinetic Study III: Mammary Concentrations in Wild-Type Balb/c Model
Curcumin
Curcumin Glucuronide
Concentration (ng/g)
Time (hours)
0
10
20
30
40
50
60
70
0
5
10
15
20
25
30

C

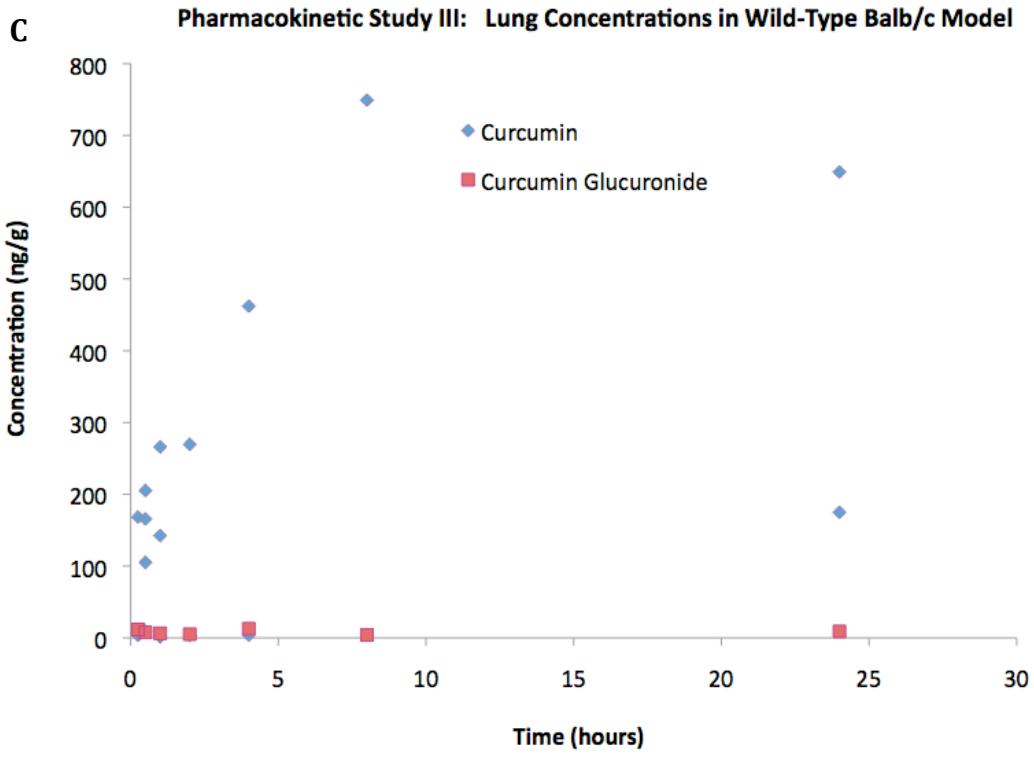
Pharmacokinetic Study III: Lung Concentrations in Wild-Type Balb/c Model
Curcumin
Curcumin Glucuronide
Concentration (ng/g)
Time (hours)
0
100
200
300
400
500
600
700
800
0
5
10
15
20
25
30

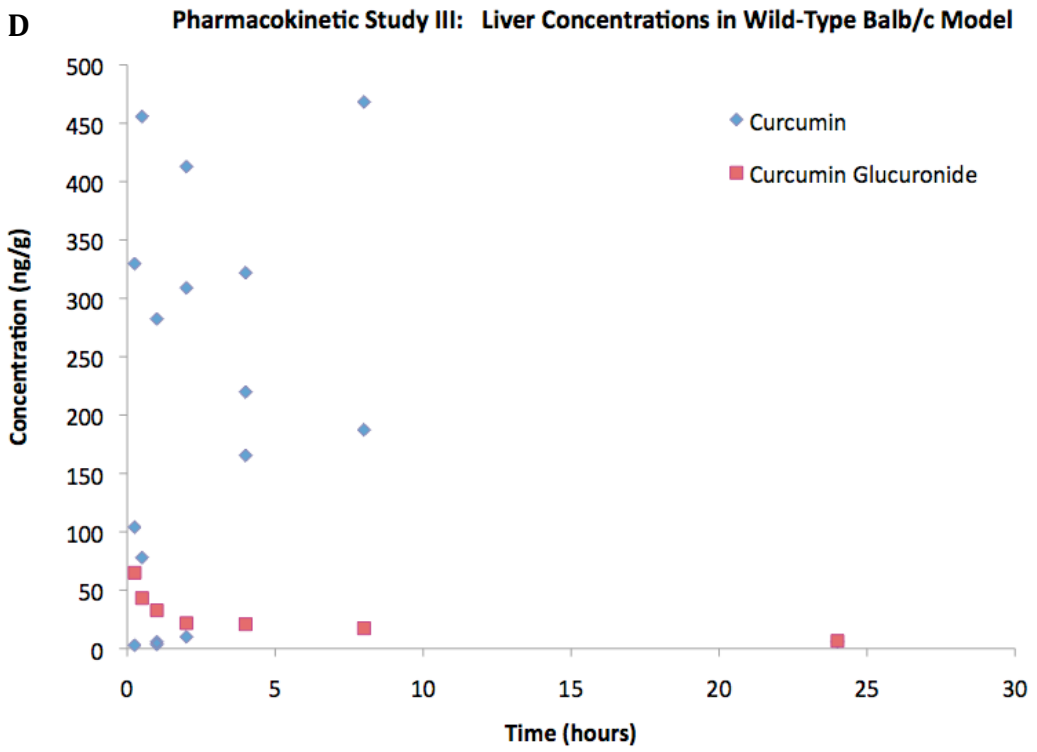

Figure 3.25. Concentration-time profiles of curcumin and its metabolite curcumin glucuronide in **(A)** plasma, **(B)** mammary, **(C)** lung, and **(D)** liver of wild-type Balb/c mice following a single intravenous dose of curcumin glucuronide dissolved in 80:20 DPBS:DMSO mixture (2 mg/kg). Curcumin and curcumin glucuronide concentrations were determined by LC-MS/MS. Points, mean (n = 3-4); bars, SE.

3.15 Accumulated Curcumin Concentrations in Tumor Tissue from Transgenic Balb-*neu*T and Orthotopic Models: JC (Triple Negative) and TuBo (HER-2+)

Curcumin is capable of long-term tissue accumulation due to its hydrophobic nature, which can be beneficial in exerting its therapeutic effects at the target site. In these set of studies, female transgenic Balb-*neu*T mice bearing spontaneously-formed tumors and wild-type female Balb/c mice bearing orthotopically implanted JC and TuBo tumors were orally administered chronic doses of curcumin SMEDDS formulation. Balb-*neu*T mice received oral doses at 100 mg/kg for 5 consecutive days, and orthotopic models received the same daily dose over a period of one month. At the end of the study, tumor tissue and plasma were collected and analyzed for accumulated curcumin concentrations by HPLC. In Balb-*neu*T mice, 0.517 ± 0.145 μM of curcumin accumulated in the tumor after 5 days of receiving daily oral doses (Figure 3.26). However, no curcumin was detected in the plasma of the same mice. Similar was the case with the orthotopic JC and TuBo models in terms of curcumin accumulation ratio between tumor and plasma. TuBo tumors accumulated 0.755 ± 0.079 μM and JC accumulated 0.095 ± 0.057 μM of curcumin in tumor, whereas plasma concentrations were comparatively negligible: 0.007 ± 0.002 μM in TuBo and 0.005 ± 0.004 μM in JC (Figure 3.27).

Interestingly, HER-2+ subtype transgenic Balb-*neu*T and orthotopic TuBo models had a 5.5-fold and 8.0-fold higher accumulation of curcumin in tumor, respectively, as compared to triple negative orthotopic JC model. This could be due to higher infiltration of inflammatory cells such as macrophages and neutrophils. Such cells would in turn

release elevated levels of β-glucuronidase, and hence greater activation and accumulation of curcumin in this subtype as compared to the triple negative (JC) model.

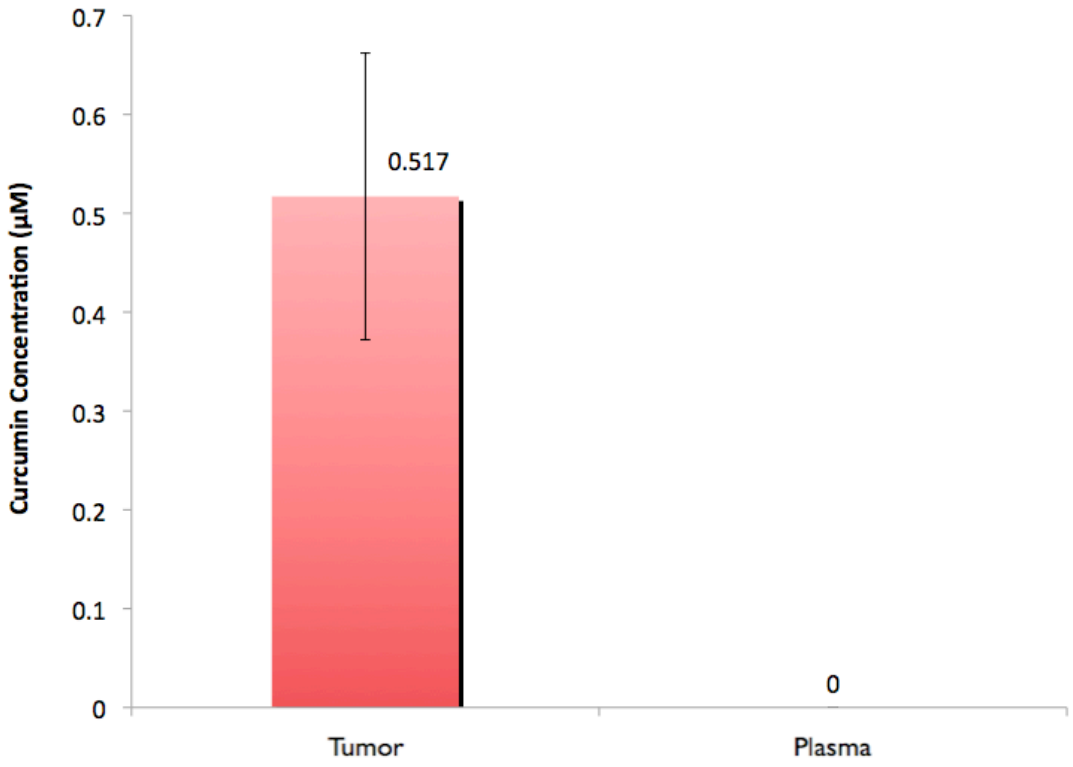

Figure 3.26. Accumulated curcumin concentrations in tumor tissue and plasma from HER-2+ transgenic Balb-*neu*T model. Female Balb-*neu*T mice bearing mammary tumors were orally dosed with curcumin SMEDDS formulation at 100 mg/kg for 5 consecutive days prior to tissue and plasma collection. Curcumin concentrations were determined by HPLC. Data shown are Mean ± SE, n = 3.

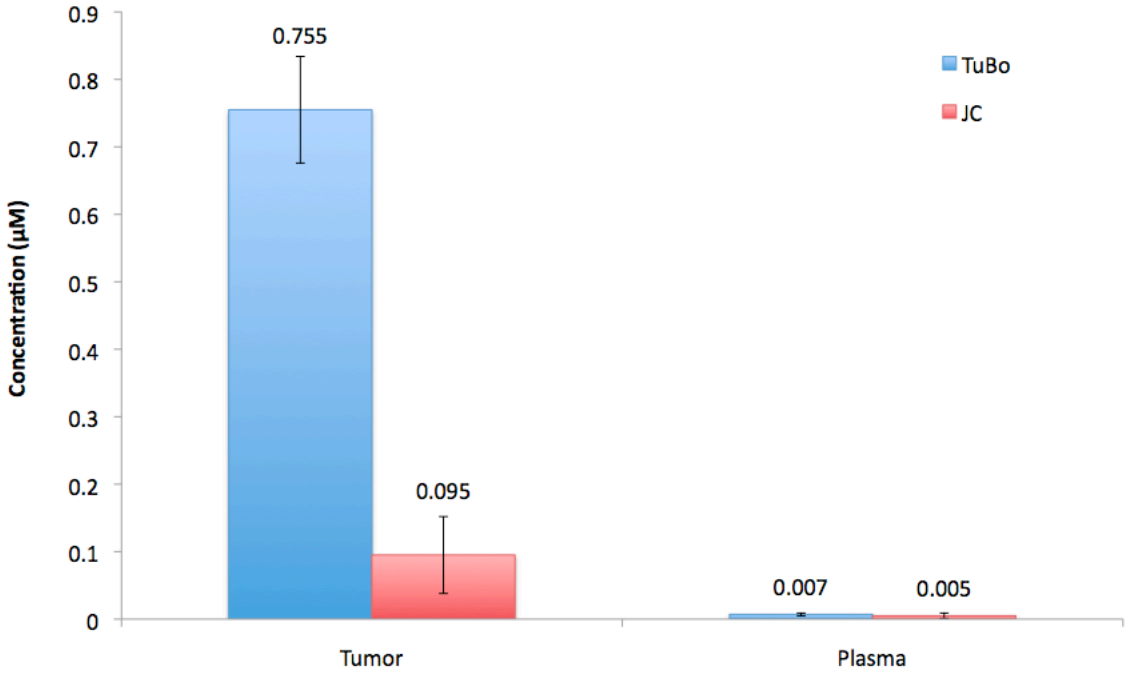

Figure 3.27. Accumulated curcumin concentrations in tumor tissue and plasma from orthotopic models: JC (triple negative) and TuBo (HER-2+). Female Balb/c mice bearing JC and TuBo orthotopic tumors were orally dosed daily with curcumin SMEDDS formulation at 100 mg/kg for 1 month prior to tissue and plasma collection. Curcumin concentration was determined by HPLC. Data shown are Mean ± SE, n = 3.

3.16 Accumulation of Curcumin and Curcumin Glucuronide in Mammary Tissue from Wild-Type Balb/c and Tumor Tissue from Orthotopic 4T1 Mouse Models after Single and Multiple Dosing of Curcumin SMEDDS

Accumulation of curcumin and curcumin glucuronide was evaluated in mammary tissue, liver, and plasma of wild-type Balb/c mice and in 4T1 tumor-bearing mice that received once-daily, oral doses of curcumin SMEDDS formulation for 14 consecutive days. Plasma and tissue were collected at 1 hour post-dose on the last day of the study. Plasma levels of curcumin glucuronide were practically the same between the wild-type (16.76 ± 2.99 μg/mL) and 4T1 tumor-bearing (15.08 ± 7.50 μg/mL) mice. No detectable levels of curcumin were found in plasma (Figure 3.28.a.). In tumor tissue from the 4T1 model, nearly 15-fold higher levels of curcumin (149.80 ± 18.00 ng/g) were present as compared to that in the mammary tissue of wild-type mice (10.52 ± 2.10 ng/g) ($P<0.05$). Curcumin glucuronide followed a similar trend in these tissues, although levels were much lower than that of curcumin (Figure 3.28.b.). In the liver, curcumin glucuronide levels were also higher in the 4T1 model (244.23 ± 25.95 ng/g) than in the wild-type model (116.04 ± 10.55 ng/g) (Figure 3.28.c.).

The degree of curcumin accumulation in the tumor tissue of 4T1 tumor-bearing mice after having received a single dose or fourteen daily doses of oral curcumin SMEDDS was compared. Results showed that chronic dosing of the curcumin SMEDDS formulation over a period of two weeks yielded significantly higher levels of curcumin in tumor as opposed to just a single dose. The group of tumor-bearing mice receiving multiple doses had an average curcumin concentration of 138.53 ± 20.04 ng/g in tumor as compared to the group receiving only a single, one-time dose, which had an average

concentration of 100.78 ± 10.30 ng/g (P<0.05). Curcumin glucuronide concentrations in tumor were much lower (<15 ng/g) in both groups (Figure 3.29).

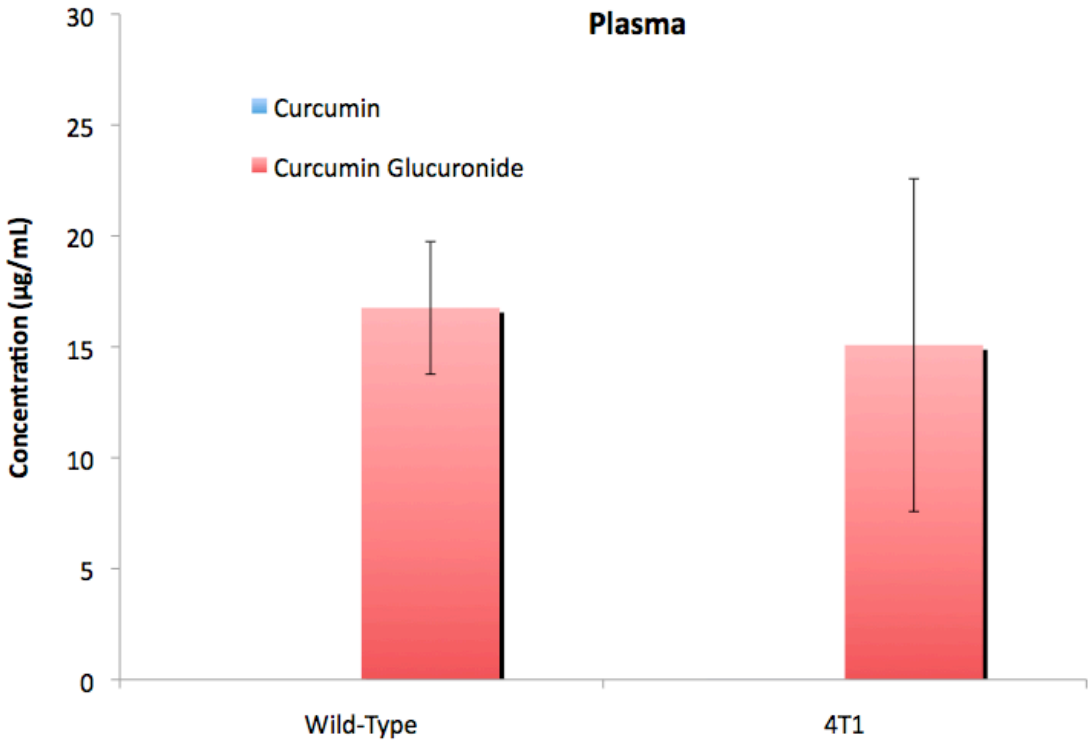

Figure 3.28.a. Curcumin and curcumin glucuronide concentrations in plasma from wild-type Balb/c and orthotopic 4T1 mouse models. Female wild-type Balb/c mice and 4T1 tumor bearing mice were orally dosed daily with curcumin SMEDDS formulation at 100 mg/kg for 14 days prior to tissue and plasma collection. Curcumin and curcumin glucuronide concentrations were determined by LC-MS/MS. Data shown are Mean ± SE, n = 5.

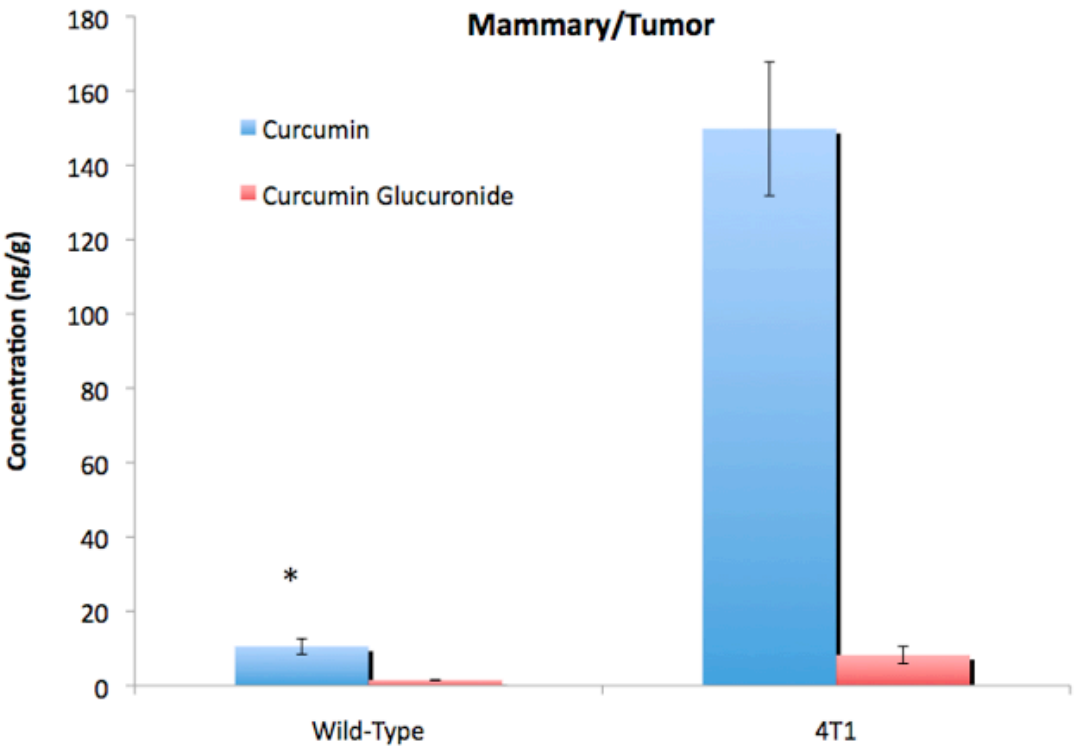

Figure 3.28.b. Accumulated curcumin and curcumin glucuronide concentrations in mammary tissue from wild-type Balb/c and tumor tissue from orthotopic 4T1 mouse models. Female wild-type Balb/c mice and 4T1 tumor bearing mice were orally dosed daily with curcumin SMEDDS formulation at 100 mg/kg for 14 days prior to tissue and plasma collection. Curcumin and curcumin glucuronide concentrations were determined by LC-MS/MS. Data shown are Mean ± SE, n = 5. * $P<0.05$, compared to curcumin concentrations in the 4T1 model, ANOVA.

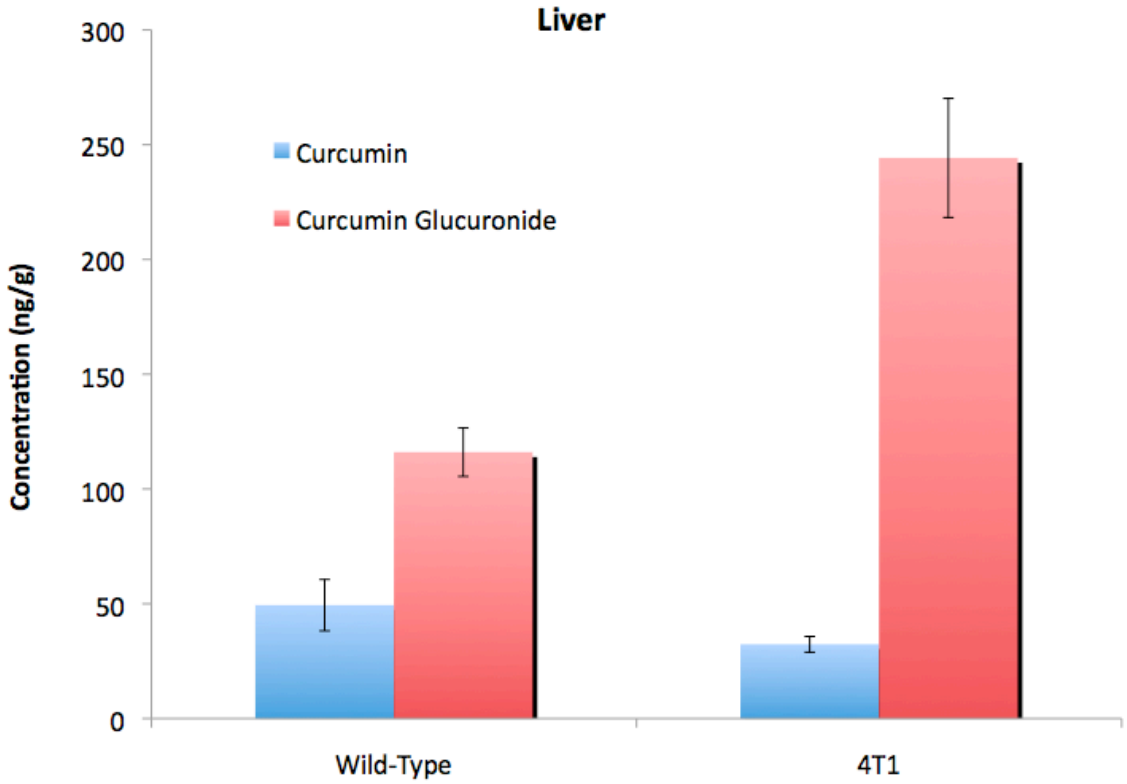

Figure 3.28.c. Accumulated curcumin and curcumin glucuronide concentrations in liver tissue from wild-type Balb/c and orthotopic 4T1 mouse models. Female wild-type Balb/c mice and 4T1 tumor bearing mice were orally dosed daily with curcumin SMEDDS formulation at 100 mg/kg for 14 days prior to tissue and plasma collection. Curcumin and curcumin glucuronide concentrations were determined by LC-MS/MS. Data shown are Mean ± SE, n = 5.

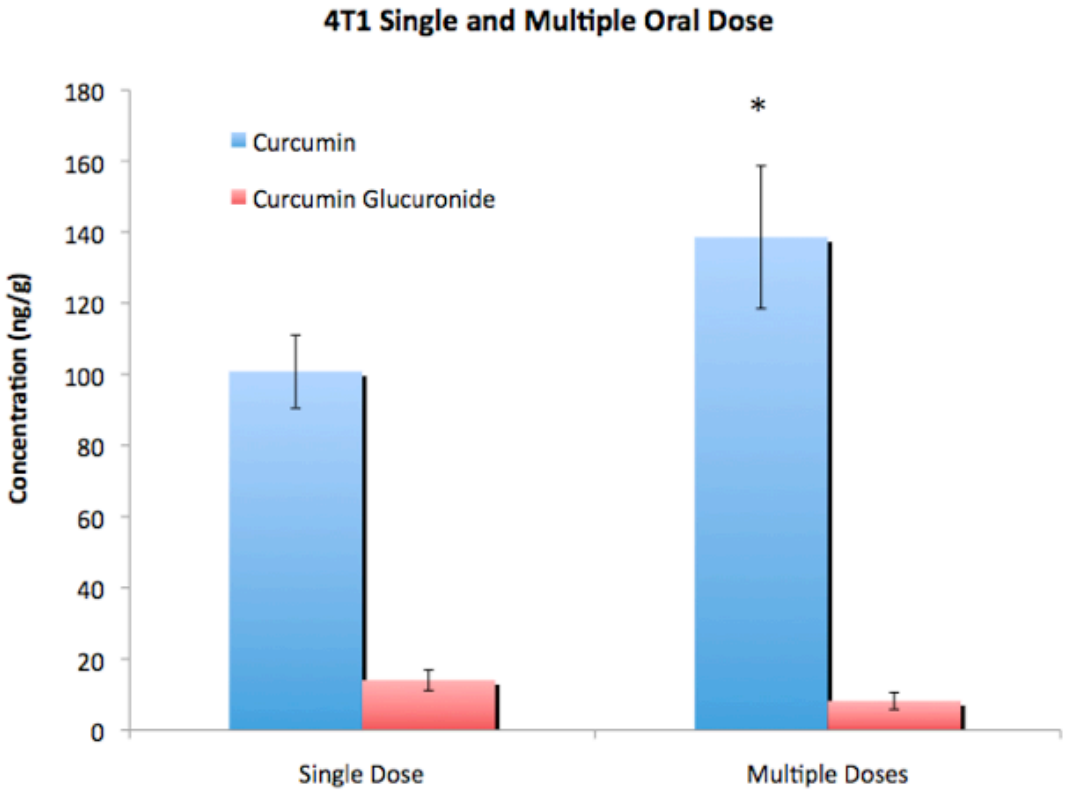

Figure 3.29. Accumulated curcumin and curcumin glucuronide concentrations in tumor tissue from orthotopic 4T1 mouse model after single and multiple oral doses of curcumin SMEDDS. 4T1 tumor bearing female mice received either a single dose or multiple doses of curcumin SMEDDS formulation daily at 100 mg/kg for 14 days prior to tissue and plasma collection. Curcumin and curcumin glucuronide concentrations were determined by LC-MS/MS. Data shown are Mean ± SE, n = 4. * $P<0.05$, compared to curcumin concentrations after one single dose, ANOVA.

3.17 Curcumin Downregulates Markers of Cell Proliferation, Angiogenesis, and Induces Apoptosis

To understand the underlying mechanisms of improved anticancer efficacy following multiple oral dosing of curcumin SMEDDS, MDA-MB-231 tumors from the chemopreventive efficacy study were analyzed for biomarkers of cell proliferation (Ki-67), angiogenesis (CD-31), and apoptosis (cleaved caspase-3). Curcumin SMEDDS treatment significantly reduced cell proliferation, as evidenced by percent of tissue stained with Ki-67 in tumors of mice receiving curcumin SMEDDS treatment (14.10 ± 0.93%) as compared to receiving blank SMEDDS (20.40 ± 1.29%) or no treatment (16.36 ± 0.88%) ($P<0.05$) (Figure 3.30). Similar was the case with microvessel density within the tumor. Microvessel density was more pronounced in blank SMEDDS (1.12 ± 0.11%) and untreated (0.76 ± 0.07%) treated tumors than in those receiving curcumin SMEDDS (0.46 ± 0.04%) ($P<0.001$). The CD-31 positive microvessels were smaller in size and less developed in the curcumin SMEDDS treated group than those in the other control groups (Figure 3.31). The trends were inverse in the case of cleaved caspase-3, a biomarker of apoptosis. Treatment with curcumin SMEDDS induced cleaved caspase-3 levels in tumor by average of greater than 7-fold compared to that caused by blank SMEDDS treatment and greater than 2-fold as compared to the untreated group (Figure 3.32). These results from immunohistological analysis support that orally dosed curcumin in a microemulsion formulation reduces tumor growth rate by inhibiting cell proliferation and angiogenesis as well as by inducing apoptosis.

Blank SMEDDS

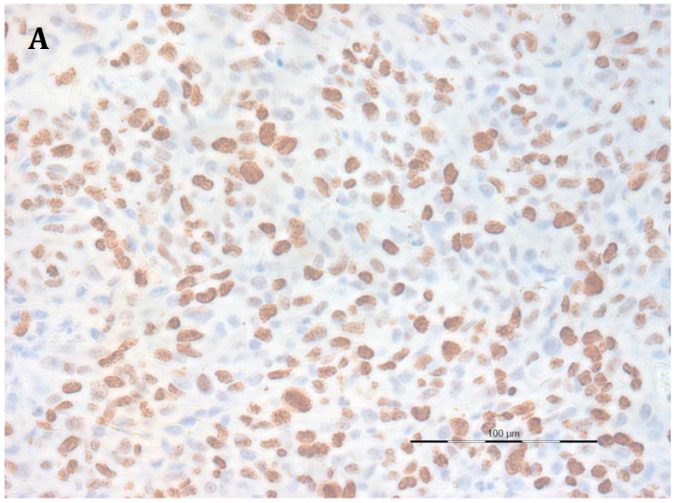

Curcumin SMEDDS

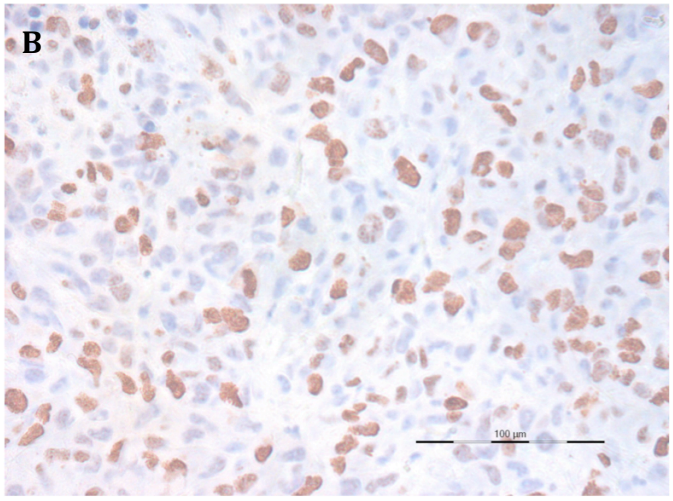

Untreated

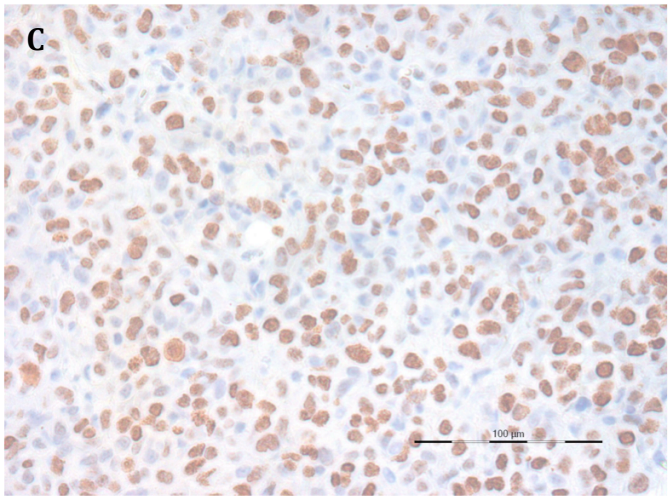

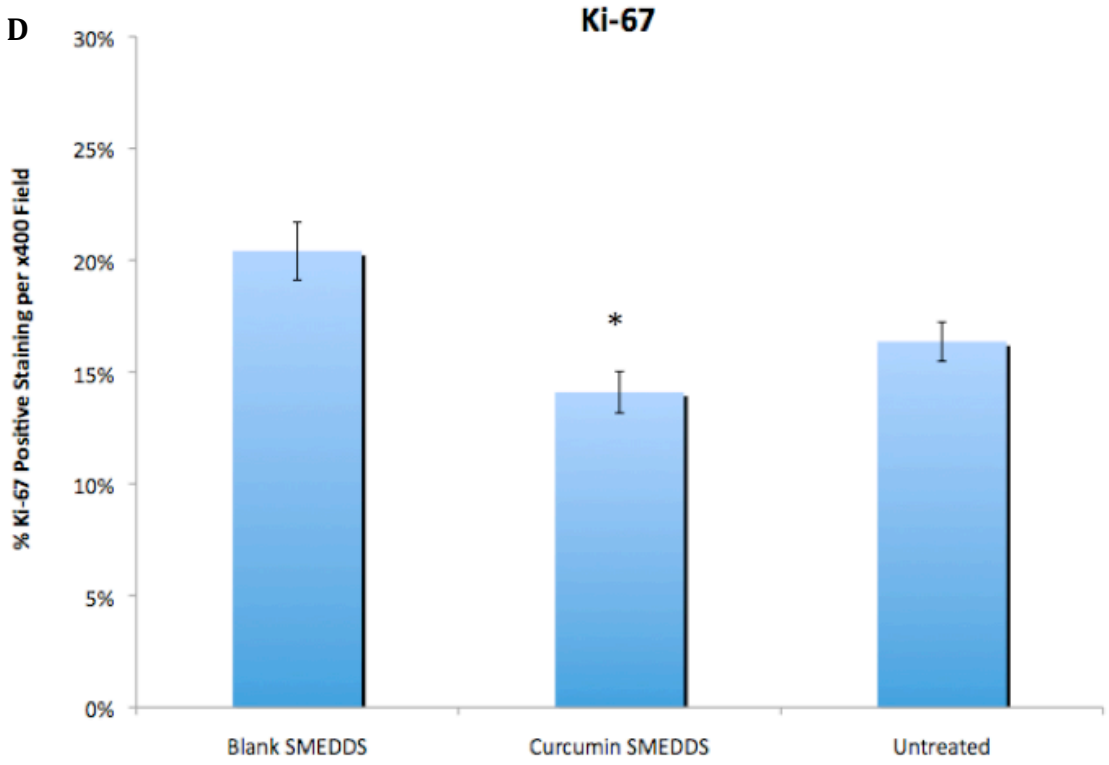

Figure 3.30. Curcumin SMEDDS treatment decreases cell proliferation in mammary tumor tissue. Female athymic nude mice bearing MDA-MB-231 human tumor xenografts were dosed daily at 100 mg/kg with **(A)** blank SMEDDS formulation, **(B)** curcumin SMEDDS formulation, or **(C)** remained untreated. Mice were sacrificed at 2 months after the initial dose and mammary tissue was stained with anti-Ki-67 antibody. **(D)** Positive Ki-67 staining was quantified as percentage stained per field of view at x400 magnification using ImageJ software. Scale bars represent 100 μm. Data are presented as average percentage of Ki-67 positive staining per x400 field ± S.E. * $P<0.05$, compared to positive staining in blank SMEDDS treated and untreated groups, ANOVA followed by post-hoc Newman-Keuls' testing.

Blank SMEDDS

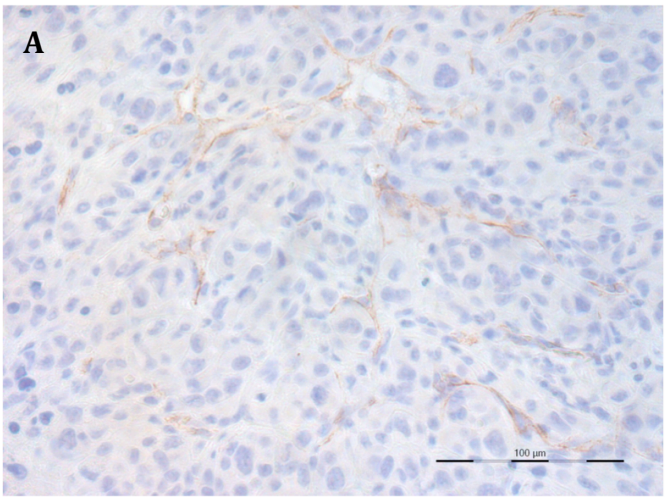

Curcumin SMEDDS

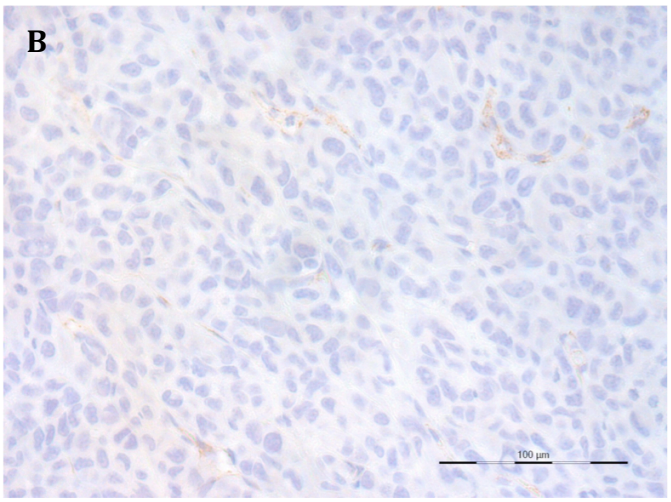

Untreated

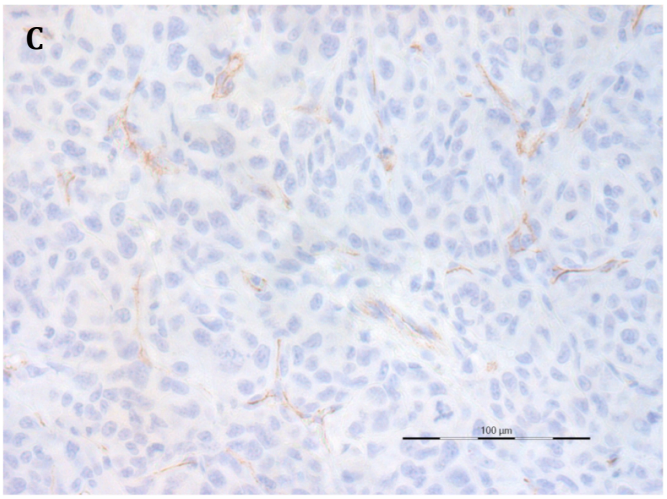

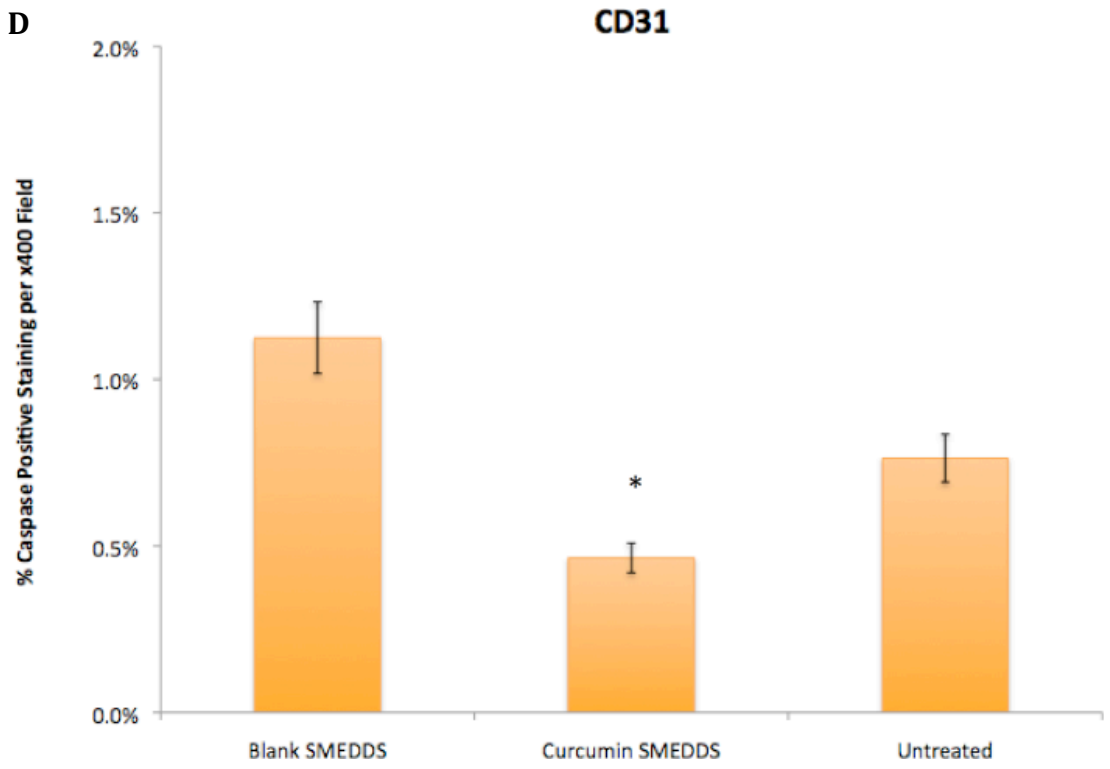

Figure 3.31. Curcumin SMEDDS treatment decreases microvascularization in mammary tumor tissue. Female athymic nude mice bearing MDA-MB-231 human tumor xenografts were dosed daily at 100 mg/kg with **(A)** blank SMEDDS formulation, **(B)** curcumin SMEDDS formulation, or **(C)** remained untreated. Mice were sacrificed at 2 months after the initial dose and mammary tissue was stained with anti-CD31 antibody. **(D)** Positive CD31 staining was quantified as percentage stained per field of view at x400 magnification using ImageJ software. Scale bars represent 100 μm. Data are presented as average percentage of CD31 positive staining per x400 field ± S.E. * $P<0.05$, compared to positive staining in blank SMEDDS treated and untreated groups, ANOVA followed by post-hoc Newman-Keuls' testing.

Blank SMEDDS

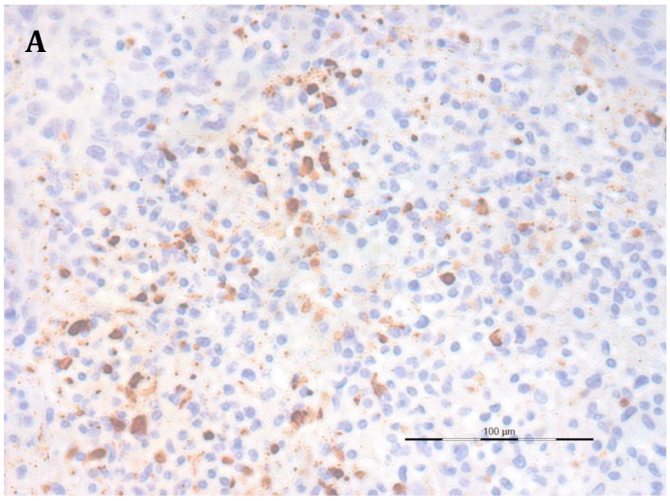

Curcumin SMEDDS

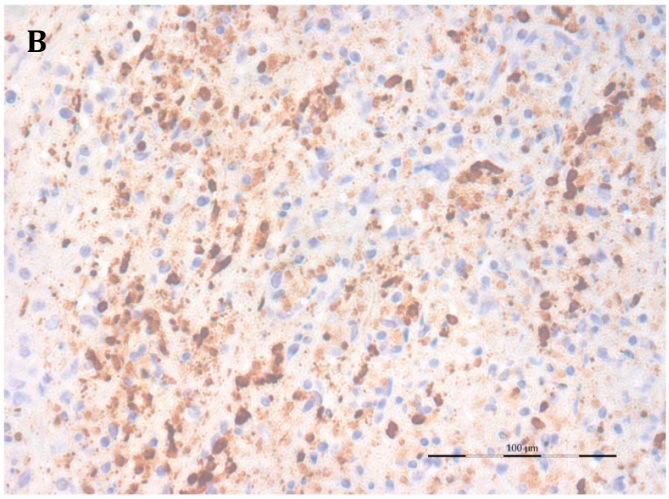

Untreated

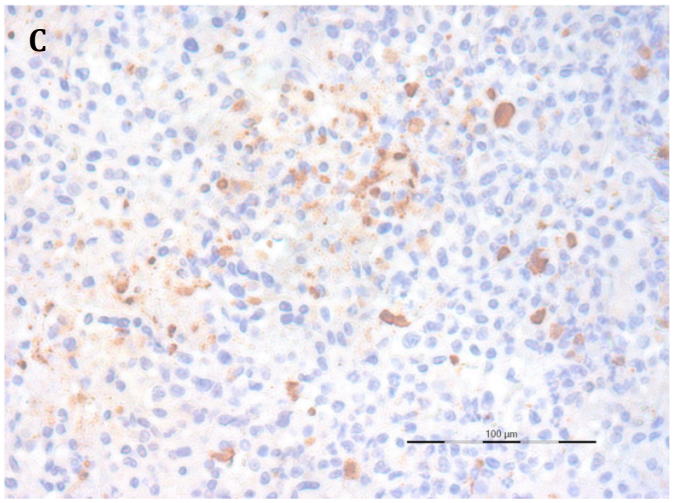

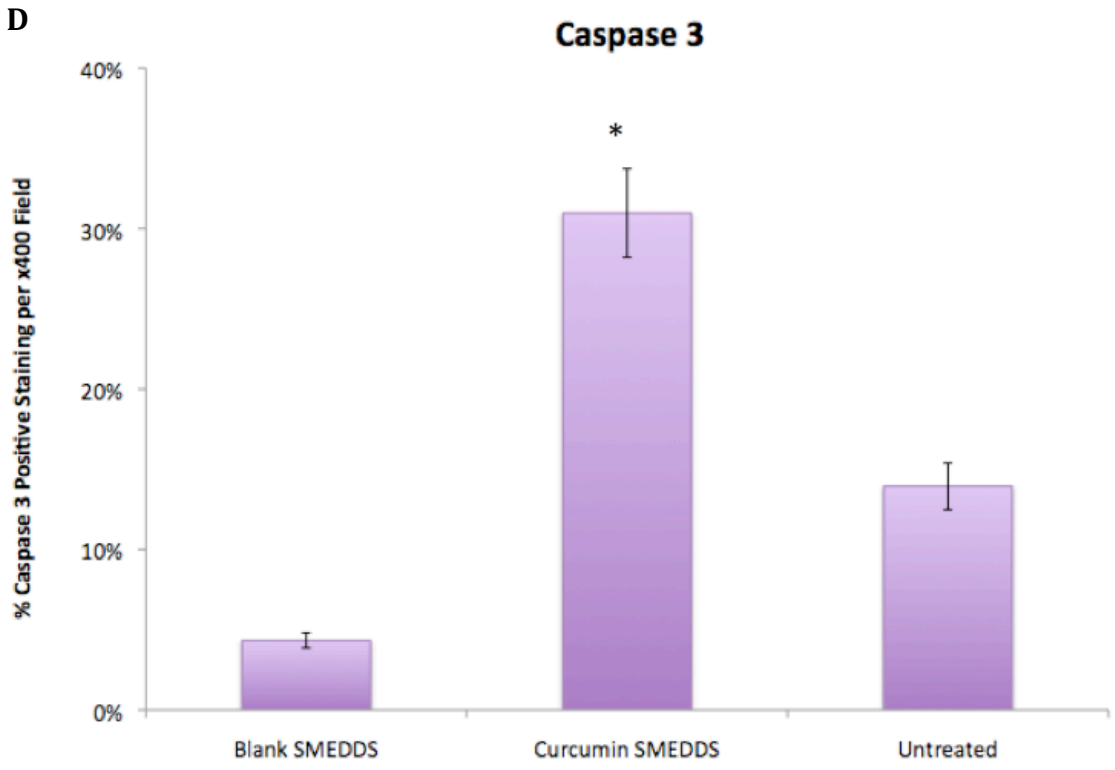

Figure 3.32. Curcumin SMEDDS treatment increases apoptosis in mammary tumor tissue. Female athymic nude mice bearing MDA-MB-231 human tumor xenografts were dosed daily at 100 mg/kg with **(A)** blank SMEDDS formulation, **(B)** curcumin SMEDDS formulation, or **(C)** remained untreated. Mice were sacrificed at 2 months after the initial dose and mammary tissue was stained with anti-caspase-3 antibody. **(D)** Positive caspase-3 staining was quantified as percentage stained per field of view at x400 magnification using ImageJ software. Scale bars represent 100 μm. Data are presented as average percentage of caspase-3 positive staining per x400 field ± S.E. * $P<0.05$, compared to positive staining in blank SMEDDS treated and untreated groups, ANOVA followed by post-hoc Newman-Keuls' testing.

Chapter IV

Discussion

The primary goal of this dissertation is to evaluate the chemopreventive potential of orally dosed curcumin in breast cancer based on the prodrug activation hypothesis. According to the prodrug hypothesis, orally administered curcumin that is absorbed along the gastrointestinal tract is rapidly metabolized to form curcumin glucuronide. The inactive glucuronide metabolite present in systemic circulation is then either re-activated back to active curcumin by β-glucuronidase present at high concentrations at the tumor or inflammation site, where it may exert its pharmacological effects, or is renally eliminated. A self-microemulsifying drug delivery system (SMEDDS) formulation was employed for the oral dosing studies to improve curcumin absorption in the gut. The studies in this thesis investigated several aspects of the prodrug hypothesis to elucidate its validity, including quantifying β-glucuronidase expression levels and specific activity according to the stage and subtype of breast cancer, determining the chemopreventive efficacy, evaluating the potential for curcumin accumulation in tumor tissue, and analyzing pharmacokinetics of both curcumin and curcumin glucuronide.

Two key questions were posed that set the stage for these studies:

1.) How does oral curcumin exhibit chemopreventive and therapeutic activity despite not being absorbed into the systemic circulation in its active form?
2.) Is the inactive metabolite curcumin glucuronide a natural prodrug?

The prodrug activation hypothesis proposes to explain the mechanisms behind this 'bioavailability paradox.' That is, this hypothesis is a potential explanation for the

seemingly paradoxical phenomenon that despite the less than 1% bioavailability of oral curcumin due to its poor intestinal absorption and extensive metabolism, curcumin still exhibits numerous health and therapeutic benefits when administered orally.

In the initial studies, β-glucuronidase expression levels were determined according to breast cancer stage and subtype in human breast carcinoma tissue, which were surgically resected from patients to form a tissue microarray for multiplexed histological analysis. Tumors at the most advanced stage of development and HER-2+ subtype tumors had the highest expression levels of β-glucuronidase among all other subtypes due most likely to its aggressive nature and hence greater recruitment of immune cells such as macrophages and neutrophils, which are responsible for liberating β-glucuronidase into the extracellular matrix [110]. Similar is the logic for the most advanced stages of tumorigenesis to yield the highest levels of β-glucuronidase expression. As the tumor grows in size, there is an increased tendency for it to develop a dysregulated vasculature [181]. Thus, large tumors tend to be hypoxic, causing tumor cells in these central hypoxic regions to die and form a necrotic core [114, 181]. These regions of tumor necrosis are largely responsible for high infiltration of monocytes (macrophages) and granulocytes (neutrophils) in response to the associated increased levels of inflammation in necrotic regions [114], hence the greater levels of β-glucuronidase within larger, more advanced tumors.

Based on our histological studies, it is clear that β-glucuronidase is overexpressed in human adenocarcinoma as compared to normal tissue. Enzyme expression levels were highly variable based on the subtype and stage of the mammary tumor. Malignant HER-2+ breast cancer tumors were predicted to yield the highest β-glucuronidase specific

activity, and hence may potentially benefit the most from prodrug administration and release of the active compound at the desired site of action. Since it was established that β-glucuronidase overexpression occurred in human tissue and that levels were variant, the next set of studies aimed at determining β-glucuronidase expression and specific activity levels *in vitro*, both in cell culture and in tissue from animal models.

In vitro experiments that aimed to quantify β-glucuronidase activity levels in breast carcinoma cells in culture (intact and lysed cells) that were subjected to either normal atmospheric conditions or hypoxic (< 5% O_2) conditions showed no detectable levels of β-glucuronidase activity. MDA-MB-231 cells were subjected to hypoxic conditions to mimic the conditions found in the tumor microenvironment and to determine whether hypoxia would affect the β-glucuronidase expression and activity levels within these cells. No intracellular β-glucuronidase activity was observed in any of the six adenocarcinoma cell lines of HER-2+, triple negative, and ER/PR+ type originating from both human and mouse species. These results suggest that β-glucuronidase is present extracellularly, and that the activity by β-glucuronidase occurs in the extracellular matrix. This makes sense, as infiltration of macrophages and neutrophils occurs into the extracellular matrix of the tumor [114], from which β-glucuronidase would be liberated. While it is known that there is some inherent β-glucuronidase activity in the lysosomes of all mammalian cells [104], the overexpressed enzyme levels present in the extracellular matrix likely is much greater than what is present within the cell.

Prior to conducting experiments to determine β-glucuronidase expression and specific activity as a function of breast cancer stage, subtype, and tumor model, two preliminary studies were performed to confirm the activity of β-glucuronidase within the

tumor. β-glucuronidase activities were determined by monitoring 4-Nitrophenyl β-D-glucuronide (NPG) conversion to parent 4-Nitrophenol (NP). The first study sought to ensure that β-glucuronidase was in fact the enzyme that was cleaving the glucuronide moiety to yield the active parent compound. Saccharolactone, a known inhibitor of β-glucuronidase [182], proved to effectively inhibit the activity of β-glucuronidase in mammary tumor tissue homogenate from Balb-*neu*T transgenic mice (Figure 3.8). This not only confirmed that β-glucuronidase was the enzyme responsible for glucuronide activation to the parent compound, but that the decrease in NPG levels with the proportional increase in NP levels was not due to natural or spontaneous degradation of the glucuronide compound. The second study showed that the glucuronide compound is activated to the parent drug compound only in the tumor where β-glucuronidase is overexpressed, and not in the plasma while the glucuronide is in systemic circulation (Figure 3.7). This is crucial, as the prodrug hypothesis holds only if the glucuronidated drug remains inactive and intact in the plasma, but is then activated specifically within the tumor or inflammatory site by β-glucuronidase.

β-glucuronidase expression and specific activity levels were quantified in mammary tumors in transgenic female Balb-*neu*T mice at 5 different age groups – 3, 8, 12, 16, and 23 weeks – to represent each progressive stage of tumorigenesis. The Balb-*neu*T model mimics the complex interplay between the developing mammary tumor and the host immune system by forming autochthonous tumors from a single cell [171], and so this model is representative of the HER-2+ type breast cancer found in human patients. Western blotting was used to determine normalized enzyme expression levels in tumor, and β-glucuronidase activity assays that monitor NPG conversion to parent NP were

conducted to determine specific activities. Interestingly, both enzyme expression and specific activity followed nearly identical trends. The trend in the β-glucuronidase expression as determined by Western blotting was similar to that of the β-glucuronidase specific activities in the same age groups. This shows that β-glucuronidase expression correlates closely with specific activity levels. The greater the levels of β-glucuronidase present within the tumor or disease site, the higher the specific activity. Expression levels and specific activities were the lowest at 3 weeks of age when the mammary glands were hyperplastic [171], and both gradually increased with the progression of tumorigenesis as tumors developed from hyperplastic to *in situ* carcinoma to invasive carcinoma, until finally at the most advanced stage of metastasis at 23 weeks of age. Because of higher levels of β-glucuronidase present, these advanced stages would be more prone to activate greater amounts of glucuronidated prodrug at the target site.

The slightly elevated β-glucuronidase specific activity levels observed at 12 weeks of age as compared to at 16 weeks in this model may be due to multiple reasons. At 6-10 weeks, microvessel density and growth tends to be increased, along with levels of growth factors (i.e., VEGF, FGF) and pro-inflammatory cytokines [171]. By approximately 15 weeks, microvasculature is lessened in density and growth factor levels are decreased as compared to at 5-8 weeks of age [172]. This is the stage when carcinoma *in situ* progresses to becoming invasive. Previous studies have shown that 13 weeks of age is a critical stage in Balb-*neu*T tumorigenesis, in that treatment with curcumin SMEDDS prior to 13 weeks has shown efficacy in reducing tumor growth rate, whereas after 13 weeks, curcumin treatment showed little to no effect [183]. Specific activity proved to be the highest at the most advanced stage of tumorigenesis (metastasis) at 23

weeks, showing that the greater the tumor aggression and stage, the higher the β-glucuronidase specific activity.

The overexpression of β-glucuronidase in the transgenic tumor model is further reiterated by the higher specific activity levels in each of the stages of tumorigenesis of the Balb-*neu*T model as compared to the activities in wild-type mammary tissue from mice of the same age groups (Figure 3.6). It is noteworthy that even at 3 weeks of age, when the mammary cells in the Balb-*neu*T model are hyperplastic, the specific activity of β-glucuronidase is already greater (2.58 ± 0.72 nmol NP formed/hr/mg protein) than that of healthy mammary tissue (0.74 ± 0.40 nmol NP formed/hr/mg protein) from wild-type Balb/c mice of the same age. This may be due to the genetic predisposition of mammary tumors to form in the Balb-*neu*T model at such a nascent age, and so this is reflected in the immune cell infiltration of macrophages and neutrophils of the tumor and therefore β-glucuronidase activity is increased as a result.

In addition to quantifying β-glucuronidase specific activity levels in the transgenic Balb-*neu*T model and correlating them with enzyme expression, the next set of studies aimed at quantifying specific activities in orthotopic mammary tumor models: JC, TuBo, MDA-MB-231, and 4T1. Of the four models, TuBo showed the lowest β-glucuronidase specific activity in all tumor volumes when compared to that of the MDA-MB-231, JC, and 4T1 models, which all had comparable activities. This is despite the fact that TuBo cells are HER-2 overexpressing cells. According to the immunohistochemistry studies with the human mammary tissue microarray, HER-2+ type tissues showed the highest levels of β-glucuronidase expression, but these activity

data with TuBo seems to contradict this generalization of HER-2+ tissue having the highest expression levels of β-glucuronidase enzyme. The low specific activity observed in TuBo may be due to minimal macrophage and neutrophil immune cell infiltration within the tumor tissue of this model [114]. These results support that β-glucuronidase activity levels are not only linked to breast cancer subtype alone, but other factors such as immune cell infiltration also play a crucial role.

One additional point to highlight when comparing enzyme specific activities across the orthotopic models is that the levels of β-glucuronidase activity plateau off at volumes above 400 mm^3. While the actual amount of increase in specific activity from volume to volume is variable between models (lower in TuBo and higher in the other 3 models), the percent increase in activity is comparable across the 4 models. This "plateauing" of specific activities beyond a tumor volume of 400 mm^3 is important to note, as the pharmacokinetic and curcumin accumulation studies are based on this fact. In these studies, since the β-glucuronidase specific activity is similar and does not increase significantly as the tumor grows beyond 400 mm^3, this was the tumor volume chosen to begin oral dosing of the curcumin microemulsion formulation. It should be noted that most tumor inhibition and drug accumulation studies start the treatments when tumors are relatively small (~100 mm^3). In general, smaller tumors respond better to treatments than larger ones [184]. Thus, the fact that oral curcumin significantly accumulates in the tumor even when the treatment was started at a later stage in tumor growth is particularly noteworthy.

Since the 4T1 model is the most aggressive of the 4 models in the study and is prone to metastasis to distant sites at later stages of development, lungs were collected in

addition to the tumor in order to determine specific activity in these tissues as well. Results showed that while specific activities were lower in lungs than in tumor in 4T1, the specific activity of the lungs from the 4T1 model was significantly higher than the activity of lungs from the wild-type model. These results show that metastatic tumors at distant sites – in this case, the lungs – also have increased expression of β-glucuronidase. This suggests that curcumin glucuronide activation could occur not just in the tumor but also at the metastatic sites.

Based on these results, chemopreventive efficacy studies were performed to elucidate the effects of oral curcumin on inhibiting tumor growth. In the 4T1 model, the average volume of the curcumin SMEDDS group was significantly lower only when compared to the average volume of the blank SMEDDS group after one month; there was no statistical difference between the average volumes of the curcumin SMEDDS and untreated groups. This is due most likely to the aggression of the model itself [185], and not to the specific activity of β-glucuronidase present within the tumor. Though it is evident that some level of β-glucuronidase activity is present, as seen with the lower volume of the curcumin SMEDDS treated group in comparison with the blank SMEDDS treated group, the aggression of 4T1 may potentially overcome the therapeutic effects of curcumin. In JC and MDA-MB-231, for example, the tumor growth is less aggressive, and so curcumin delivery results in a therapeutic benefit. In the TuBo model, however, there was no significant difference in tumor volumes between the treatment groups. This is attributable to the low specific activity levels of β-glucuronidase in TuBo mammary tumors, as determined from the activity assays. These results strongly support the notion

that orally administered curcumin in a microemulsion formulation has an efficacious effect on limiting tumor growth rate based on the prodrug activation hypothesis.

It is important to note that the tumor growth rate inhibition is dependent not only on β-glucuronidase specific activity, but also on the tumor cell sensitivity to curcumin. Interestingly, of the 4 cell lines, TuBo cells showed the greatest resistance to curcumin treatment *in vitro*. Thus, in addition to the limited conversion of curcumin glucuronide to active curcumin in the extracellular matrix of the tumor, the inherent resistance of the TuBo cells to curcumin resulted in poor efficacy of orally delivered curcumin in this tumor model.

In addition to measuring β-glucuronidase specific activity ex-vivo in extracted tumor tissue from various mouse models, activity levels were also determined *in vivo* in an MDA-MB-231 LM2 (or LM2) model using an activity-based near-infrared fluorescent difluoromethylphenol-glucuronide probe. Fluorescence imaging was used to determine levels of β-glucuronidase expression and activity based on enzyme activity *in vivo*. The glucuronidated probe is non-fluorescent; however, when the glucuronide is cleaved by β-glucuronidase in the tumor and the fluorescent probe is released, fluorescence can be detected by the imager [180]. According to the results, an increase in fluorescence was observed with increasing tumor volume in the LM2 model, indicating that β-glucuronidase activity is present in activating the fluorescent parent probe by cleaving the glucuronide.

According to the ex-vivo studies determining β-glucuronidase specific activity in the JC, 4T1, MDA-MB-231, and TuBo models, specific activity increases from 100 mm^3

to 400 mm^3, but then plateaus at volumes higher than 400 mm^3. Since this trend was observed in all 4 models studied, this most likely occurs in the LM2 model as well. Thus, in the LM2 model in these *in vivo* imaging studies, it may also be that enzyme specific activity increases initially at smaller tumor volumes, but at larger tumor volumes, the activity would remain practically constant. The higher levels of fluorescence observed in the larger tumor sizes, then, would mainly be due to increased levels of β-glucuronidase in the tumor. Imaging studies do not allow for estimation of specific activity of the enzyme in the tumor. The main goal of these imaging studies was to show a visual representation of the presence of β-glucuronidase activity in the tumor of live animals.

One point to highlight in these *in vivo* imaging studies is the considerable level of fluorescence that occurs in the liver in the more advanced stages of tumor growth, such as at tumor volumes of 700 mm^3 and 1200 mm^3. This may suggest an elevated β-glucuronidase activity in the liver or the presence of metastases in the liver. This, however, was unlikely because fluorescence in the liver region was observed even when the tumor was in the earliest stages of development (100 mm^3 in size) but not in healthy animals. Furthermore, no fluorescence was observed in the lungs, the major site of metastasis for the LM2 cells. The most likely cause of fluorescence in the liver region even from the earliest stages of tumorigenesis is the potential re-circulation of the fluorescent probe after activation by β-glucuronidase in the tumor. Clearance of the fluorescent probe from the tumor into the systemic circulation would result in significant levels of the probe accumulating in the liver, one of the major eliminating organs. As tumor volume increases, the fluorescence in liver increases in correlation with that in the

tumor, indicating greater levels of fluorescent probe re-circulating after having been activated by β-glucuronidase at the tumor site.

The next set of studies investigated the pharmacokinetics of curcumin and its metabolite curcumin glucuronide following either oral dosing of curcumin SMEDDS or intravenous dosing of curcumin glucuronide in the 4T1 and TuBo models. The ultimate goal of these studies was to correlate the curcumin levels generated in the tumor with the β-glucuronidase specific activity in that tumor type. The two models were chosen specifically for their high (4T1) and low (TuBo) specific activities of β-glucuronidase. The plasma levels of curcumin glucuronide following oral dosing of curcumin SMEDDS far exceeded the levels of the parent curcumin compound itself, indicating that curcumin undergoes rapid first-pass metabolism upon absorption from the gut. In tumor, however, curcumin levels were far greater than that of curcumin glucuronide. Curcumin concentrations in 4T1 tumors were greater than in TuBo tumors. These results point to the strong correlation between curcumin generation and the β-glucuronidase specific activity.

Curcumin concentrations in liver were highly variable in both models. This may very well be due to the high variability in curcumin absorption from the gastrointestinal tract. Despite receiving the same dose (100 mg/kg), absorption rates of curcumin from the gut may be wide ranging, which would result in minimal to excessive amounts of curcumin present in the liver at a given point in time. It is interesting to note, however, that despite this variance in liver curcumin concentrations from animal to animal, the concentration-time profiles for curcumin glucuronide in plasma and curcumin in tumor

follow distinct trends and are typical of what would be observed in a pharmacokinetic profile of drug concentrations in plasma and target tissue following oral dosing. In other words, since curcumin concentrations are highly variable in liver, it is intriguing that the curcumin and metabolite concentrations in plasma and tumor do not follow similarly scattered profiles. One reason for this could be that despite the variable concentrations, the liver may metabolize curcumin at only a certain maximal rate, and so any excess curcumin may be eliminated by enterohepatic recirculation from the liver back into the gastrointestinal tract. The gut may absorb far more curcumin than what the liver is capable of metabolizing. According to the results, the maximal concentration of curcumin glucuronide in plasma following intravenous dosing is ~ 65 – 70 μg/mL, the extrapolated initial concentration of glucuronide at time zero. Thus, in addition to the glucuronidation that takes place in the enterocytes along the gastrointestinal wall, the liver would theoretically only need to be presented with enough curcumin from the portal vein in order to metabolize and produce combined curcumin glucuronide concentrations of ~ 65 – 70 μg/mL in plasma following oral dosing.

Curcumin tumor disposition was rather interesting. In both the 4T1 and TuBo models, the curcumin concentrations in tumor following oral dosing was slightly elevated as compared to that at the 4-hour time point. This suggests the potential for slow and sustained curcumin accumulation in tumor from even a single oral dose. In a typical pharmacokinetic profile following oral dosing, once C_{max} (absorption rate = elimination rate) has been reached and the elimination rate becomes greater than the absorption rate, drug concentrations in the plasma and tissue begin to steadily decline at a linear rate (i.e., elimination phase). This explains the decline in curcumin levels from C_{max} at 1 hour to 4

hours post-dose in both models. However, with the oral dosing of curcumin, the drug concentration is lowest at the 4-hour time point, and then increases again at the 8-hour time point. This is could be due to redistribution of curcumin and/or glucuronide from other tissue sites (i.e., liver and lungs) to the tumor. Curcumin glucuronide was still present in the plasma even after 8 hours post-oral dose (~8 μg/mL), and so a constant and steady supply of glucuronide to the tumor site was available between 4 and 8 hours post-dose. With the half-life of curcumin elimination from tumor as calculated by non-compartmental analysis to be at 40.5 hours, curcumin would steadily accumulate in the tumor, given that glucuronide is still presented by circulation and β-glucuronidase continues to activate the metabolite back to curcumin within the tumor. In terms of rates, the absorption rate of curcumin into the tumor (conversion of curcumin glucuronide to curcumin) and elimination rate of curcumin from the tumor (clearance of curcumin from tumor) remain constant, but since absorption rate > elimination rate (low due to longer elimination half-life), curcumin levels in tumor would accumulate until eventually the plasma levels of the glucuronide decline. Additional studies examining the disposition of curcumin and its metabolite beyond 24 hours are needed to confirm these findings.

The second study sought to determine the pharmacokinetic parameters of just the metabolite, curcumin glucuronide, and confirm the values with those determined from the curcumin glucuronide formed endogenously by first-pass metabolism in the first study. This study involved the intravenous dosing of glucuronide so as to bypass the absorption barrier that would occur with oral dosing. The resulting concentration-time profiles of curcumin glucuronide following IV dosing of the metabolite were practically identical between the 4T1 and TuBo models. Non-compartmental analysis by Phoenix WinNonlin

6.3 (Pharsight, St. Louis, MO) of the pharmacokinetic parameters revealed the half-life of curcumin glucuronide elimination from plasma ($t_{1/2}$ = 3.9 hours) to be the same, whether the glucuronide was formed endogenously following oral dosing of curcumin or intravenously dosed directly into the systemic circulation. In addition, a third study in which glucuronide was dosed intravenously into healthy, tumor-free, wild-type female mice of the same age yielded a similar half-life of elimination. Because the pharmacokinetic parameters were the same for curcumin glucuronide in plasma across these three studies, it was concluded that the route of administration and the disease status of the animal model did not have an effect on the glucuronide biodistribution in circulation.

Curcumin concentrations in the tumor of 4T1 and TuBo were greater than that of what was seen in the mammary tissue of wild-type mice. This was the case with both the oral dosing of curcumin SMEDDS and the intravenous dosing of curcumin glucuronide. These observations strongly support the prodrug hypothesis not only in the sense that curcumin levels are significantly higher in tumor despite curcumin glucuronide being the predominant form present in plasma, but the concentration levels of curcumin are elevated in the tumor models as compared to in the wild-type model. Increased β-glucuronidase activity due to elevated levels of the enzyme in the tumor increases the rate at which curcumin glucuronide is converted to active curcumin, and thus increased concentrations of curcumin are present in the tumor microenvironment. Since the specific activity of enzyme is lower in mammary tissue of healthy mice due to minimal expression of β-glucuronidase, it follows that the glucuronide activation rate would consequently be lower and hence lower levels of curcumin would be formed in the tumor.

The prodrug activation hypothesis is well supported by the results from multiple oral dosing and pharmacokinetic studies: curcumin glucuronide levels in plasma far exceed that of curcumin itself, glucuronide plasma levels were relatively the same between the wild-type and the tumor models, curcumin levels in tumor were much greater than glucuronide levels, and curcumin concentrations were by far significantly higher in the tumor from the 4T1 model than in the mammary tissue from the wild-type model. Curcumin is a hydrophobic polyphenolic compound, and is therefore capable of tissue accumulation over an extended period of time of regular dosing. It is interesting to note that while curcumin accumulation was evident in both the orthotopic TuBo and JC models after one month of daily oral dosing with curcumin SMEDDS, accumulation levels in TuBo tumors were significantly higher than in JC tumors. This can be explained by the potential higher infiltration levels of macrophages and neutrophils to the tumor site in the TuBo model as compared to that of JC. Curcumin concentration in 4T1 tumor after two weeks of daily oral dosing was significantly higher than that achieved after a single, one-time oral dose. Tumor volumes were 400 mm^3 at the time of initiating the oral dosing in both the single and multiple dosing groups so that β-glucuronidase specific activity levels would be comparable. In the multiple dosing group though, since the treatments were given for 14 consecutive days, the average tumor size in this group increased to approximately 700 mm^3 by the end of the study, which may have had an impact on the β-glucuronidase specific activity. However, our studies show that the enzyme activity in 4T1 tumors plateau after having reached 400 mm^3 in volume, and so tumor volumes greater than 400 mm^3 have comparable levels of activity as tumors that are 400 mm^3 in size. Therefore, it was concluded that the higher tumor curcumin levels in the multiple

dosing group was due to curcumin accumulation, and not because of elevated β-glucuronidase specific activity as a result of larger tumor volumes at the end of the study.

Previous studies have shown that regular, low-dose drug treatments have greater therapeutic effects than dosing high concentrations of drug for a shorter duration. This concept has been termed as "metronomic treatment" [75, 76]. Conventional treatments such as chemotherapy are high-dose and acute, resulting in the direct killing of cancer cells and potentially the surrounding healthy cells, causing undesirable side effects. However, with metronomic treatment, sustained, low levels of drug are maintained in the systemic circulation, and so the drug is able to exert its pharmacological effects at the targeted site of action over an extended period of time. The results of the efficacy and accumulation studies suggest that daily oral dosing of curcumin SMEDDS generates small quantities of curcumin for a prolonged period of time, and this is effective in inhibiting tumor growth. Thus, our data supports the notion of "metronomic chemoprevention" by curcumin.

Curcumin is known to regulate numerous signal transduction pathways that affect cell proliferation, angiogenesis, and apoptosis. Previous studies have shown that curcumin limits cell proliferation [54] and angiogenesis [52, 53], and induces apoptosis [55], all of which are important for inhibiting tumor growth. In the current studies, the effect of curcumin on three biomarkers – Ki-67 (cell proliferation), CD31 (angiogenesis), and cleaved caspase-3 (apoptosis) – were studied. Tumor tissue from the MDA-MB-231 model was chosen because it had the greatest response to curcumin treatment, as shown from the efficacy studies.

Results from these studies showed statistically significant differences in the levels of all 3 biomarkers from the curcumin SMEDDS treated group as compared to the blank SMEDDS and untreated control groups. There was a significantly lower level of staining for Ki-67 and CD31 in the curcumin treated group as compared to the other control groups, indicating that curcumin does exert an effect in limiting tumorigenesis by decreasing cell proliferation and the microvessel density within the tumor. It is interesting to note that levels of Ki-67 and CD31 were slightly elevated in the blank SMEDDS treated group as compared to the untreated group. This is most likely because of one of two reasons, or potentially a combination of both: 1.) blank SMEDDS formulation free of drug could in itself induce some levels of increased cell proliferation and angiogenesis, or 2.) animals treated with blank SMEDDS were subjected to increased levels of stress from handling and oral gavage procedures, thus promoting cell proliferation and microvasculature increase. Despite this, the presence of curcumin ultimately lowers cell proliferation and decreases angiogenesis in the tumor microenvironment.

Curcumin treatment elevated cleaved caspase-3 levels. Cleaved caspase-3 is a marker for cell apoptosis, and curcumin is known to induce tumor cell apoptosis. These effects of curcumin are apparent on a larger scale as well in the chemopreventive efficacy study, in that MDA-MB-231 tumors from the curcumin SMEDDS treated group were less than half the volume of those from the blank SMEDDS or untreated group after two months of receiving such treatments. The results from these immunohistological studies further confirm the chemopreventive efficacy of orally dosed curcumin at a cellular level.

Numerous reports in literature have correlated β-glucuronidase overexpression in inflammatory and tumor tissue with its specific activity and therapeutic potential in activating prodrugs to increase drug specificity to the disease site [121-127]. Previous studies have shown that necrotic regions of tumors that are highly infiltrated with immune response cells such as macrophages and neutrophils reveal the greatest levels of β-glucuronidase upregulation [121]. In other studies, β-glucuronidase expression and specific activity levels were determined to be lowest in healthy pancreatic tissue and highest in pancreatitis and pancreatic adenocarcinoma tissue, as determined by activity assays that monitored MUG to parent MU conversion [122]. Other reports have studied specifically the therapeutic potential of prodrug forms of various chemotherapeutic compounds – specifically irinotecan, or CPT-11 [123], and doxorubicin [124] – according to the increased specific activity of β-glucuronidase in disease pathology. It was determined in these studies that healthy normal tissues that expressed marginal levels of β-glucuronidase yielded negligible levels of active SN-38 and doxorubicin, whereas in inflammatory and tumor tissue, the increased levels of β-glucuronidase resulted in higher levels of active drug being present at the target site. Additionally, efficacy in inhibiting tumor growth was observed to be increased in EJ/mβG tumor-bearing mice as compared to in mice bearing wild-type EJ tumors that do not overexpress β-glucuronidase when both groups were treated with the endogenously glucuronidated drug CPT-11 [125]. These previous reports illustrate the potential for the natural phenomenon of β-glucuronidase overexpression in the malignant tissue to be employed as a therapeutic approach to improving drug delivery.

The data and results presented in this thesis highly correlate with what has been previously reported in literature, and further reinforces the notion that β-glucuronidase overexpression in inflammatory and tumor tissue can be exploited for therapeutic benefit. One of the goals of the work here was to determine whether β-glucuronidase would be upregulated in breast cancer, and if so, would this type of cancer also respond to treatments that would involve the activation activity of β-glucuronidase as described in the literature. It was determined from our studies that β-glucuronidase is indeed overexpressed in several mammary tumor models as well, and that treatment with a polyphenol that is known to be highly glucuronidated results in significant efficacy based on β-glucuronidase expression and activity at the tumor site. The results from this thesis work are in strong agreement with previous reports [122-126], in that mammary tumors express minimal levels of β-glucuronidase at initial stages of tumorigenesis but levels increase significantly as the disease progresses, specific activity is highly correlated with enzyme expression levels, and efficacy in limiting tumor growth rate is exhibited based on the enzymatic activation activity of β-glucuronidase at the tumor site.

These studies with curcumin, a relatively non-toxic, dietary polyphenolic molecule, have the potential to have global implications in being applied to other chemopreventive agents that can be targeted to specifically the tumor site following oral administration. Since many other chemopreventive compounds undergo glucuronidation [187-190], the research presented here could very well serve as a model for future studies involving the evaluation of other dietary compounds for therapeutic efficacy and chemoprevention. These studies, based on the prodrug hypothesis, would suggest that for a chemopreventive agent that has poor bioavailability and low plasma concentrations but

exhibits efficacy, the concentration of inactive metabolite in plasma should be evaluated as an indicator of efficacy rather than that of the active parent compound. The applicability of these promising results that support the prodrug hypothesis, in combination with β-glucuronidase activity typically being upregulated during inflammation, could potentially not only transform the field of cancer chemoprevention, but also impact a wide array of inflammatory diseases in general.

Chapter V

Recapitulation

Curcumin, a naturally occurring polyphenol derived from turmeric, has been shown to possess anti-cancer and anti-inflammatory effects, and hence chemopreventive potential in epidemiological studies. However, curcumin has poor bioavailability (<1%) due to low absorption and rapid first-pass metabolism. The main objective of this thesis was to examine and evaluate the validity of an enzymatic prodrug activation hypothesis that proposes to explain this 'bioavailability paradox.' According to the hypothesis, the inactive glucuronide metabolites are naturally occurring prodrugs of curcumin that are selectively activated only in the tumor site to generate the active parent compound. β-glucuronidase, an enzyme that hydrolyzes the glycosidic bond of glucuronides, is of primary interest in these studies, as this hypothesis posits that β-glucuronidase generates the active agent from the glucuronide metabolites 'on demand' at the required sites of action, such as in tumor or sites of inflammation.

The objective of the first set of studies was to determine the relationship between disease stage/tumor subtype and β-glucuronidase activity in human and mouse mammary tumors. Based on immunohistochemistry studies with human mammary adenocarcinoma tissue of varying stages and subtypes, advanced stage and HER-2+ subtype tumors showed the highest levels of β-glucuronidase overexpression. Normal and benign stages of tumor showed the lowest levels of β-glucuronidase while the invasive/metastatic stage showed the highest levels. It was observed, however, that of the 4 orthotopic mammary adenocarcinoma models (JC, TuBo, MDA-MB-231, 4T1) studied, TuBo, a HER-2+ overexpressing model, had the lowest β-glucuronidase specific activity, while 4T1, a triple negative subtype model, had the greatest enzymatic specific activity. Moreover, since 4T1 is an aggressive model that is prone to metastasis, lungs from the advanced

stages of tumorigenesis in this model also showed elevated β-glucuronidase levels as compared to lungs from healthy, wild-type mice, suggesting that these distant sites may also be susceptible to curcumin intervention.

β-glucuronidase expression and activity levels were also determined in the transgenic Balb-*neu*T model, in which levels were compared both between the stages of tumorigenesis as well as between the Balb-*neu*T model and the wild-type Balb/c model. Once again, the results from these studies reiterated that β-glucuronidase expression and activity levels increase with successive stages in tumor development and that β-glucuronidase is overexpressed in inflammatory and tumor tissue as compared to healthy tissue. With each progressive stage of tumorigenesis in Balb-*neu*T, the enzyme expression levels gradually increased, as shown from Western blotting studies, and specific activities of β-glucuronidase also increased in correlation, as seen in the enzyme activity assays. Fluorescent imaging studies with the MDA-MB-231 LM2 model presented a visual representation of β-glucuronidase activity *in vivo*, and further confirmed that enzyme activity increases with tumor growth and volume.

We next sought to investigate the role of β-glucuronidase activity in the chemopreventive efficacy of oral curcumin. The orthotopic models that were evaluated in the β-glucuronidase expression and activity studies showed therapeutic efficacy from oral curcumin treatment, with the exception of the TuBo model. Aside from the low levels of β-glucuronidase activity in TuBo, it was also determined that TuBo cells were inherently resistant to curcumin treatment, giving further reason to the limited efficacy of curcumin treatment in this model. In the 4T1 model, despite the high β-glucuronidase activity that was observed from the specific activity assays, efficacy was not the highest, as would be

expected with 4T1. This can be explained by the aggression of the 4T1 model, which may in fact overcome the therapeutic effects of curcumin treatment. MDA-MB-231 was the model that showed the most promising results, in that efficacy data strongly correlated with the significant specific β-glucuronidase activity seen in this model. Based on immunohistological analysis of Ki-67, CD31, and caspase-3, it was determined that curcumin significantly reduces cell proliferation, tumor vasculature size and density, and induces apoptosis. These results hold great potential since MDA-MB-231 is an orthotopic human xenograft model, making this study potentially more translatable to the clinic.

The final set of studies aimed to evaluate the pharmacokinetics and drug accumulation of curcumin and curcumin glucuronide in both wild-type and tumor-bearing mouse models. The 4T1 and TuBo orthotopic models were used for these pharmacokinetic studies due to their respective high and low β-glucuronidase specific activities, as determined from the activity assay studies. Data from these studies showed that curcumin glucuronide levels in plasma were much greater than that of curcumin itself following oral dosing of curcumin SMEDDS, curcumin levels in tumor far exceeded that of glucuronide levels, glucuronide plasma levels were practically the same between the wild-type and tumor models, and curcumin concentrations in 4T1 tumors were significantly higher than in the healthy, mammary tissue from wild-type mice.

Since curcumin is hydrophobic in nature and is capable of tissue accumulation, drug accumulation studies revealed the potential for curcumin to accumulate in the tumor tissue of both transgenic (Balb-*neu*T) and orthotopic (JC, TuBo, 4T1) models. In the orthotopic models, evidence of curcumin accumulation following multiple dosing of curcumin SMEDDS was present, with 4T1 tumors having accumulated the highest levels

and TuBo tumors having accumulated the lowest levels. This is in correlation with their respective β-glucuronidase specific activities. In all of the models studied for curcumin accumulation, significant levels of curcumin were present in the tumor while levels were marginal in the plasma. When accumulation of curcumin in 4T1 tumor was compared with that of in mammary tissue of wild-type mice for the same multiple dosing timeframe, significantly greater levels of curcumin were present in 4T1 tumors than in healthy mammary tissue. Additionally, higher levels of curcumin were found in 4T1 tumors after multiple dosing of oral curcumin as compared to receiving just a single dose. Such findings from both the pharmacokinetic and drug accumulation studies strongly support the prodrug activation hypothesis.

The results from this thesis work convincingly demonstrate the presence of β-glucuronidase in mammary tumors and point to a potential mechanism of action for natural chemopreventives such as curcumin that have poor oral bioavailability but have potent chemopreventive activity after oral administration. Our studies show that the expression of β-glucuronidase is highly correlated with tumor progression in both human and mouse tumors, and that oral administration of curcumin results in significant tumor concentrations of the parent compound without detectable levels in plasma, thus supporting the central hypothesis. Overall, this research establishes the foundations for the validity of the enzymatic prodrug activation hypothesis, which would have important implications for how chemopreventives such as curcumin are evaluated. Many other natural chemopreventive agents undergo glucuronidation, and so the research in this thesis could potentially serve as a model for studies with other dietary chemopreventive compounds and have an impact on the treatment strategies for numerous inflammatory

diseases. Moreover, results from this thesis will enable the advancement of an effective and clinically translatable oral dosing strategy for breast cancer chemoprevention and therapy.

Bibliography

1. Prasad, K., Mantha, S.V., Kalra, J., Lee, P. Prevention of hypercholesterolemic atherosclerosis by garlic, an antioxidant. *J. Cardiovas. Pharmacol. Ther.,* **1997**. 2: 309-320.

2. Vogel, E., Pelletier, S. *J. Pharm.,* **1818**. 2:50.

3. Daybe, F.V. Über Curcumin, den Farbstoff der Curcumawurzzel. *Ber.,* **1870**. 3: 609.

4. Milobedzka, J.V., Kostanecki, S., Lampe, V. Zur Kenntnis des Curcumins. *Ber. Dtsch. Chem. Pharm.*, **1910**. 43: 2163-2170.

5. Goel, A., Kunnumakkara, A.B., Aggarwal, B.B. Curcumin as "Curecumin": from kitchen to clinic. *Biochem. Pharm.*, **2008**. 75: 787-809.

6. Pan, M.H., Huang, T.M., Lin, J.K. Biotransformation of curcumin through reduction and glucuronidation in mice. *Drug Metab. Dispos*, **1999**. 27: 486-494.

7. Tomren, M.A., Masson, M., Loftsson, T., Tonnesen, H.H. Studies on curcumin and curcuminoids XXXI. Symmetric and asymmetric curcuminoids: stability, activity and complexation with cyclodextrin. *Int. J. Pharm.*, **2007**. 338: 27-34.

8. Bharti, A.C., Donato, N., Aggarwal, B.B. Curcumin diferuloylmethane inhibits constitutive and IL-6-inducible STAT3 phosphorylation in human multiple myeloma cells. *J. Immunol.*, **2003**. 7: 3863-3871.

9. Vadhan, V.S., Weber, D., Giralt, S., Alexanian, R., Thomas, S., Zhou, X., Patel, P., Bueso-Ramos, C., Newman, R., Aggarwal, B.B. Curcumin downregulates NF-κB and related genes in patients with multiple myeloma: results of a phase 1/2 study. *Am. Soc. Hematol.*, **2007**.

10. Dhillon, N., Aggarwal, B.B., Li, L., Chiao, P., Sarkar, F., Wolff, R.A., Kurzrock, R. Phase II tria of curcumin (diferuloylmethane), an NF-κB inhibitor, in patients with advanced pancreatic cancer. *J. Clin. Oncol.*, **2006**. 24: 14151.

11. Aggarwal, B.B., Surh, Y.H., Shishodia, S. The molecular targets and therapetics of curcumin in health and disease. *Advances in Experimental Medicine and Biology, Springer Publication*, **2007**. 995.

12. Aggarwal, B.B., Bhatt, I.D., Ichikawa, H., Ahn, K.S., Sethi, G., Sandur, S., Sundaram, C., Seeram, N., Shishodia, S. Curcumin – Biological and Medicinal Properties. *The CRC Press*, Boca Raton, FL, **2006**. 297-368.

13. Wang, Z., Zhang, Y., Banerjee, S., Li, Y., Sarkar, F.H. Notch-1 down-regulation by curcumin is associated with the inhibition of cell growth and the induction of apoptosis in pancreatic cancer cells. *Cancer*, **2006**. 106: 2503-2513.

14. Park, C.H., Ham, E.R., Park, S., Kim, H.K., Yang, C.H. The inhibitory mechanism of curcumin and its derivative against beta-catenin/Tcf signaling. *FEBS Lett.,* **2005**. 579: 2965-2971.

15. Jaiswal, A.S., Marlow, B.P., Gupta, N., Narayan, S. Beta-catenin-mediated transactivation and cell-cell adhesion pathways are important in curcumin (diferuloylmethane)-induced growth arrest and apoptosis in colon cancer cells. *Oncogene*, **2002**. 21: 8414-8427.

16. Pendurthi, U.R., Rao, L.V. Suppression of transcription factor Egr-1 by curcumin. *Thromb. Res.,* **2000**. 97: 179-189.

17. Chen, A., Xu, J., Johnson, A.C. Curcumin inhibits human colon cancer cell growth by suppressing gene expression of epidermal growth factor receptor through reducing the activity of the transcription factor Egr-1. *Oncogene*, **2006**. 25: 278-287.

18. Jobin, C., Bradham, C.A., Russo, M.P., Juma, B., *et al.* Curcumin blocks cytokine-mediated NF-kappa B activation and proinflammatory gene expression by inhibiting inhibitory factor I-kappa B kinase activity. *J. Immunol.,* **1999**. 163: 3474-3483.

19. Bours, V., Bentires-Alj, M., Hellin, A.C., Viatour, P., *et al.* Nuclear factor-kappa B, cancer, and apoptosis. *Biochem. Pharmacol.,* **2000**. 60: 1085-1089.

20. Surh, Y.J., Chun, K.S., Cha, H.H., Han, S.S., *et al.* Molecular mechanisms underlying chemopreventive activities of anti-inflammatory phytochemicals: down-regulation of COX-2 and iNOS through suppression of NF-kappa B activation. *Mutat. Res. Fundam. Mol. Mech. Mutagen.,* **2001**. 480,481, 243-268.

21. Aggarwal, B.B., Shishodia, S., Takada, Y., Jackson-Bernitsas, D., Ahn, K.S., Sethi, G., Ichikawa, H. TNF blockage: an inflammatory issue. *Ernst Schering Res. Found Workshop*, **2006**. 161-186.

22. Fu, Y., Zheng, S., Lin, J., Ryerse, J., Chen, A. Curcumin protects the rat liver from CCl4-caused injury and fibrogenesis by attenuating oxidative stress and suppressing inflammation. *Mol. Pharmacol.*, **2008**. 73: 399-409.

23. Gulcubuk, a., Altunatmaz, K., Sonmez, K., Haktanir-Yatkin, D., Uzun, H., Gurel, A., Aydin, S. Effects of curcumin on tumour necrosis factor-alpha and interleukin-6 in the late phase of experimental cute pancreatitis. *J. Vet. Med. A. Physiol. Pathol. Clin. Med.*, **2006**. 53, 49-54.

24. Kuhad, A., Chopra, K. Curcumin attenuates diabetic encephalopathy in rats: behavioral and biochemical evidences. *Eur. J. Pharmacol*., **2007**. 576: 34-42.

25. Dinarello, C.A. The paradox of pro-inflammatory cytokines in cancer. *Cancer Metastasis Rev.,* **2006**. 25: 307-313.

26. Cho, J.W., Lee, K.S., Kim, C.W. Curcumin attenuates the expression of IL-1beta, IL-6, and TNF-alpha as well as cyclin E in TNF-alpha-treated HaCaT cells; NF-kappaB and MAPKs as potential upstream targets. *Int. J. Mol. Med.,* **2007**. 19: 469-474.

27. Ranjan, D., Chen, C., Johnston, T.D., Jeon, H., Nagabhushan, M. Curcumin inhibits mitogen stimulated lymphocyte proliferation, NFkappaB activation, and IL-2 signaling. *J. Surg. Res.,* **2004**. 121: 171-177.

28. Kobayashi, T., Hashimoto, S., Horie, T. Curcumin inhibition of *Dermatophagoides farinea*-induced interleukin-5 (IL-5) and granulocyte macrophage-colony stimulating factor (GM-CSF) production by lymphocytes from bronchial asthmatics, *Biochem. Pharmacol.,* **1997**. 54: 819-824.

29. Fahey, A.J., Adrian Robins, R., Constantinescu, C.S. Curcumin modulation of IFN-beta and IL-12 signalling and cytokine induction in human T cells. *J. Cell. Mol. Med.,* **2007**. 11: 1129-1137.

30. Grandjean-Laquerriere, A., Antonicelli, F., Gangloff, S.C., Guenounou, M., Le Naour, R. UVB-induced IL-18 production in human keratinocyte cell line NCTC 2544 throuh NF-kappaB activation. *Cytokine*, **2007**. 37: 76-83.

31. Cobb, M.H., Goldsmith, E.J. How MAP kinases are regulated. *J. Biol. Chem.,* **1995**. 270: 14843-14846.

32. Kyriakis, M.J., Avruch, J. Protein kinase cascades activated by stress and inflammatory cytokines. *Bioessays*, **1996**. 18: 567-577.

33. Chen, Y.R., Wang, X., Templeton, D., Davis, R.J., Tan, T.H. The role of c-Jun N-terminal kinase (JNK) in apoptosis induced by ultraviolet C and gamma radiation. Duration of JNK activation may determine cell death and proliferation. *J. Biol. Chem.,* **1996**. 271: 31929-31936.

34. Karin, M. The regulation of AP-1 activity by mitogen-activated protein kinases. *J. Biol. Chem,* **1995**. 270: 16483-16486.

35. Lee, K.W., Kim, J.H., Lee, H.J., Surh, Y.J. Curcumin inhibits phorbol ester-induced up-regulation of cyclooxygenase-2 and matrix metalloproteinase-9 by blocking ERK1/2 phosphorylation and NF-kappaB transcriptional activity in MCF10A human breast epithelial cells. *Antioxid. Redox. Signal.,* **2005**. 7: 1612-1620.

36. Chen, Y.R., Tan, T.H. Inhibition of the c-Jun N-terminal kinase (JNK) signaling pathway by curcumin. *Oncogene*, **1998**. 17: 173-178.

37. Dhandapani, K.M., Mahesh, V.B., Brann, D.W. Curcumin suppresses growth and chemoresistance of human glioblastoma cells via AP-1 and NFkappaB transcription factors. *J. Neurochem.,* **2007**. 102: 522-538.

38. Hussain, A.R., Al-Rasheed, M., Manogaran, P.S., Al-Hussein, K.A., et al. Curcumin induces apoptosis via inhibition of PI3'-kinase/AKT pathway in acute T cell leukemias. *Apoptosis*, **2006**. 11: 245-254.

39. Gururajan, M., Dasu, T., Shahidain, S., Jennings, C.D., *et al.* Spleen tyrosine kinase (Syk), a novel target of curcumin, is required for B lymphoma growth. *J. Immunol.,* **2007**. 178: 111-121.

40. Hatcher, H., Planalp, R., Cho, J., Torti, F.M., Torti, S.V. Curcumin: from ancient medicine to current clinical trials. *Cell Mol. Life Sci.,* **2008**. 65: 1631-1652.

41. Squires, M.S., Hudson, E.A., Howells, L., Sale, S., *et al.* Relevance of mitogen activated protein kinase (MAPK) and phosphotidylinositol-3-kinase/protein kinase B (PI3K/PKB) pathways to induction of apoptosis by curcumin in breast cells. *Biochem. Pharmacol.,* **2003**. 65: 361-376.

42. Goel, A., Boland, C.R., Chauhan, D.P. Specific inhibition of cyclooxygenase-2 (COX-2) expression by dietary curcumin in HT-29 human colon cancer cells. *Cancer Lett.,* **2001**. 172: 111-118.

43. Surh, Y.J., Chun, K.S., Cha, H.H., Han, S.S., *et al.* Molecular mechanisms underlying chemopreventive activities of anti-inflammatory phytochemicals: down-regulation of COX-2 and iNOS through suppression of NF-kappa B activation. *Mutat. Res. Fundam. Mol. Mech. Mutagen.,* **2001**. 480,481, 243-268.

44. Plummer, S.M., Holloway, K.A., Manson, M.M., Munks, R.J., *et al.* Inhibition of cyclo-oxygenase 2 expression in colon cells by the chemopreventive agent curcumin involves inhibition of NF-kappaB activation via the NIK/IKK signalling complex. *Oncogene*, **1999**. 18: 6013-6020.

45. Shehzad, A., Khan, S., Shehzad, O., Lee, Y.S. Curcumin therapeutic promises and bioavailability in colorectal cancer. *Drugs Today*, **2010**. 46: 523-532. DOI: 10.1358/dot.2010.46.7.1509560.

46. Zucker, S., Vacirca, J. Role of matrix metalloproteinases (MMPs) in colorectal cancer. *Cancer Metastasis Rev.,* **2004**. 23: 101-117.

47. Woo, M.S., Jung, S.H., Kim, S.Y., Hyun, J.W., *et al.* Curcumin suppresses phorbol ester-induced matrix metalloproteinase-9 expression by inhibiting the PKC to MAPK signaling pathways in human astroglioma cells. *Biochem. Biophys. Res. Commun.,* **2005**. 335: 1017-1025.

48. Kunnumakkara, A.B., Guha, S., Krishnan, S., Diagaradjane, J., Gelovani, J., Aggarwal, B.B. Curcumin potentiates antitumor activity of gemcitabine in an orthotopic model of pancreatic cancer through suppression of proliferation, angiogenesis, and inhibition of nuclear factor-kappaB-regulated gene products. *Cancer Res.,* **2007**. 67: 3853-3861.

49. Lin, Y.G., Kunnumakkara, A.B., Nair, A., Merritt, W.M., Han, L.Y., Armaiz-Pena, G.N., Kamat, A.A., Spanuth, W.A., Gershenson, D.M., Lutgendor, S.K., Aggarwal, B.B., Sood, A.K. Curcumin inhibits tumor growth and angiogenesis in ovarian carcinoma by targeting the nuclear factor-kappaB pathway. *Clin. Cancer Res.,* **2007**. 13: 3423-3430.

50. Camacho-Barquero, L., Villegas, I., Sánchez-Calvo, J.M., Talero, E., Sánchez-Fidalgo, S., Motilva, V., Alarcón de la Lastra, C. Curcumin, a *Curcuma longa* constituent, acts on MAPK p38 pathway modulating COX-2 and iNOS expression in chronic experimental colitis. *Int. Immunopharmacol.*, **2007**. 3: 333-342.

51. Kortula, L., Cheung, J.Y., Mendelsohn, J., Kumar, R. Inhibition of ligand-induced activation of epidermal growth factor receptor tyrosine phosphorylation by curcumin. *Carcinogenesis*, **1995**. 18: 1741-1745.

52. Arbiser, K.N.J.L., Rohan, R., van Leeuwen, R., Huang, M.T., Fisher, C., Flynn, E., HR, B. Curcumin is an in vivo inhibitor of angiogenesis. *Mol. Med.,* **1998**. 4: 376-383.

53. Gururaj, B.M.A.E., Venkatesh, D.A., Marmé, D., Salimath, B.P. Molecular mechanisms of anti-angiogenic effect of curcumin. *Biochem. Biohys. Res. Commun.,* **2002**. 297: 934-942.

54. Verma, G.B., Lin, P.S. The inhibition of the estrogenic effects of pesticides and environmental chemicals by curcumin and isoflavonoids. *Environ. Health Perspect.,* **1998**. 12: 807-812.

55. Chin, S.S., Geng, J.J., Mao, L.T., Gung, C.J., *et al.* Curcumin-induced apoptosis of human colon cancer colon 205 cells through the production of ROS, Ca2+ and the activation of caspase-3. *Anticancer Res.,* **2006**. 26: 4379-4389.

56. Shishodia, S., Amin, H.M., Lai, R., Aggarwal, B.B. Curcumin (diferuloylmethane) inhibits constitutive NF-kappaB activation, induces G1/S arrest, suppresses proliferation, and induces apoptosis in mantle cell lymphoma. *Biochem. Pharmacol.,* **2005**. 70: 700-713.

57. Sarkar, F., Li, Y. Cell signaling pathways altered by natural chemopreventive agents. *Mutat. Res. Fundam. Mol. Mech. Mutagen.,* **2004**. 555: 53-64.

58. Sa, G., Das, T. Anti cancer effects of curcumin: cycle of life and death. *Cell Div.*, **2008**. 3: 14.

59. Han, S.S., Chung, S.T., Robertson, D.A., Ranjan, D., Bondada, S. Curcumin causes the growth arrest and apoptosis of B cell lymphoma by downregulation of egr-1, c-myc, bcl-XL, NF-kappa B, and p53. *Clin. Immunol.,* **1999**. 93: 152-161.

60. Bush, J.A., Cheung, J. K.-J., Li, G. Curcumin induces apoptosis in human melanoma cells through a Fas receptor/caspase-8 pathway independent of p53. *Exp. Cell Res.*, **2001**. 271: 305-314.

61. Liu, E., Wu, J., Cao, W., Zhang, J., Liu, W., Jiang, X., Zhang, X. Curcumin indudes G2/M cell cycle arrest in a p53-dependent manner and upregulates ING4 expression in human glioma. *J. Neurooncol.,* **2007**. 85: 263-270.

62. Mukhopadhyay, A., Banerjee, S., Stafford, L.J., Xia, X., et al. Curcumin-induced suppression of cell proliferation correlates with down-regulation of cyclin D1 expression and CDK4-mediated retinoblastoma protein phosphorylation. *Oncogene*, **2002**. 21: 8852-8862.

63. Park, M.J., Kim, E.H., Park, I.C., Lee, H.C., *et al.* Curcumin inhibits cell cycle progression of immortalized human umbilical vein endothelial (ECV304) cells by up-regulating cyclin-dependent kinase inhibitor, p21WAF1/CIP1, p27KIP1 and p53. *Int. J. Oncol.,* **2002**. 21: 379-383.

64. Ravindranath, V., Chandrasekhara, N. Absorption and tissue distribution of curcumin in rats. *Toxicology*, **1980**. 16: 259-265.

65. Wahlstrom, B., Blennow, G. A study on the fate of curcumin in the rat. *Acta Pharmacol. Toxicol. (Copenh.),* **1978**. 43: 86-92.

66. Pan, M.H., Huang, T.M., Lin, J.K. Biotransformation of curcumin through reduction and glucuronidation in mice. *Drug Metab. Dispos.,* **1999**. 27: 486-494.

67. Cheng, A.L., Hsu, C.H., Lin, J.K., Hsu, M.M., *et al.* Phase I clinical trial of curcumin, a chemopreventive agent, in patients with high-risk or pre-malignant lesions. *Anticancer Res.,* **2001**. 21: 2895-2900.

68. Garcea, G., Berry, D.P., Johns, D.J., Singh, R., *et al.* Consumption of the putative chemopreventive agent curcumin by cancer patients: assessment of curcumin levels in the colorectum and their pharmacodynamic consequences. *Cancer Epidemiol. Biomarkers Prev.,* **2005**. 14: 120-125.

69. Ireson, C., Orr, S., Jones, D.J., Verschoyle, R., *et al.* Characterization of metabolites of the chemopreventive agent curcumin in human and rat hepatocytes and in the rat

in vivo, and evaluation of their ability to inhibit phorbol ester-induced prostaglandin E2 production. *Cancer Res.,* **2001**. 61: 1058-1064.

70. Yang, K.Y., Lin, L.C., Tseng, T.Y., Wang, S.C., Tsai, T.H. Oral bioavailability of curcumin in rat and the herbal analysis from Curcuma longa by LC-MS/MS. *J. Chromatogr., B.*, **2007**. 853: 183-189.

71. Maiti, K., Mukherjee, K., Ganai, A., Saha, B.P., Mukherjee, P.K. Curcumin-phospholipid complex: Preparation, therapeutic evaluation and pharmacokinetic study in rats. *Int. J. Pharm.,* **2007**. 330: 155-163.

72. Perkins, S., Verschoyle, R.D., Hill, K., Parveen, I., *et al.* Chemopreventive efficacy and pharmacokinetics of curcumin in the min/+ mouse, a model of familial adenomatous polyposis. *Cancer Epidemiol. Biomarkers Prev.*, **2002**. 11: 535-540.

73. Cheng, A.L., Hsu, C.H., Lin, J.K., Hsu, M.M., Ho, Y.F., Shen, T.S., Ko, J.Y., Lin, J.T., Lin, B.R., Ming-Shiang, W., *et al.* Phase I clinical trial of curcumin, a chemopreventive agent, in patients with high-risk or pre-malignant lesions. *Anticancer Res*., **2001**. 21: 2895-2900.

74. Goel, A., Kunnumakkara, A.B., Aggarwal, B.B. Curcumin as "Curecumin": from kitchen to clinic. *Biochem. Pharmacol.,* **2008**. 75: 787-809.

75. Bertolini, F., Paul, S., Mancuso, P., *et al.* Maximum tolerable dose and low-dose metronomic chemotherapy have opposite effects on the mobilization and viability of circulating endothelial progenitor cells. *Cancer Res.,* **2003**. 63: 4342-4346.

76. Kerbel, R.S., Kamen, B.A. The anti-angiogenic basis of metronomic chemotherapy. *Nat. Rev. Cancer,* **2004**. 4: 423–436.

77. Maiti, K., Mukherjee, K., Gantait, A., Saha, B.P., Mukherjee, P.K. *Int. J. Pharm.,* **2007**. 330: 155-163.

78. Marczylo, T.H., Verschoyle, R.D., Cooke, D.N., Morazzoni, P., *et al. Cancer Chemothera. Pharmacol.,* **2007**. 60, 171-177.

79. Hassaninasab, A., Hashimoto, Y., Tomita-Yokotani, K., and Kobayashi, M. Discovery of the curcumin metabolic pathway involving a unique enzyme in an intestinal microorganism. *Proc. Natl. Acad. Sci.,* **2011**. 108: 6615-20.

80. Mukhopadhyay, A., Basu, N., Ghatak, N., Gujral, P.K. Anti-inflammatory and irritant activities of curcumin analogues in rats. *Agents Actions*, **1982**. 12: 508–515.

81. Pari, L., Murugan, P. Antihyperlipidemic effect of curcumin and tetrahydrocurcumin in experimental type 2 diabetic rats. *Ren. Fail.,* **2007**. 29: 881–889.

82. Sugiyama, Y., Kawakishi, S., Osawa, T. Involvement of the β-diketone moiety in the antioxidative mechanism of tetrahydrocurcumin. *Biochem. Pharmacol.,* **1996**. 52: 519–525.

83. Shoba, G., Joy, D., Joseph, T., Majeed, M., Rajendran, R., and Srinivas, P.S. Influence of piperine on the pharmacokinetics of curcumin in animals and human volunteers. *Planta Med*, **1998**. 64: 353-356.

84. Karikar, C., Maitra, A., Bisht, S., Feldmann, G., Soni, S., Ravi, R. Polymeric nanoparticle-encapsulated curcumin ("nanocurcumin"): a novel strategy for human cancer therapy. *J. Nanobiotechnol.,* **2007**. 5:3.

85. Tiyaboonchai, W., Tungpradit, W., Plianbangchang, P. Formulation and characterization of curcuminoids loaded solid lipid nanoparticles. *Int. J. Pharm.,* **2007**. 337: 299-306.

86. Suresh, D., Srinivasan, K. Studies on the in vitro absorption of spice principles – Curcumin, capsaicin and piperine in rat intestines. *Food Chem. Toxicol.,* **2007**. 45: 1437-1442.

87. Ma, Z., Shayeganpour, A., Brocks, D.R., Lavasanifar, A., Samuel, J. High-performance liquid chromatography analysis of curcumin in rat plasma: application to pharmacokinetics of polymeric micellar formulation of curcumin. *Biomed. Chromatogr.,* **2007**. 21: 546-552.

88. Li, L., Braiteh, F.S., Kurzrock, R. Liposome-encapsulated curcumin: in vitro and in invo effects on proliferation, apoptosis, signaling, and angiogenesis. *Cancer*, **2005**. 104: 1322-1331.

89. Li, L., Ahmed, B., Mehta, K., Kurzrock, R. Liposomal curcumin with and without oxaliplatin: effects on cell growth, apoptosis, and angiogenesis in colorectal cancer. *Mol. Cancer Ther.,* **2007**. 6: 1276-1282.

90. Kunwar, A., Barik, A., Pandey, R., Priyadarsini, K.I. Transport of liposomal and albumin loaded curcumin to living cells: an absorption and fluorescence spectroscopic study. *Biochem. Biophys. Acta,* **2006**. 1760: 1513-1520.

91. Gatti, G., Perucca, E. Plasma concentrations of free and conjugated silybin after oral intake of a silybin-phosphatidylcholine complex (silipide) in healthy volunteers. *Int. J. Clin. Pharmacol. Ther.,* **1994**. 32: 614-617.

92. Kimura, T., Takeda, K., Kageyu, A., Toda, M., Kurosaki, Y., Nakayama, T. Intestinal absorption of dolichol from emulsions and liposomes in rats. *Chem. Pharm. Bull. (Tokyo),* **1989**. 37: 463-466.

93. Ireson, C.R., Jones, D.J., Orr, S., Coughtrie, M.W., Boocock, D.J., Williams, M.L., Farmer, P.B., Steward, W.P., and Gescher, A.J. Metabolism of the cancer chemopreventive agent curcumin in human and rat intestine. *Cancer Epidemiol. Biomarkers Prev.*, **2002**. 11: 105-111.

94. Hoehle, S.I., Pfeiffer, E., Solyom, A.M., and Metzler, M. Metabolism of curcuminoids in tissue slices and subcellular fractions from rat liver. *J. Agric. Food Chem.*, **2006**. 54: 756-764.

95. Hoehle, S.I., Pfeiffer, E., and Metzler, M. Glucuronidation of curcuminoids by human microsomal and recombinant UDP-glucuronosyltransferases. *Mol. Nutr. Food Res.*, **2007**. 51: 932-938.

96. Pan, M.H., Huang, T.M., and Lin, J.K. Biotransformation of curcumin through reduction and glucuronidation in mice. *Drug Metab. Dispos.*, **1999**. 27: 486-494.

97. Pfeiffer, E., Hoehle, S.I., Walch, S.G., Riess, A., Solyom, A.M., and Metzler, M. Curcuminoids form reactive glucuronides in vitro. *J. Agric. Food Chem.,* **2007**. 55: 538-544.

98. Nishimuta, H., Ohtani, H., Tsujimoto, M., Ogura, K., Hiratsuka, A. and Sawada, Y. Inhibitory effects of various beverages on human recombinant sulfotransferase isoforms SULT1A1 and SULT1A3. *Biopharm. Drug Dispos*., **2007**. 28: 491-500.

99. Hacker, M., Messer II, W.S., Bachmann, K.A. *Pharmacology: Principles and Practice. Academic Press*, **2009**. 216-217.

100. Wermuth, C.G, Ganellin, C.R., Lindberg, P., Mitscher, L.A., Ganellin, Lindberg, Mitscher. Glossary of terms used in medicinal chemistry (IUPAC Recommendations 1998)". *Pure and Applied Chemistry*, **1998**. 70 (5): 1129.

101. Malhotra, B., Gandelman, K., Sachse, R., Wood, N., Michel, M. C. The design and development of fesoterodine as a prodrug of 5-hydroxymethyl tolterodine (5-HMT), the active metabolite of tolterodine. *Curr Med Chem.*, **2009**. 16 (33): 4481–4489.

102. Stella, V.J., Charman, W.N., Naringrekar, V.H. Prodrugs. Do they have advantages in clinical practice? *Drugs,* **1985**. 29 (5): 455–473.

103. Kim, H.W., Mino, K., Ishikawa, K. Crystallization and preliminary X-ray analysis of endoglucanase from Pyrococcus horikoshii. *Acta Crystallogr.,* **2008**. 64: 1169-1171.

104. Bosslet, K., Czech, J., Hoffmann, D. A novel one-step tumor-selective prodrug activation system. *Tumor Targeting,* **1995**. 1: 45.

105. Brot, F.E., Bell, C.E., Sly, W.S. Purification and properties of β-glucuronidase from human placenta. *Biochemistry*, **1978**. 17: 385-391.

106. Islam, M.R., Tomatsu, S., Shah, G.N., Grubb, J.H., Sanjeev, J., Sly, W.S. Active site residues of human β-glucuronidase. Evidence for Glu(540) as the nucleophile

and Glu(451) as the acid-base residue. *J. Biol. Chem.,* **1998**. 274 (33): 23451–23455.

107. Jain, S., Drendel, W.B., Chen, Z.W., Mathews, F.S., Sly, W.S., Grubb, J.H. Structure of humanbeta-glucuronidase reveals candidate lysosomal targeting and active-site motifs. *Nat. Struct. Biol.,* **1996**. 3 (4): 375–81.

108. Smith, R.L. The biliary excretion and enterohepatic circulation of drugs and other organic compounds. *Fortschr Arzneimittelforsch*, **1966**. 9: 299-360.

109. Mürdter T.E., Sperker B., Kivistö K.T., *et al*. Enhanced Uptake of Doxorubicin into Bronchial Carcinoma: β-Glucuronidase Mediates Release of Doxorubicin from a Glucuronide Prodrug (HMR 1826) at the Tumor Site. *Cancer Research,* **1997**. 57: 2440-2445.

110. Bosslet K., Straub R., Blumrich M., *et al.* Elucidation of the Mechanism Enabling Tumor Selective Prodrug Monotherapy. *Cancer Research,* **1998**. 58: 1195-1201.

111. Schumacher, U., Adam, E., Zangemeister-Wittke, U., Gossrau, R. Histochemistry of therapeutically relevant enzymes in human tumours transplanted into severe combined immunodeficient (SCID) mice: nitric oxide synthase-associated diaphorase, beta-D-glucuronidase and non-specific alkaline phosphatase. *Acta Histochem.,* **1996**. 98: 381-387.

112. Houba, P.H., Boven, E., Erkelens, C.A., Leenders, R.G., Scheeren, J.W., Pinedo, H.M., Haisma, H.J. The efficacy of the anthracycline prodrug daunorubicin-GA3 in human ovarian cancer xenografts. *Br. J. Cancer,* **1998**. 78: 1600-1606.

113. Houba, P.H., Boven, E., Van der Meulen-Muileman, I.H., Leenders, R.G., Scheeren, J.W., Pinedo, H.M., Haisma, H.J. A novel doxorubicin-glucuronide prodrug DOX-GA3 for tumour-selective chemotherapy: distribution and efficacy in experimental human ovarian cancer. *Br. J. Cancer,* **2001**. 84: 550-557.

114. Bosslet, K., Straub, R., Blumrich, M., Czech, J., Gerken, M., Sperker, B., Kroemer, H.K., Gesson, J.P., Koch, M., Monneret, C. Elucidation of the mechanism enabling tumor selective prodrug monotherapy. *Cancer Res.,* **1998**. 58: 1195-1201.

115. Sperker, B., Werner, U., Murdter, T.E., Tekkaya, C., Fritz, P., Wacke, R., Adam, U., Gerken, M., Drewelow, B., Kroemer, H.K. Expression and function of beta-glucuronidase in pancreatic cancer: potential role in drug targeting. *Naunyn Schmiedebergs Arch. Pharmacol.,* **2000**. 362: 110-115.

116. Sinnott, M. Comprehensive Biological Catalysis. *Manchester, UK: Academic Press,* **1998**. 119–138.

117. McCarter, J.D., Withers, S.G. Mechanisms of enzymatic glycoside hydrolysis. *Curr. Opin. Struct. Biol.,* **1994**. 4 (6): 885–892.

118. Sinnott, M.L. Catalytic mechanisms of enzymatic glycosyl transfer. *Chem Rev,* **1990**. 90: 1171–1202.

119. Hoehle, S.I., Pfeiffer, E., and Metzler, M. Glucuronidation of curcuminoids by human microsomal and recombinant UDP-glucuronosyltransferases. *Mol. Nutr. Food Res.*, **2007**. 51: 932-938.

120. Bock, K., Köhle, C. UDP-glucuronosyltransferase 1A6: structural, functional, and regulatory aspects. *Methods Enzymol.*, **2005**. 400: 57–75.

121. Bosslet, K., Straub, R., Blumrich, M., Czech, J., Gerken, M., Sperker, B., Kroemer, H.K., Gesson, J.P., Koch, M., Monneret, C. Elucidation of the mechanism enabling tumor selective prodrug monotherapy. *Cancer Res.,* **1998**. 58 (6):1195-1201.

122. Sperker, B., Werner, U., Mürdter, T.E., Tekkaya, C., Fritz, P., Wacke, R., Adam, U., Gerken, M., Drewelow, B., Kroemer, H.K. Expression and function of beta-glucuronidase in pancreatic cancer: potential role in drug targeting. *Naunyn Schmiedebergs Arch. Pharmacol.,* **2000**. 362 (2): 110-115.

123. Dodds, H.M., Tobin, P.J., Stewart, C.F., Cheshire, P., Hanna, S., Houghon, P., Rivory, L.P. The importance of tumor glucuronidase in the activation of irinotecan in a mouse xenograft model. *J. Pharmacol. Exp. Ther.,* **2002**. 303 (2): 649-655.

124. Mürdter, T.E., Sperker, B., Kivistö, K.T., McClellan, M., Fritz, P., Friedel, G., Linder, A., Bosslet, K., Toomes, H., Dierkesmann, R., Kroemer, H.K. Enhanced uptake of doxorubicin into bronchial carcinoma: beta-glucuronidase mediates release of doxorubicin from a glucuronide prodrug (HMR 1826) at the tumor site. *Cancer Res.,* **1997**. 57 (12): 2440-2445.

125. Prijovich, Z.M., Chen, K.C., Roffler, S.R. Local enzymatic hydrolysis of an endogenously generated metabolite can enhance CPT-11 anticancer efficacy. *Mol. Cancer Ther.,* **2009**. 8 (4): 940-946.

126. Mürdter, T.E., Friedel, G., Backman, J.T., McClellan, M., Schick, M., Gerken, M., Bosslet, K., Fritz, P., Toomes, H., Kroemer, H.K., Sperker, B. Dose optimization of a doxorubicin prodrug (HMR 1826) in isolated perfused human lungs: low tumor pH promotes prodrug activation by beta-glucuronidase. *J. Pharmacol. Exp. Ther.,* **2002**. 301 (1): 223-228.

127. Juan, T.Y., Roffler, S.R., Hou, H.S., Huang, S.M., Chen, K.C., Leu, Y.L, Prijovich, Z.M, Yu, C.P., Wu, C.C., Sun, G.H., Cha, T.L . Antiangiogenesis targeting tumor microenvironment synergizes glucuronide prodrug antitumor activity. *Clin. Cancer Res.,* **2009**. 15 (14): 4600-4611.

128. Savjani, K.T., Gajjar, A.K., Savjani, J.K. Drug Solubility: Importance and Enhancement Techniques. *ISRN Pharm.,* **2012**. 195727.

129. Gursoy, R.N., Benita, S. Self-emulsifying drug delivery systems (SEDDS) for improved oral delivery of lipophilic drugs. *Biomed. Pharmacother.,* **2004**. 58: 173-182.

130. Bagwe, R.P., Kanicky, J.R., Palla, B.J., Patanjali, P.K., Shah, D.O. Improved drug delivery using microemulsions: Rationale, recent progress, and new horizons. *Crit. Rev. Ther. Drug,* **2001**. 18(1): 77–140.

131. Lawrence, M.J., Rees, G.D. Microemulsion-based media as novel drug delivery systems. *Adv. Drug Deliv. Rev.,* **2000**. 45(1): 89–121.

132. Attwood, D. *Microemulsions*, **1994**. Marcel Dekker, New York.

133. Tenjarla, S. Microemulsions: an overview and pharmaceutical applications. *Crit. Rev. Ther. Drug Carrier Syst*, **1999**. 16: 461-521.

134. Thevenin, M.A., Grossiord, J.L., Poelman, M.C. Sucrose esters/cosurfactant microemulsion systems for transdermal delivery: Assessment of bicontinuous structures. *International Journal of Pharmaceutics*, **1996**. 137: 177-186.

135. Hirunpanich, V., Sato, H. Improvement of cyclosporine A bioavailability by incorporating ethyl docosahexaenoate in the microemulsion as an oil excipient. *Eur. J. Pharm. Biopharm.*, **2009**. 73: 247-252.

136. Aboofazeli, R., Lawrence, C.B., Wicks, S.R., Lawrence, M.J. Investigations into the formation and characterization of phospholipid microemulsions. III. Pseudo-ternary phase diagrams of systems containing water-lecithin-isopropyl myristate and either an alkanoic acid, amine, alkanediol, polyethylene glycol alkyl ether or alcohol as cosurfactant. *International Journal of Pharmaceutics*, **1994**. 111: 63-72.

137. Vonderscher, J., Meinzer, A. Rationale for the development of Sandimmune Neoral. *Transplant Proc.*, **1994**. 26: 2925-2927.

138. Baselga, J., Perez, E.A., Pienkowski, T., Bell, R. Adjuvant trastuzumab: a milestone in the treatment of HER-2-positive early breast cancer. *Oncologist*, **2006**. 11 Suppl 1: 4-12.

139. 2015. American Cancer Society Breast Cancer Facts & Figures 2014-2015.

140. U.S. Breast Cancer Statistics, *Breastcancer.org.* Available from: http://www.breastcancer.org/symptoms/understand_bc/statistics.

141. Hanahan, D., Weinberg, R.A. The hallmarks of cancer. *Cell*, **2000**. 100: 57-70.

142. Ursini-Siegel, J., Schade, B., Cardiff, R.D., Muller, W.J. Insights from transgenic mouse models of ERBB2-induced breast cancer. *Nat. Rev. Cancer*, **2007**. 7: 389-397.

143. Carter, C.L., Allen, C., Henson, D.E. Relation of tumor size, lymph node status, and survival in 24,740 breast cancer cases. *Cancer*, **1989**. 63: 181-187.

144. Jemal, A., Siegel, R., Ward, E., Hao, Y., Xu, J., Murray, T., Thun, M.J. Cancer statistics, 2008. *CA Cancer J. Clin.,* **2008**. 58: 71-96.

145. Wilcken, N., Dear, R. Chemotherapy in metastatic breast cancer: A summary of all randomised trials reported 2000-2007. *Eur. J. Cancer*, **2008**. 44: 2218-2225.

146. Richert, M.M., Schwertfeger, K.L., Ryder, J.W., Anderson, S.M. An atlas of mouse mammary gland development. *J. Mammary Gland Biol. Neoplasia*, **2000**. 5: 227-241.

147. McSherry, E.A., Donatello, S., Hopkins, A.M., McDonnell, S. Molecular basis of invasion in breast cancer. *Cell. Mol. Life Sci.,* **2007**. 64: 3201-3218.

148. Breast Cancer Health Center: What are the stages of breast cancer? *WebMD.* Available from: http://www.webmd.com/breast-cancer/guide/stages-breast-cancer.

149. Tamimi, R.M., Baer, H.J., Marotti, J., *et al.* Comparison of molecular phenotypes of ductal carcinoma in situ and invasive breast cancer. *Breast Cancer Res.,* **2008**. 10 (4): R67.

150. Clark, S.E., Warwick, J., Carpenter, R., Bowen, R.L., Duffy, S.W., Jones, J.L. Molecular subtyping of DCIS: heterogeneity of breast cancer reflected in pre-invasive disease. *Br J Cancer,* **2011**. 104 (1): 120-7.

151. Carey, L.A., Perou, C.M., Livasy, C.A., *et al.* Race, breast cancer subtypes, and survival in the Carolina Breast cancer Study. *JAMA*, **2006**. 295(21): 2492-2502.

152. Potemski, P., Kusinska, R., Watala, C., Pluciennik, E., Bednarek, A.K., Kordek, R. Prognostic relevance of basal cytokeratin expression in operable breast cancer. *Oncology*, **2005**. 69(6): 478-485.

153. Hu, Z., Fan, C., Oh, D.S., *et al.* The molecular portraits of breast tumors are conserved across microarray platforms. *BMC Genomics,* **2006**. 7: 96.

154. Fan, C., Oh, D.S., Wessels, L., *et al.* Concordance among gene-expression-based predictors for breast cancer. *N. Engl. J. Med.,* **2006**. 355(6): 560-569.

155. Voduc, K.D., Cheang, M.C., Tyldesley, S., Gelmon, K., Nielsen, T.O., Kennecke, H. Breast cancer subtypes and the risk of local and regional relapse. *J Clin Oncol*, **2010**. 28(10): 1684-91.

156. Carey, L.A. Molecular intrinsic subtypes of breast cancer. In: UpToDate. Hayes, D.F., Dizon, D.S. (eds.). Waltham, M.A.: UpToDate, **2013**.

157. Fossati, R., Confalonieri, C., Torri, V., Ghislandi, E., Penna, A., Pistotti, V., Tinazzi, A., Liberati, A. Cytotoxic and hormonal treatment for metastatic breast cancer: a systematic review of published randomized trials involving 31,510 women. *J. Clin. Oncol.*, **1998**. 16: 3439-3460.

158. van Londen, G.J., Perera, S., Vujevich, K., Rastogi, P., Lembersky, B., Brufsky, A., Vogel, V., Greenspan, S.L. The impact of an aromatase inhibitor on body composition and gonadal hormone levels in women with breast cancer. *Breast Cancer Research and Treatment,* **2011**. 125 (2): 441-446.

159. Yarden, Y. Biology of HER2 and its importance in breast cancer. *Oncology*, **2001**. 61 Suppl 2: 1-13.

160. Baselga, J., Perez, E.A., Pienkowski, T., Bell, R. Adjuvant trastuzumab: a milestone in the treatment of HER-2-positive early breast cancer. *Oncologist*, **2006**. 11 Suppl 1: 4-12.

161. Vargo-Gogola, T., Rosen, J.M. Modelling breast cancer: one size does not fit all. *Nature Reviews Cancer,* **2007**. 7: 659-672.

162. Morton, C.L., Houghton, P.J. Establishment of human tumor xenografts in immunodeficient mice. *Nat Protoc.,* **2007**. 2 (2): 247-250.

163. Bosma, M.J., Carroll, A.M. The SCID mouse mutant: definition, characterization, and potential uses. *Annu. Rev. Immunol.,* **1991**. 9: 323-350.

164. Ross, D.T., Scherf, U., Eisen, M.B., Perou, C.M., Rees, C., Spellman, P., Iyer, V., Jeffrey, S.S., Van de Rijn, M., Waltham, M., *et al.* Systematic variation in gene expression patterns in human cancer cell lines. *Nat. Genet.*, **2000**. 24: 227-235.

165. Neve, R.M., Chin, K., Fridlyand, J., Yeh, J., Baehner, F.L., Fevr, T., Clark, L., Bayani, N., Coppe, J.P., Tong, F., *et al.* A collection of breast cancer cell lines for the study of functionally distinct cancer subtypes. *Cancer Cell*, **2006**. 10: 515-527.

166. Ursini-Siegel, J., Schade, B., Cardiff, R.D., Muller, W.J. Insights from transgenic mouse models of ERBB2-induced breast cancer. *Nat. Rev. Cancer*, **2007**. 7: 389-397.

167. Sinn, E., Muller, W., Pattengale, P., Tepler, I., Wallace, R., Leder, P. Coexpression of MMTV/v-Ha-ras and MMTV/c-myc genes in transgenic mice: synergistic action of oncogenes in vivo. *Cell*, **1987**. 49: 465-475.

168. Sutherland, R.L., Musgrove, E.A. Cyclin D1 and mammary carcinoma: new insights from transgenic mouse models. *Breast Cancer Res.,* **2002**. 4: 14-17.

169. Guy, C.T., Webster, M.A., Schaller, M., Parsons, T.J., Cardiff, R.D., Muller, W.J. Expression of the neu protooncogene in the mammary epithelium of transgenic mice induces metastatic disease. *Proc. Natl. Acad. Sci. U S A*, **1992**. 89: 10578-

10582.

170. Talmadge, J.E., Singh, R.K., Fidler, I.J., Raz, A. Murine Models to Evaluate Novel and Conventional Therapeutic Strategies for Cancer. *Am. J. Pathol.,* **2007**. 170 (3): 793-804.

171. Di Carlo, E., Diodoro, M.G., Boggio, K., Modesti, A., Modesti, M., Nanni, P., Forni, G., Musiani, P. Analysis of mammary carcinoma onset and progression in HER-2/neu oncogene transgenic mice reveals a lobular origin. *Lab Invest*, **1999**. 79: 1261-1269.

172. Calogero, R.A., Cordero, F., Forni, G., Cavallo, F. Inflammation and breast cancer. Inflammatory component of mammary carcinogenesis in ErbB2 transgenic mice. *Breast Cancer Res.*, **2007**. 9: 211.

173. Sharma, R.A., *et al*. Phase I clinical trial of oral curcumin biomarkers of systemic activity and compliance. *Clinical Cancer Research,* **2004**. 10 (20): 6847-6854.

174. Shimoi, K., Tsutomu, N. Glucuronidase deconjugation in inflammation. *Methods in enzymology,* **2005.** 400: 263-272.

175. Aggarwal, B.B., Kumar, A., Bharti, A.C. Anticancer potential of curcumin: preclinical and clinical studies. *Anticancer Res.,* **2003**. 23: 363-398.

176. Mohandas, K.M., Desai, D.C. Epidemiology of digestive tract cancers in India. V. Large and small bowel. *Indian J. Gastroenterol.,* **1999**. 18: 118-121.

177. Aggarwal, B.B. Prostate cancer and curcumin: add spice to your life. *Cancer Biology & Therapy,* **2008**. 7:9, 1436-1440.

178. Boggio, K., Nicoletti, G., Di Carlo, E., Cavallo, F., Landuzzi, L., Melani, C., Giovarelli, M., Rossi, I., Nanni, P., De Giovanni, C., *et al.* Interleukin 12-mediated prevention of spontaneous mammary adenocarcinomas in two lines of Her-2/neu transgenic mice. *J. Exp. Med.*, **1998**. 188: 589-596.

179. Boggio, K., Di Carlo, E., Rovero, S., Cavallo, F., Quaglino, E., Lollini, P.L., Nanni, P., Nicoletti, G., Wolf, S., Musiani, P., *et al.* Ability of systemic interleukin-12 to hamper progressive stages of mammary carcinogenesis in HER2/neu transgenic mice. *Cancer Res*., **2000**. 60: 359-364.

180. Cheng, T.C., Roffler, S.R., Tzou, S.C., Chuang, K.H., Su, Y.C., Chuang C.H., Kao, C.H., Chen, C.S., Harn, I.H., Liu, K.Y., Cheng, T.L., Leu, Y.L. An activity-based near-infrared glucuronide trapping probe for imaging β-glucuronidase expression in deep tissues. *J. Am. Chem. Soc.,* **2012**. 134 (6): 3103-3110.

181. Höckel, M., Vaupel, P. Tumor Hypoxia: Definitions and Current Clinical, Biologic, and Molecular Aspects. J. Natl. Cancer Inst., **2001**. 93 (4): 266-276.

182. Oleson, L., Court, M.H. Effect of the β-glucuronidase inhibitor saccharolactone on glucuronidation by human tissue microsomes and recombinant UDP-glucuronosyltransferases. *J. Pharm. Pharmacol.,* **2008**. 60(9): 1175-1182.

183. Grill, A., Shahani, K., Kalscheuer, S., Koniar, B., Panyam, J. Chemopreventive efficacy of sustained release curcumin microparticles depends on tumorigenesis stage during initial treatment. *Cancer Res.,* **2012**. 72: 602.

184. DeAngelis, L.M., Posner, J.B. Neurologic Complications of Cancer, Second Edition. *Oxford University Press,* **2009**.

185. Kaur, P., Negaraja, G.M., Zheng, H., Gizachew, D., Galukande, M., Krishnan, S., Asea, A. A mouse model for triple-negative breast cancer tumor-initiating cells (TNBC-TICs) exhibits similar aggressive phenotype to the human disease. *BMC Cancer,* **2012**. 12: 120.

186. Choi, C., Helfman, D.M. The Ras-ERK pathway modulates cytoskeleton organization, cell motility and lung metastasis signature genes in MDA-MB-231 LM2. *Oncogene,* **2014**. 33: 3668-3676.

187. Brüsselbach, S. Extracellular beta-glucuronidase for gene-directed enzyme-prodrug therapy. *Methods Mol. Med.,* **2004**. 90: 303-330.

188. Delmas, D., Lançon, A., Colin, D., Jannin, B., Latruffe, N. Resveratrol as a chemopreventive agent: a promising molecule for fighting cancer. *Curr. Drug Targets*, **2006**. 7(4): 423-442.

189. Sabolovic, N., Humbert, A.C., Radominska-Pandya, A., Magdalou, J. Resveratrol is efficiently glucuronidated by UDP-glucuronosyltransferases in the human gastrointestinal tract and in Caco-2 cells. *Biopharm. Drug Dispos.,* **2006**. 27(4): 181-189.

190. Sharan, S., Iwuchukwu, O.F., Canney, D.J., Zimmerman, C.L., Nagar, S. In vivo-formed versus preformed metabolite kinetics of trans-resveratrol-3-sulfate and trans-resveratrol-3-glucuronide. *Drug Metab. Dispos.,* **2012**. 40(10): 1993-2001.